Biologically-Important Reactions of Ruthenium Arene Anticancer Complexes

A Thesis Submitted for the Degree of

Doctor of Philosophy

by

Jingjing Xu, *BSc.*

School of Chemistry

The College of Science and Engineering

The University of Edinburgh

December 2007

Abstract

Ru(II) half-sandwich "piano-stool" complexes $[(\eta^6\text{-arene})Ru(en)Cl]^+$ (en = ethylenediamine), such as $[(\eta^6\text{-bip})Ru(en)Cl]^+$ (bip = biphenyl) and $[(\eta^6\text{-tha})Ru(en)Cl]^+$ (tha = tetrahydroanthracene), show anticancer activity both *in vitro* and *in vivo* via hydrolysis, including activity against ciplatin-resistant cell lines. However, potential physiological and medical applications of these Ru(II) arene anticancer complexes are impeded by a lack of knowledge of competition between S-donor peptides/proteins by which cisplatin is deactivated and N-donor nucleotides for these Ru(II) complexes.

It is reported here that the Ru(II) arene anticancer complex $[(\eta^6\text{-bip})Ru(en)Cl]^+$ binds strongly to guanine (as cGMP and 14-mer DNA oligonucleotides) under physiologically-relevant conditions (micromolar concentrations, pH 7, 22 mM NaCl, 310 K), even in the presence of a 250-fold molar excess of glutathione (GSH). Reactions between the Ru(II) complex and GSH carried out in water without buffering follow a different course: a tri-glutathione-bridged dinuclear Ru(II) complex $[((\eta^6\text{-bip})Ru)_2(GS)_3]$ is the final product, and three intermediates $[(\eta^6\text{-bip})Ru(en)(GS)]$ (same formula but different binding sites) are obtained as well; whereas in reactions of the Ru(II) complex with GSH in phosphate buffer (pH 7), only a mono-ruthenium-glutathione complex $[(\eta^6\text{-bip})Ru(en)(GS)]$ was obtained, the same as one intermediate in the same reaction carried out in aqueous solution without buffering. In the presence of air, this thiolate $[(\eta^6\text{-bip})Ru(en)(GS)]$ is susceptible to oxidation, forming the sulfenate $[(\eta^6\text{-bip})Ru(en)(G(O)S)]$ which protonates to the unstable sulfenic acid $[(\eta^6\text{-bip})Ru(en)(G(OH)S)]^+$ that can be readily substituted by guanine bases (as cGMP and 14-mer DNA oligonucleotides in this thesis) ; whereas a dinuclear Ru(0) complex $\{[(\eta^6\text{-bip})Ru(0)(GSO_2)](\mu\text{-S-GSO})_2[(GSO_2)Ru(0)(\eta^6\text{-}$

bip)]}$^{9-}$ is observed when bubbling with Ar, and it probably plays a similar role to [(η^6-bip)Ru(en)(G(O)S)] described above.

The Ru(II) arene complex [(η^6-hmb)Ru(en)(SPh)]$^+$ (hmb = hexamethylbenzene; Ph = phenyl) was reported to be cytotoxic to cancer cells (IC_{50} = 23 μM, A2780 cells) but cannot hydrolyse to form the active aqua species. It is demonstrated here that GSH acts as catalyst in the oxidation of the Ru(II) thiolato complex [(η^6-hmb)Ru(en)(S-*i*Pr)]$^+$ to the sulfenato adduct [(η^6-hmb)Ru(en)(S(O)-*i*Pr)]$^+$, which is a key intermediate in the formation of cGMP adduct [(η^6-hmb)Ru(en)(cGMP-*N7*)]$^+$. The sulfenate [(η^6-hmb)Ru(en)(S(O)-*i*Pr)]$^+$ can protonate to form action of the sulfenic acid [(η^6-hmb)Ru(en)(S(OH)-*i*Pr)]$^+$ which readily hydrolyses and binds to cGMP.

Acknowledgements

I would like to thank Professor Peter J. Sadler for his supervision and encouragement throughout my project. I am grateful to him for all his help, advice and everything he has taught me, and I really have enjoyed these past three years working in his group.

I would also like to thank Professor Fuyi Wang who started this project and introduced me to the subject. I am very grateful for all his great help and invaluable advice. Many thanks are due to Dr. Holm Petzold who has helped me so much in the work shown in Chapter 6 in this thesis. Thanks are also due to Dr. C. Logan Mackay and Stefan Weidt, especially Stefan Weidt, for their efficient FT-ICR mass spectroscopy support. I am grateful to Juraj Bella for his help with NMR, Robert Smith and John Dalrymple for help with ESI-MS.

I would like to thank the ORS and the University of Edinburgh for financial support during this project. I would also like to thank the University of Edinburgh Chemistry Department and Development Trust for financial assistance, allowing me to present my work at a conference in South Africa.

Big thanks are due to all members of the Sadler group, both past and present, for being such a pleasure to work with. A special thanks to Dr. Abraha Habtemariam for his important Ru(II) arene complex. I would also like to thank Sarah Dougan for her support and huge help while I have been writing up.

Thank you to all the friends I have made since being in Edinburgh, both in and out of the chemistry department.

Finally very special thanks go to my parents for their eternal support and encouragement.

Contents

Abbreviations

bip	biphenyl
tha	tetrahydroanthracene
hmb	hexamethylbenzene
p-cym	*para*-cymene
Ph	phenyl
en	enthylenediamine
GSH	glutathione
cGMP	guanosine-3',5'-cyclic monophosphate
DNA	deoxyribonucleic acid
D_2O	water-d_2
MeOD	methanol- d_4
UV-Vis	ultraviolet-visible
HPLC	high performance liquid chromatography
PLRP	polymer reverse phase
ESI-MS	electrospray ionisation mass spectrometry
FT-ICR MS	fourier transform ion cyclotron resonance mass spectrometry
NMR	nuclear magnetic resonance
COSY	correlation spectroscopy
TOCSY	total correlation spectroscopy
NOESY	nuclear overhauser enhancement spectroscopy
HSQC	heteronuclear single quantum correlation spectroscopy
ICP-OES	inductively coupled plasma optical emission spectroscopy
ca.	circa (about)
mol equiv	molar equivalent
IC_{50}	50% growth inhibition concentration

Chapter 1

Introduction

This thesis is concerned with investigations into the mechanism of cytotoxic action of ruthenium(II) arene complexes. In this Chapter an introduction to inorganic anticancer complexes is given, particularly focusing on ruthenium(II) arene complexes, and oxidation of thiols. The aims of this thesis are also described.

1.1 Metals in Life

The first metal (from Greek 'Metallon') discovered on Earth was gold in 6000 BC due to Process Metallurgy which is one of the oldest applied sciences.[1] Metals at low levels in human body fluids and tissues (nanograms or micrograms per gram or per millilitre) are called trace elements which are composed of essential and non-essential elements, and in the absence of an essential element, such as chromium, cobalt, copper, iron, manganese, molybdenum, nickel, selenium, tin, vanadium and zinc, a deficiency syndrome develops.[2] Transition metal ions are present in living organisms mainly bound to the usual donor atoms: N, O and S which are present in proteins in their amino acid residues.[3] The first-transition-series elements Zn, Cu, Mn, Fe and Co are found in metallo-enzymes in the human body.[3]

1.2 Inorganic Drugs Used in Cancer Therapy

Cancer is a group of diseases in which cells are aggressive (grow and divide without respect to normal limits), invasive (invade and destroy adjacent tissues), and/or metastatic (spread to other locations in the body), which differentiate cancers from benign tumours.[4] Cancer can cause 13% of all deaths,[5] which is the second main cause of death in the western world.[6] Much more interest has been focused on research into metal-based anticancer drugs since the discovery of cisplatin [*cis*-

$PtCl_2(NH_3)_2$] by Barnett Rosenberg in the 1960's. Pt, Ti, V, Mo and Ru have been used as metal centres in antitumour compounds.[7-9]

1.2.1 Platinum

Several platinum anticancer complexes were synthesized since the anticancer activity of Cisplatin was discovered in the 1960's.[10,11] Cisplatin is the most successful anticancer drug in the world, and is used to treat a wide range of cancers, including testicular, ovarian, cervical, bladder, and head and neck cancers.[12] Cisplatin is administered to the blood stream, and hydrolysis is inhibited due to the relatively high chloride ion concentration in blood (ca. 100 mM). Upon entering the cell, the chloride concentration drops to ca. 20 mM, and cisplatin is hydrolysed to *cis*-[$PtCl(NH_3)_2(H_2O)]^+$ and *cis*-[$Pt(NH_3)_2(H_2O)_2]^{2+}$, which are more active forms of the drug.[13] These aqua species bind preferentially to the N7 position of guanine bases of DNA, which is the most electron rich site of DNA, to form 1,2-intrastrand adduct by binding at two neighbouring G-N7 bases.[14] Cisplatin is considered to block replication and inhibit transcription by binding to DNA, leading to apoptosis of the cancer cell.[15]

However, cisplatin has some serious drawbacks, including (1) severe toxicity such as nausea, ear damage, vomiting, loss of sensation in hands and kidney toxicity; (2) tumour resistance.[14] It is also only effective to a narrow range of cancers, which led to the development of new generations of platinum drugs (Figure 1.1). Furthermore, the high affinity between Pt(II) and sulfur-containing biological molecules, such as cysteine, methionine, glutathione and metallothionein, is known. It is believed that the sites on proteins are the most likely origin of the toxic side effects of cisplatin and its several derivatives.[16,17] Significant amounts of cisplatin are lost due to

binding to S atoms. To date over 3000 platinum complexes have been synthesised and tested for antitumour activity,[18] but only a few of these have been made into clinical trials,[19] and there are only five other platinum drugs approved for clinical use (in at least one country).[20]

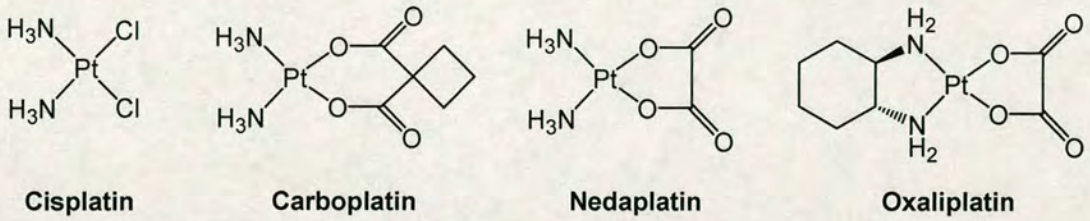

Figure 1.1 The chemical structures of the platinum anticancer drug ciplatin and some 2nd generation platinum drugs: carboplatin, nedaplatin and oxaliplatin.

1.2.2 Ruthenium

Both the success of cisplatin and its limitations have led to the search for other metal-based anticancer drugs. Ruthenium along with Os, Rh, Ir, Pd and Pt, forms the platinum group metals. Ruthenium is a group 8 transition metal of the platinum group, and its oxidation states range from 0 to +8, though oxidation states of +2 and +3 are most common in aqueous solution. Approaches to the design of new active ruthenium complexes have rapidly evolved in recent years. Many ruthenium complexes increase the lifetime expectancy of tumour-bearing hosts due to their low cytotoxic potential *in vivo*.[21] However, they were still expected to reduce tumour growth by a mechanism of interaction with cellular DNA, similar to that of cisplatin.[21] At present, ruthenium is probably the second after platinum in the number of its complexes that exhibit anticancer activity.[22]

1.2.2.1 Rutheium(III) Complexes

Ruthenium(III) was considered as a promising candidate,[23] due to the similar spectrum of kinetic acitivity as platinum(II)[22] and its lower toxicity. In the 1970's, anticancer activity was reported for several ruthenium amine compounds by Clarke, particularly *fac*-$[RuCl_3(NH_3)_3]$,[24] but it has very poor water solubility. Since this discovery, two ruthenium(III) compounds have entered clinical trials, *trans*-$[RuCl_4(DMSO)(Im)]ImH$ (NAMI-A; Im = imidazole) which is an antimetastatic complex, meaning that it is relatively inactive to primary tumours but prevents the spread of cancer from the primary site to other sites in the body,[25] and *trans*-$[RuCl_4(Ind)_2]IndH$ (KP1019; Ind = indazole) which is active against colorectal tumours,[26] as shown in Figure 1.2.

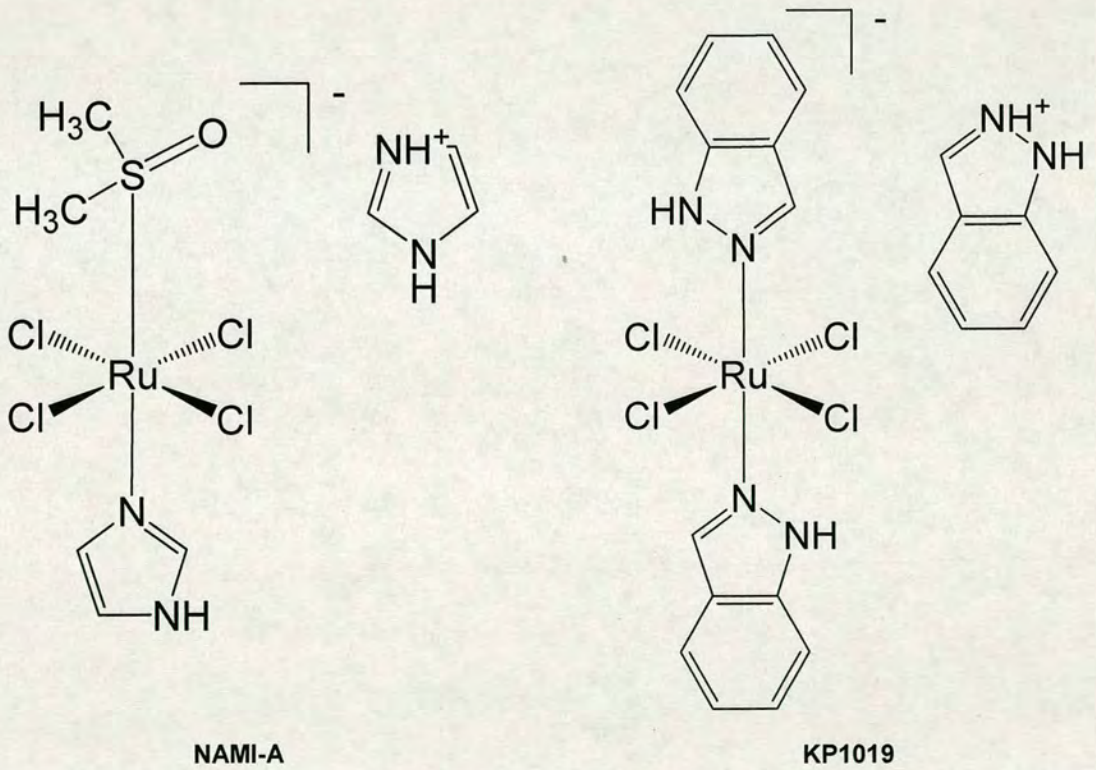

Figure 1.2 Chemical structures of NAMI-A and KP1019.

It has been suggested that ruthenium(III) anticancer complexes remain in their relatively inert Ru(III) oxidation state until they reach the tumour site, and reduce to the more reactive Ru(II) complexes due to its lower oxygen content and more acidic pH in tumours than those in normal tissue.[21] Therefore, ruthenium(II) complexes were widely studied.

1.2.2.2 Ruthenium(II) Arene Anticancer Complexes

Based on the proposal that Ru(II) may be the active species of ruthenium(III) anticancer drugs, work in our group has turned to researches into Ru(II) anticancer complexes, especially these organometallic ruthenium(II) arene complexes with a "piano-stool" structure as shown in Figure 1.3(A).

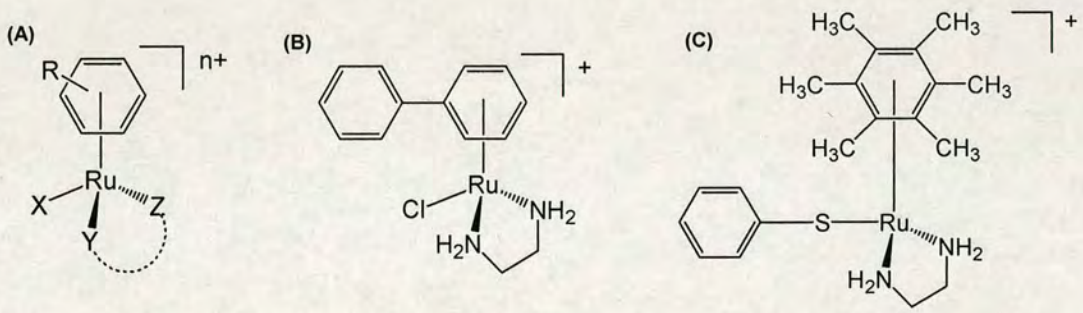

Figure 1.3 (A) General chemical structure of Ru(II) arene complexes with "piano-stool" structure, $[(\eta^6\text{-arene})Ru(X)(YZ)]^{n+}$; (B) Chemical structure of complex $[(\eta^6\text{-bip})Ru(en)Cl]^+$ (bip = biphenyl, en = ethylenediamine); (C) Chemical structure of complex $[(\eta^6\text{-hmb})Ru(en)(SPh)]^+$ (hmb = hexamethylbenzene).

Ruthenium(II) arene complexes containing an arene like biphenyl (bip) or hexamethylbenzene (hmb), a chelating ligand (YZ) such as ethylenediamine (en), and a leaving group (X) such as halide (Cl, Br and I) or thiolate SR (R = Ph, isopropyl), Figure 1.3(B) and (C), have been reported to be cytotoxic to cancer cells.[27-31]

1.2.2.2.1 Mode of Action

The mechanism of cytotoxic action of Ru(II) arene complexes, e.g. $[(\eta^6\text{-bip})Ru(en)Cl]^+$, is generally thought that the intact chloro complex is a "pro-drug" which is activated *in vivo* by hydrolysis of the Ru-Cl bond, and it is inhibited in the blood where high chloride concentrations are present (ca. 100 mM), while in the cell (4-25 mM $[Cl^-]$) the chloro complex is mainly hydrolysed to form the reactive species $[(\eta^6\text{-bip})Ru(en)(H_2O)]^{2+}$.[32] The aqua form then selectively binds to the N7 position of guanine (G) bases in DNA (Scheme 1.1).[33,34]

Scheme 1.1 Mechanism of cytotoxic action of Ru(II) arene complexes.

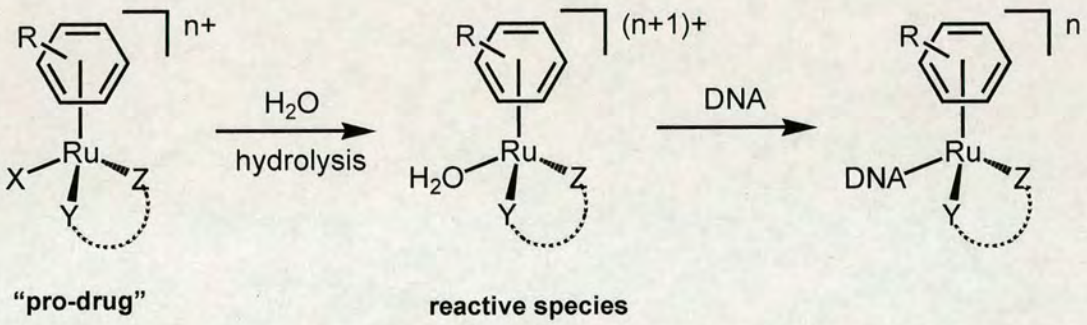

Interestingly, one novel ruthenium(II) arene complex $[(\eta^6\text{-hmb})Ru(en)(SPh)]^+$ (Figure 1.3(C)) was found to have anticancer activity but no hydrolysis was observed.[31] The mechanism of cytotoxic action of this complex was proposed to involve the oxidation of sulphur (discussed in Chapter 5).

Ruthenium(II) arene complexes $[(\eta^6\text{-arene})Ru(en)Cl]^+$ were found to be active against cisplatin-resistant cell lines.[35] Their binding to DNA can only give rise to monofuctional adducts compared to the bifunctional adducts of cisplatin, and DNA

was more difficult to repair after treated with $[(\eta^6\text{-arene})Ru(en)Cl]^+$ than that treated with cisplatin.[36,37]

1.2.2.2.2 Role of Coordinated Arene

The arene group appears to play a major role in the anticancer activity of complexes, which is considered as a π-acid / π-acceptor ligand towards Ru(II). The IC_{50} values (the dose which inhibits growth of 50% of the cells) decrease (increase in activity) with increase in hydrophobicity of arenes (see Figure 1.4 and Table 1.1).[35]

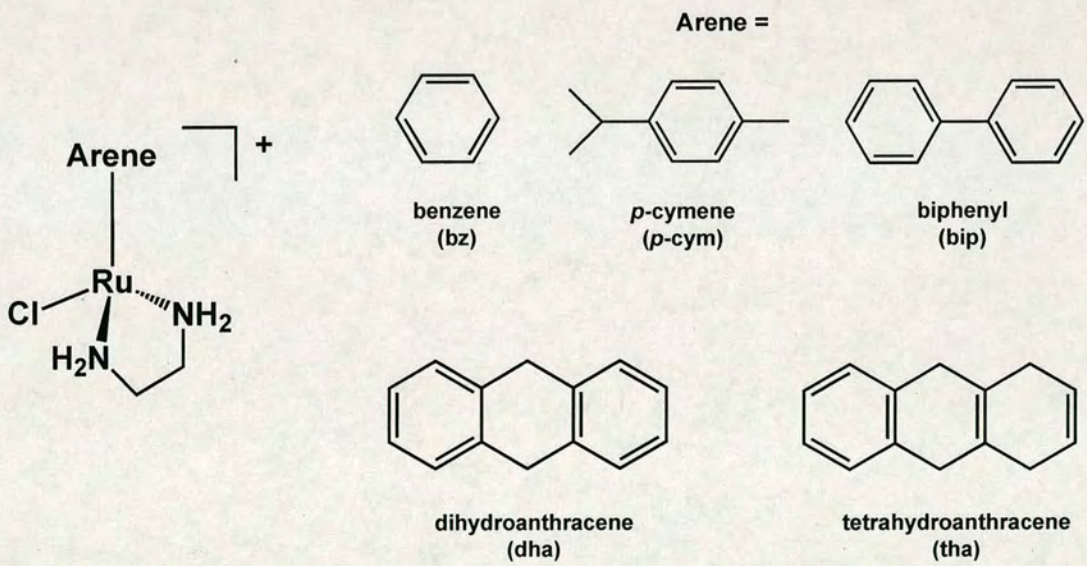

Figure 1.4 Ruthenium(II) arene complexes with different arenes.

Table 1.1 IC_{50} values against human ovarian A2780 cancer cells after 24 h complex exposure.[35]

Arene or Pt complex	IC_{50} / μM
bz	17
p-cym	10
bip	5
dha	2
tha	0.5
cisplatin	0.6
carboplatin	6

The arene can stabilise ruthenium in its +2 oxidation state, as well as makes the whole molecule hydrophobic which may assist in crossing cell membranes. The reason for the increase in activity with increase in hydrophobicity of arenes is that the extended arenes can intercalate into DNA to form strong intramolecular π-π arene-nucleobase stacking,[34,36] which is supported by the X-ray crystal structures of 9-ethylguanine (9EtG) adducts $[(\eta^6\text{-arene})Ru(en)(9EtG)]^{2+}$ (Figure 1.5).[38]

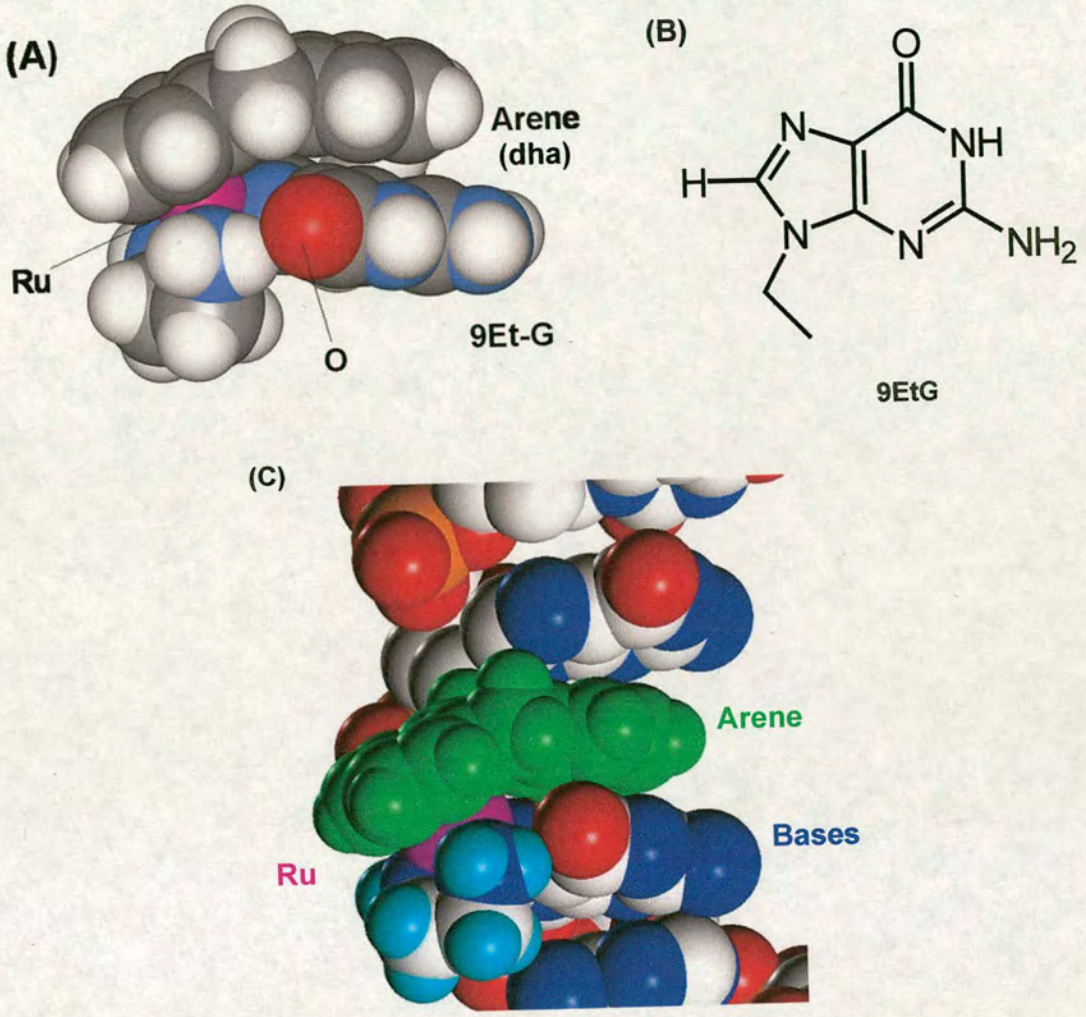

Figure 1.5 π-π arene-nucleobase stacking. (A) X-ray crystal structure of $[(\eta^6$-dha)Ru(en)(9EtG-*N7*)$]^{2+}$; (B) Chemical structure of 9-ethylguanine (9EtG); (C) Model of the ruthenium(II) arene complex binding to B-DNA, showing how the coordinated arene can insert between G base pairs. Figure reproduced from reference 38.

The rate of reaction with cyclic guanosine monophophate (cGMP) increases with the increase in hydrophobicity of arenes due to the π-π arene-nucleobase stacking (Table 1.2).[39]

Table 1.2 Half lives ($t_{1/2}$) for reactions of $[(\eta^6\text{-arene})Ru(en)Cl]^+$ (2 mM) with cGMP (Ru:G = 1:1) containing 100 mM $NaClO_4$ at 298 K.[39]

Arene	$t_{1/2}$ / h
tha	1.1
bip	2.0
dha	3.6
p-cym	7.1
bz	13

1.2.2.2.3 Chelating Ligand (YZ)

The chelating ligand, which increase the thermodynamic stability of the complex due to the chelate effect, showed significant effect on the reactivity of Ru(II) arene complexes. It was found that monodentate ligands on Ru(II) arene complexes are more labile than bidentate ligands, and Ru(II) arene complexes with monodentate ligands, like $[(\eta^6\text{-}p\text{-cym})Ru(CH_3CN)_2Cl]^+$ and $[(\eta^6\text{-}p\text{-cym})Ru(\text{isonicotinamide})_2Cl]^+$, are inactive against human ovarian A2780 cancer cells.[29] Ethylenediamine (en) is mostly used as the chelating ligand in Ru(II) arene anticancer complexes.

1.2.2.2.4 Leaving Group (X)

Hydrolysis of the Ru-X bond is believed to be correlated with the cytotoxicity of Ru(II) arene complexes because the aqua adduct $[(\eta^6\text{-arene})Ru(YZ)(H_2O)]^{(n+1)+}$ is the reactive species to biological molecules. The correlations between hydrolysis rates and cytotoxicity have been investigated for the Ru(II) complexes $[(\eta^6\text{-hmb})Ru(en)X]^+$, in which high activity is for complexes that aquate readily, e.g. X = halide, whereas inactivity for those that do not aquate, e.g. X = pyridine (see Figure

1.6).[31] An exception to this rule is the complex $[(\eta^6\text{-hmb})Ru(en)(SPh)]^+$, which is active against human ovarian A2780 cancer cells (IC_{50} = 23 μM) although it is relatively inert to hydrolysis.[31] It is proposed that it follows different mechanism of activation, in which oxidation of the thiolate may be involved (discussed in Chapter 6).

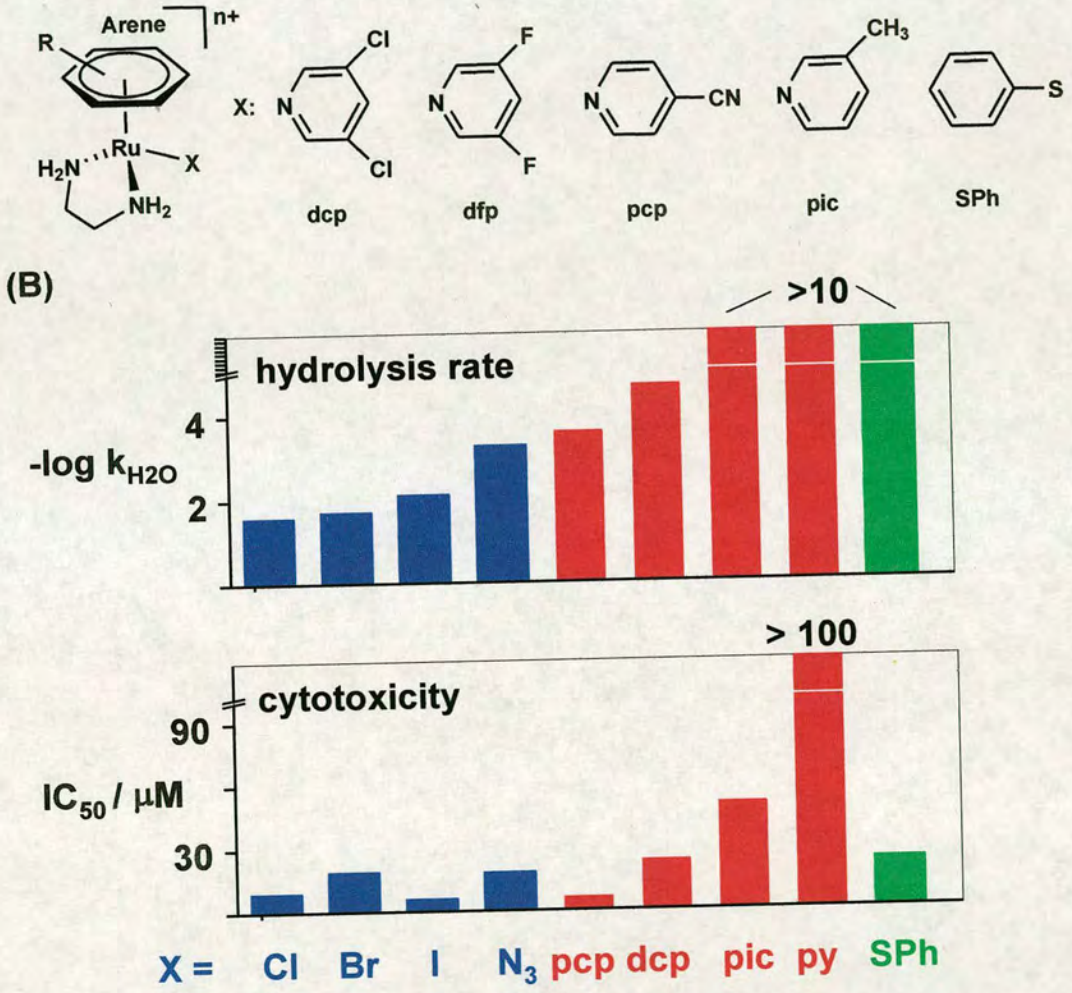

Figure 1.6 Correlation of hydrolysis with cytotoxicity. (A) Chemical structures of Ru(II) arene complexes with different leaving groups; (B) Hydrolysis rates and equilibrium percentage of total Ru as $[(\eta^6\text{-hmb})Ru(en)(H_2O)]^{2+}$ (top); cytotoxicity (IC_{50} values) for $[(\eta^6\text{-hmb})Ru(en)X]^+$ against human ovarian A2780 cancer cells (bottom). Figure reproduced from reference 31.

1.3 Glutathione

Glutathione (γ-L-Glu-L-Cys-Gly, abbreviated GSH) is a tripeptide composed of glutamate acid, cysteine and glycine (Figure 1.7(A)), which is a potentially polydentate ligand, and is widely used as a model system for the binding of metal ions by peptides and proteins. It is an abundant (millimolar) intracellular thiol responsible for the deactivation of heavier transition metal ions, including some platinum and ruthenium anticancer complexes.[40-41] Glutathione is present in several additional forms in cells, tissues and plasma, such as glutathione disulfide (GSSG; Figure 1.7(B)) which is one of the oxidation forms from GSH, sulfonates which are further oxidation products.[42]

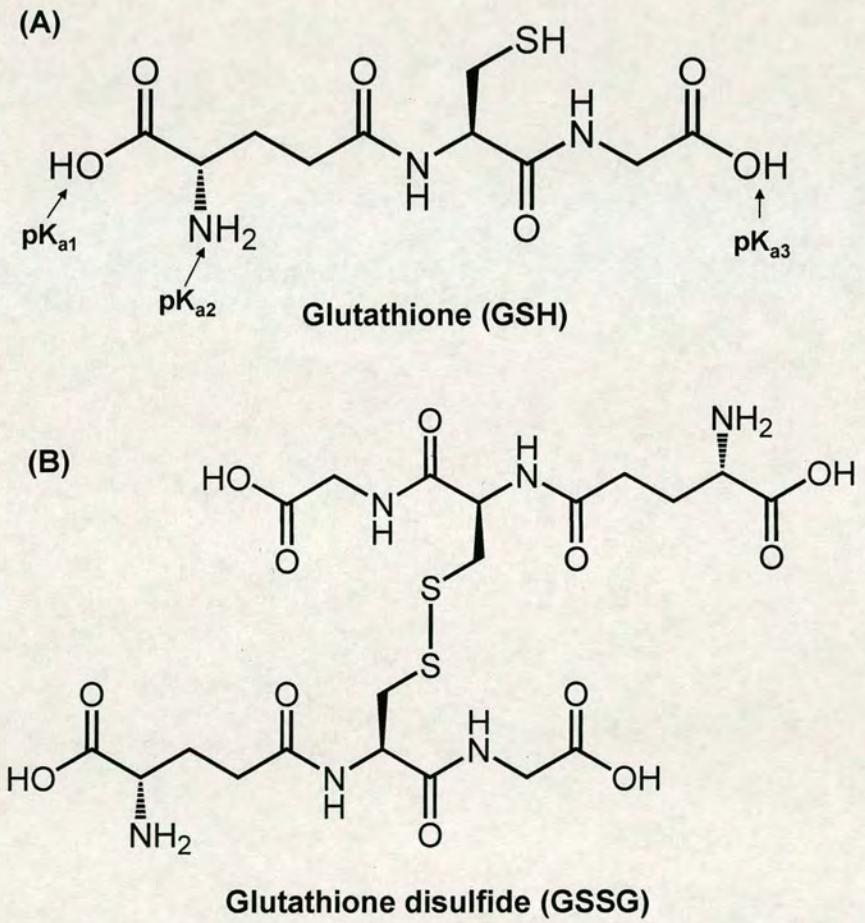

Figure 1.7 Chemical structures of GSH (A) and GSSG (B). $pK_{a1} = 2.19$, $pK_{a2} = 9.67$, $pK_{a3} = 2.34$.[43]

GSH is synthesized from L-glutamate, L-cysteine and glycine in two steps, catalyzed by γ-glutamyl-cysteine synthase and glutathione synthase, requiring two moles of ATP as shown in Scheme 1.2.[44]

Scheme 1.2 Synthesis of GSH in human body.

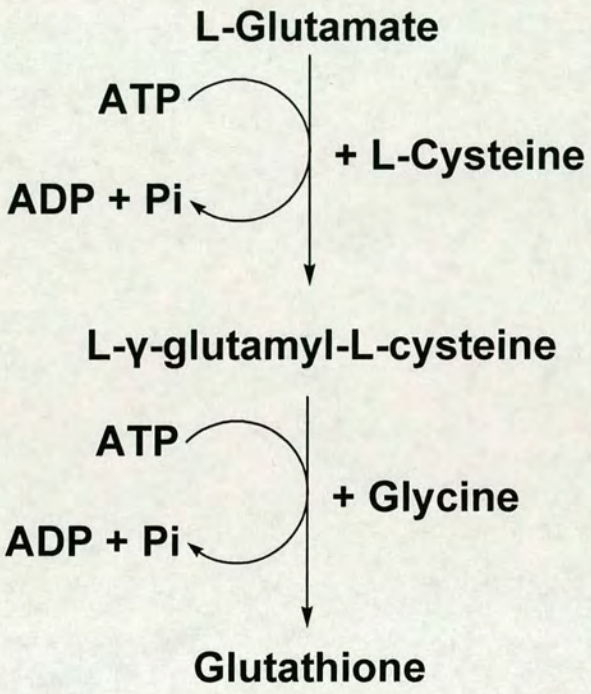

Glutathione has numerous important functions within cells. It serves as a reductant and is conjugated to drugs to make them more water soluble. It is also involved in amino acid transport across cell membranes (the γ-glutamyl cycle) and is a part of the peptidoleukotrienes, and serves as a cofactor for some enzymatic reactions and as an aid in the rearrangement of protein disulfide bonds.[42]

The role of GSH as a reductant is extremely important particularly in the highly oxidizing environment of the erythrocyte, in which the sulfhydryl of GSH can reduce peroxides forming during oxygen transport and the resulting oxidized form of GSH

consists of two molecules disulfide bonded together (GSSG, structure shown in Figure 1.7(B)).[42] The enzyme glutathione reductase utilizes NADPH as a cofactor to reduce GSSG back to two moles of GSH. Several mechanisms exist for the transport of amino acids across cell membranes. Many are symport or antiport mechanisms that couple amino acid transport to sodium transport. The γ-glutamyl cycle is an example of a group transfer mechanism of amino acid transport. Although this mechanism requires more energy input, it is rapid and has a high capacity. The cycle functions primarily in the kidney, particularly renal epithelial cells.[42] The enzyme γ-glutamyl transpeptidase is located in the cell membrane and shuttles GSH to the cell surface to interact with an amino acid. Reaction with an amino acid liberates cysteinylglycine and generates a γ-glutamyl-amino acid which is transported into the cell and hydrolyzed to release the amino acid.[42] Glutamate is released as 5-oxoproline and the cysteinylglycine is cleaved to its component amino acids. Regeneration of GSH requires an ATP-dependent conversion of 5-oxoproline to glutamate and then the 2 additional moles of ATP that are required during the normal generation of GSH.[42]

1.4 Thiols and Their Oxidation Adducts

Sulfur complexes are widely present in nature. Sulfur-containing substances play important biological roles.

1.4.1 Oxidation of Thiols

Thiol (RSH) is one of the most reactive functional groups in cells, and biologically, the most important reactions of thiols are their oxidations to disulfides and higher

sulphur oxides, and in all these reactions sulfenic acids (RSOH) are involved. The pathways are shown in Scheme 1.3.[45,46]

Scheme 1.3 Major pathways for thiol oxidation.

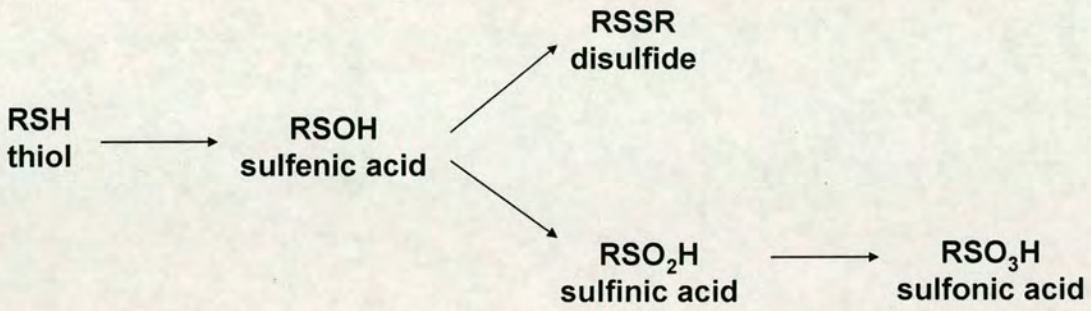

1.4.2 Sulfenic Acids

Sulfenic acids are transient intermediates during the oxidation of thiols with mild oxidants such as a stoichiometric quantity of hydrogen peroxide (H_2O_2). They are recognised to be important intermediates in many organic reactions such as hydrolysis of sulfenyl halides,[47,48] decomposition of alkyl sulfoxides and thiosulfinates,[49,50] autoxidation of thiols,[51] etc. Sulfenic acids were discovered in the 1940's and found to play an important role in reactions of extracts of *Allium* plants.[52] Three thiolato complexes $RS(O)CH_2CH(NH_2)COOH$ (R = methyl, propyl and 2-propenyl) were detected in *Allium sativum* L (garlic), and alliinase was induced to cleave the S-C bond, leading to the corresponding sulfenic acids RSOH which quickly condensed and gave the relatively stable thiosulfinic-S esters (thiosulfinates) RS(O)SR as shown in Scheme 1.4.[53]

Scheme 1.4 Formation of sulfenic acids in *Allium sativum* (garlic).

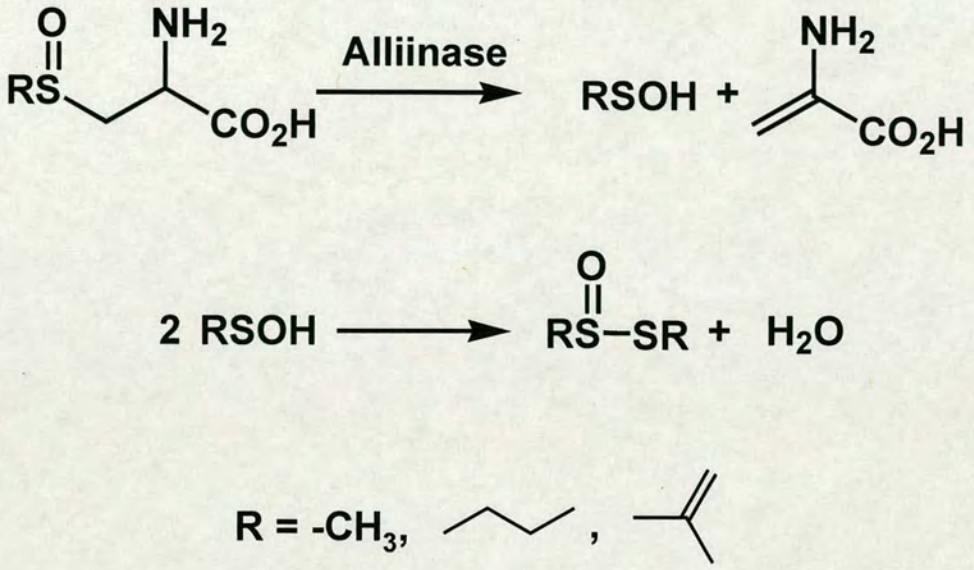

Sulfenic acids are generally very unstable and highly reactive. They can act as either nucleophile (binding to transition metals)[54-57] or an electrophile (attacked by another sulfenic acid)[53] under different reaction conditions. The main reason for their instability is the facile self-condensation reaction to form the corresponding thiosulfinates RS(O)SR as shown in Scheme 1.4.[53] Two possible tautomeric structures have been considered for sulfenic acids in Scheme 1.5.[58]

Scheme 1.5 Two tautomeric structures of sulfenic acids

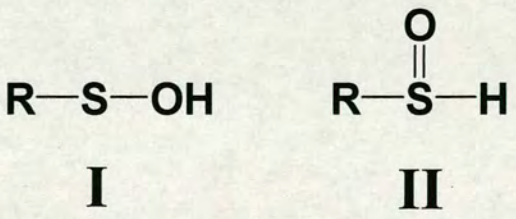

Sulfenic acids are generally thought to be stabilised either by steric inhibition or by formation of intramolecular hydrogen bonding between the sulfenic acid moiety and a suitable hydrogen bond acceptor.[59] The observation of hydrogen-bonded sulfenic acids in the reaction of sulfenic acid self-condensation,[60] and the intermolecular hydrogen bonding is believed to be particularly effective in lowering the potential energy or enthalpy of the reaction shown in Scheme 1.6.[59] However, Weigand et al. focused on stabilising anions of sulfenic acids by transition metal complexes to form sulfenates.[58] The first report of a metal-sulfenato complex was published by George et al., in which the iridium compound $IrCl_2[S(O)CH_3](CO)(PR_3)_2$ was prepared.[61] Then the controlled monooxidation of thiolates coordinated to cobalt(III) to Co-coordinated sulfenates was reported.[62,63] Transition metal fragments in lower oxidation states exhibit excellent π-donor ability, so the mesomeric structure **VI** shown in Scheme 1.7 has to be taken into account.[58]

Scheme 1.6 Formation of intermolecular hydrogen bonding in the conversion of sulfenic acids to thiosulfinates.[59]

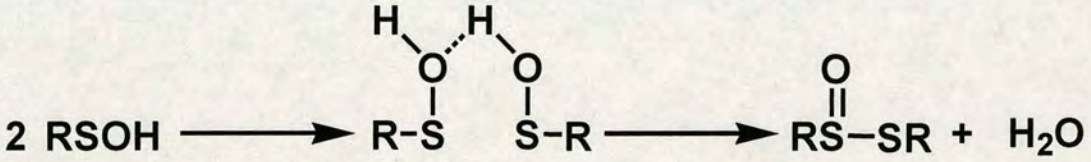

Scheme 1.7 Metal-coordinated sulfenate and its mesomeric structure.[58]

1.4.3 Cys-SOH in Proteins

In contrast, oxidation of cysteinyl side chains in proteins can be controlled to form cysteine-sulfenic acid (Cys-SOH) instead of forming a disulfide bond. The reactivity-control of Cys-SOH has been shown to yield stable active-site Cys-SOH derivatives of papain and glyceraldehydes-3-phophate dehydrogenase.[46] Cys-SOH stabilisation requires the absence of other sulfhydryl groups in the vicinity, furthermore, limited solvent access and association with apolar elements of protein structure should contribute to this stabilisation.[64] Although protein disulfides play an important role in the protein folding process, formation of protein disulfides can inactivate the activity of proteins due to the disappearance of the active-site Cys-SH in proteins. Therefore, oxidation of Cys-SH to Cys-SOH were used to protect the active-sites in proteins sometimes.[64] Recently, Cys-SOH has been found to be involved in redox catalysis,[65-67] redox regulation[68-70] (see Scheme 1.7) and redox signalling.[71] Also in the iron-containing nitrile hydratase (NHase), two Cys residues coordinated to the iron were found to be post-translationally modified to Cys-SOH and Cys-SO_2H,[72] and NHase was irreversibly inactivated by the oxidation of Cys-SOH to Cys-SO_2H.[73]

Scheme 1.7 Diverse roles for Cys-SOH in redox catalysis and redox regulation. R is H, FADH or alkyl; R_1SH is either GSH, DTT or another as-yet-unidentified thiol(s).[70]

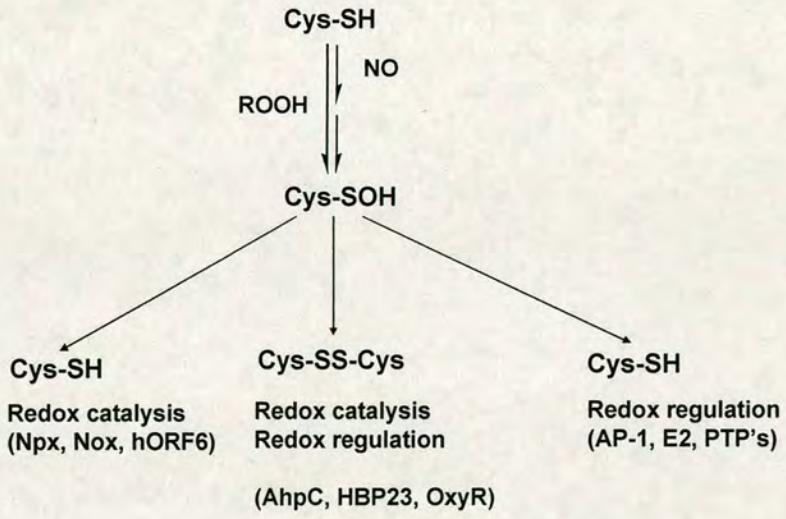

1.5 Aims

The overall aim of this thesis is to investigate the mechanisms of the cytotoxic action of ruthenium(II) arene complexes. As illustrated in section **1.2.1**, significant amounts of cisplatin are lost due to binding to S atoms, and some work in our group focusing on investigations of reactions of Ru(II) arene complexes with either cysteine, histidine, or 14-mer DNA oligonucleotides was carried out. This thesis is concerned with the competitive reactions of N-donor (G N7-DNA) and S-donor (GSH) ligands with Ru(II) arene anticancer complexes. More specific aims are shown as follows.

(1) Investigations of the reactions of $[(\eta^6\text{-bip})Ru(en)Cl]^+$ with GSH both in unbuffered water (pH ca. 3) and in phosphate buffer (pH 7).

(2) Studies of the mechanism for the competitive reaction of $[(\eta^6\text{-bip})Ru(en)Cl]^+$ with GSH and cGMP at pH 7.

(3) Investigation of possible reactions of $[(\eta^6\text{-bip})Ru(en)Cl]^+$ with thiol-containing protein glutathione S-transferase (GST) at ca. pH 7.

(4) Investigation of the competition between GSH and 14-mer DNA oligonucleotides for $[(\eta^6\text{-arene})Ru(en)Cl]^+$.

(5) Studies of the mechanism of reaction of the cytotoxic Ru(II) arene thiolate complexes $[(\eta^6\text{-hmb})Ru(en)(SR)]^+$.

1.6 References

[1] Aicheson, L. *A History of Metals* Interscience, New York, USA, **1960**.

[2] Merian E. *Metals and Their Compounds in the Environment: Occurrence, Analysis and Biological Relevance* VCH Verlagsgesellschaft mbH, Weinheim, Germany & VCH Publishers, Inc., New York, USA, **1991**.

[3] Bertini, I.; Messori, L.; Viezzoli, M. S. *Coord. Chem. Rev.* **1992**, *120*, 163-192.

[4] Guyton, A. C. *Textbook of Medical Physiology, Vol. Eighth Edition*, W. B. Saunders Company, Philadelphia, USA, **1991**.

[5] www.who.int

[6] www.deathreference.com/B1-Ce/Causes-of -Death.html

[7] Saxena, A. K.; Huber, F. *Coord. Chem. Rev.* **1989**, *95*, 109-123.

[8] Koepf-Maier, P.; Kopef, H. *Chem. Rev.* **1987**, *87*, 1137-1152.

[9] Sava, G.; Zorzet, S.; Giraldi, T.; Zassinovich, G. E. *J. Cancer Clin. Oncol.* **1984**, *20*, 841-847.

[10] Rosenberg, B.; VanCamp, L.; Trosko, J. E.; Mansour, V. H. *Nature* **1969**, *222*, 385-386.

[11] Rosenberg, B.; VanCamp, L.; Krigas, T. *Nature* **1965**, *205*, 698-699.

[12] Barnard, C. F. J. *Plat. Met. Rev.* **1989**, *33*, 162-167.

[13] Jennerwein, M.; Andrews, P. A. *Drug Metab. Dispos.* **1995**, *23*, 178-184.

[14] Jamieson, E. R.; Lippard, S. J. *Chem. Rev.* **1999**, *99*, 2467-2498.

[15] Guo, Z.; Sadler, P. J. *Adv. Inorg. Chem.* **2000**, *49*, 183-306.

[16] Lempers, E. L. M.; Reedijk, J. *Adv. Inorg. Chem.* **1991**, *37*, 175-217.

[17] Corden, B. J. *Inorg. Chim. Acta* **1987**, *137*, 125-130.

[18] Weiss, R. B.; Christian, M. C. *Drugs* **1993**, *46*, 360-377.

[19] Wong, E.; Giandomenico, C. M. *Chem. Rev.* **1999**, *99*, 2451-2466.

[20] Galanski, M.; Jakupec, M. A.; Keppler, B. K. *Curr. Med. Chem.* **2005**, *12*, 2075-2094.

[21] Sava, G.; Bergamo, A. *Int. J. Oncol.* **2000**, *17*, 353-365.

[22] Clarke, M. J.; Zhu, F.; Frasca, D. R. *Chem. Rev.* **1999**, *99*, 2511-2333.

[23] Clarke, M. J. *Coord. Chem. Rev.* **2002**, *232*, 69-93.

[24] Durig, J. R.; Danneman, J.; Behnke, W. D.; Mercer, E. E. *Chem. Biol. Interact.* **1976**, *13*, 287-294.

[25] Rademaker-Lakhai, J. M.; Van Den Bongard, D.; Pluim, D.; Beijnen, J. H.; Schellens, M. *Clin. Cancer Res.* **2004**, *10*, 3717-3727.

[26] Galanski, M.; Arion, V. B.; Jakupec, M. A.; Keppler, B. K. *Curr. Pharm. Design* **2003**, *9*, 2078-2089.

[27] Morris, R. E.; Aird, R. E.; Murdoch, P. D. S.; Chen, H.; Cummings, J.; Hughes, N. D.; Parsons, S.; Parkin, A.; Boyd, G.; Jodrell, D. I.; Sadler, P. J. *J. Med. Chem.* **2001**, *44*, 3616-3621.

[28] Habtemariam, A.; Melchart, M.; Fernandez, R.; Parsons, S.; Oswald, I. D. H.; Parkin, A.; Fabbiani, F. P. A.; Davidson, J. E.; Dawson, A.; Aird, R. E.; Jodrell, D. I.; Sadler, P. J. *J. Med. Chem.* **2006**, *49*, 6858-6868.

[29] Sheldrick, W. S.; Heeb, S. *Inorg. Chim. Acta* **1990**, *168*, 93-100.

[30] Allardyce, C. S.; Dyson, P. J.; Ellis, D. J.; Heath, S. L. *Chem. Commun.* **2001**, 1396-1397.

[31] Wang, F.; Habtemarian, A.; Van Der Geer, P. L.; Fernandez, R.; Melchart, M.; Deeth, R. J.; Aird, R.; Guichard, S.; Fabbiani, F. P. A.; Lozano-Casal, P.;

Oswald, I. D. H.; Jodrell, D. I.; Parsons, S.; Sadler, P. J. *Proc. Nat. Acad. Sci. USA* **2005**, *102*, 18269-18274.

[32] Wang, F.; Chen, H.; Parsons, S.; Oswald, I. D. H.; Davidson, J. E.; Sadler, P. J. *Chem. Eur. J.* **2003**, *9*, 5810-5820.

[33] Novakova, O.; Chen, H.; Vrana, O.; Rodger, A.; Sadler, P. J.; Brabec, V. *Biochemistry* **2003**, *42*, 11544-11554.

[34] Liu, H. K.; Wang, F.; Parkinson, J. A.; Bella, J.; Sadler, P. J. *Chem. Eur. J.* **2006**, *12*, 6151-6165.

[35] Aird, R. E.; Cummings, J.; Ritchie, A. A.; Muir, M.; Morris, R. E.; Chen, M.; Sadler, P. J.; Jodrell, D. I. *Br. J. Cancer* **2002**, *86*, 1652-1657.

[36] Novakova, O.; Kasparkova, J.; Bursova, V.; Hofr, C.; Vojtiskova, M.; Chen, H.; Sadler, P. J.; Brabec, V. *Chem. Biol.* **2005**, *12*, 121-129.

[37] Chen, H.; Parkinson, J. A.; Novakova, O.; Bella, J.; Wang, F.; Dawson, A.; Gould, R.; Parsons, S.; Brabec, V.; Sadler, P. J. *Proc. Nat. Acad. Sci. USA* **2003**, *100*, 14623-14628.

[38] Chen, H.; Parkinson, J. A.; Parsons, S.; Coxall, R. A.; Gould, R. O.; Sadler, P. J. *J. Am. Chem. Soc.* **2002**, *124*, 3064-3082.

[39] Chen, H.; Parkinson, J. A.; Morris, R. E.; Sadler, P. J. *J. Am. Chem. Soc.* **2003**, *125*, 173-186.

[40] Reedijk, J. *Chem. Rev.* **1999**, *99*, 2499-2510.

[41] Frasca, D. R.; Clarke, M. J. *J. Am. Chem. Soc.* **1999**, *121*, 8523-8532.

[42] Sies, H. *Free Radic. Biol. Med.* **1999**, *27*, 916-921.

[43] Tang, S. S.; Chang, G. G. *J. Biochem.* **1995**, *309*, 347-353.

[44] Griffith, O. W. *Free Radic. Biol. Med.* **1999**, *27*, 922-925.

[45] Kratochwil, N. A.; Ivanov, A. I.; Patriarca, M.; Parkinson, J. A.; Gouldsworthy, A. M.; Murdoch, P. del S.; Sadler, P. J. *J. Am. Chem. Soc.* **1999**, *121*, 8193-8203.

[46] Allison, W. S. *Acc. Chem. Res.* **1976**, *9*, 293-299.

[47] Vinkler, E.; Klivenyi, F. *Int. J. Sulfur Chem.* **1973**, *8*, 111-117.

[48] Vinkler, E.; Klivenyi, F. *Acta Chim. Acad. Sci. Hung.* **1960**, *22*, 345-350.

[49] Shelton J. R.; Davis, K. E. *Int. J. Sulfur Chem.* **1973**, 3, 205-216.

[50] Shelton, J. R.; Davis, K. E. *J. Am. Chem. Soc.* **1967**, *89*, 718-719.

[51] Berger, H. *Recl. Trav. Chim. Pays-Bas* **1963**, *82*, 773-789.

[52] Stoll, A.; Seebeck, E. *Helv. Chim. Acta* **1948**, *31*, 189-210.

[53] Block, E.; Ahmad, S.; Catalfamo, J. L.; Jain, M. K.; Apitz-Castro, R. *J. Am. Chem. Soc.* **1986**, *108*, 7045-7055.

[54] Adzamli, I. K.; Libson, K.; Lydon, J. D.; Elder, R. C.; Deutsch, E. *Inorg. Chem.* **1979**, *18*, 303-311.

[55] Buonomo, R. M.; Font, I.; Maguire, M. J.; Reibenspies, J. H.; Tuntulani, T.; Darensbourg, M. Y. *J. Am. Chem. Soc.* **1995**, *117*, 963-973.

[56] Grapperhaus, C.; Darensbourg, M. Y. *Acc. Chem. Res.* **1998**, *31*, 451-459.

[57] Aranyosiova, M.; Vollarova, O.; Benko, J.; Cernusak, I. *Int. J. Quan. Chem.* **2006**, *106*, 747-763.

[58] Weigand, W.; Wunsch, R. *Chem. Ber.* **1996**, *129*, 1409-1419.

[59] Davis, F. A.; Jenkins, L. A.; Billmers, R. L. *J. Org. Chem.* **1986**, *51*, 1033-1040.

[60] Davis, F. A.; Billmers, R. L. *J. Org. Chem.* **1985**, *50*, 2593-2595.

[61] George, T. A.; Watkins Jr., D. D. *Inorg. Chem.* **1973**, *12*, 398-402.

[62] Lange, B. A.; Libson, K.; Deutsch, E.; Elder, R. C. *Inorg. Chem.* **1976**, *15*, 2985-2989.

[63] Jackson, W. G.; Sargeson, A. M.; Whimp, P. O. *J. Chem. Soc., Chem. Commun.* **1916**, 934-936.

[64] Claiborne, A.; Miller, H.; Parsonage, D.; Ross, R. P. *FASEB J.* **1993**, *15*, 1483-1490.

[65] Poole, L. B.; Claiborne, A. *Biol. Chem.* **1989**, *264*, 12330-12338.

[66] Parsonage, D.; Claiborne, A. *Biochemistry* **1995**, *34*, 435-441.

[67] Mallett, T. C.; Parsonage, D.; Claiborne A. *Biochemistry* **1999**, *38*, 3000-3011.

[68] Abate, C.; Patel, L.; Rauscher III, F. J.; Curran, T. *Science* **1990**, *249*, 1157-1161.

[69] McBride, A. A.; Klausner, R. D.; Howley, P. M. *Proc. Natl. Acad. Sci. USA* **1992**, *89*, 7531-7535.

[70] Claiborne, A.; Yeh, J. I.; Mallett, T. C.; Luba, J.; Crane III, E. J.; Charrier, V.; Parsonage, D. *Biochemistry* **1999**, *38*, 15407-15416.

[71] Poole, L. B.; Karplus, P. A.; Claiborne, A. *Annu. Rev. Pharmacol. Toxicol.* **2004**, *44*, 325-347.

[72] Nagashima, S.; Nakasako, M.; Dohmae, N.; Tsujimura, M.; Takio, K.; Odaka, M.; Yohda, M.; Kamiya, N.; Endo, I. *Nat. Strucl. Bio.* **1998**, *5*, 347-351.

[73] Tsujimura, M.; Odaka, M.; Nakayama, H.; Dohmae, N.; Koshino, H.; Asami, T.; Hoshino, M.; Takio, K.; Yoshida, S.; Maeda, M.; Endo, I. *J. Am. Chem. Soc.* **2003**, *125*, 11532-11538.

Chapter 2

Experimental Section

This Chapter involves the main experimental techniques used in the work shown in this thesis. More specific methods relating to particular experiments are outlined in the appropriate chapters.

2.1 Ultraviolet-visible (UV-Vis) Spectroscopy

Ultraviolet and visible absorption spectra were recorded on UV-Vis spectrophotometer (Perkin Elmer Company) which is connected with a temperature controller (in the range of 200-600 nm, using a 10 mm path length quartz cuvette at 310 K. Spectra were processed with WinUV software.

2.2 High Performance Liquid Chromatography (HPLC)[1,2]

A Hewlett-Packard series 1100 quaternary pump and a Rheodyne sample injector with 100 μL and 2.0-mL loops, a HP 1100 series UV-vis detector and HP 1100 series Chemstation with a HP enhanced integrator were used.

2.2.1 Reverse Phase HPLC (RP-HPLC)

RP-HPLC is the only type of HPLC used in this thesis. RP-HPLC consists of a non-polar stationary phase (a spherical, rigid, macroporous polystyrene/divinylbenzene polymer packed in the PLPR-s column used in my work), and a moderately polar mobile phase (specific combinations of water and acetonitrile in this thesis). Therefore, the retention time is longer for non-polar molecules and shorter for polar

ones, which is also increased by the addition of polar mobile phase and decrease by the addition of more hydrophobic mobile phase.

RP-HPLC separates components on the basis of principle of hydrophobic interactions. The binding strength of the component to the stationary phase is proportional to the contact surface area around the non-polar segment of the component molecule upon association with the ligand in the aqueous eluent. The retention time can be shortened by increasing less-polar solvent like acetonetrile into the mobile phase to reduce the surface tension of water. Also structural properties of the component molecule are related to its retention characteristics. Generally, the retention time for a molecule with a larger hydrophobic surface area, such as C-H, C-C and generally non-polar atomic bonds (S-S), is increased due to the increase of the molecule's non-polar surface area which is non-interacting with water. In contrast, polar groups, such as –OH, $-NH_2$, COO– and $-NH_3^+$, result in shorter retention times as they are well integrated into water.

2.3 ElectroSpray Ionisation Mass Spectrometry (ESI-MS)

Positive-ion electrospray ionization mass spectra were obtained with a Platform II mass spectrometer (Micromass, Manchester, U.K.). A Waters 2690 HPLC system was interfaced with the mass spectrometer, using the column and gradients as described in each main chapter for the analytical HPLC separation, with a flow rate of 1.0 mL min^{-1} and a splitting ratio of 1/5. The spray voltage was 3.50-3.68 kV, and the cone voltage, 20 V. The capillary temperature was 410 K with a 450 L h^{-1} flow of nitrogen drying gas. The quadrupole analyzer, operated at a background pressure of 2

$\times 10^{-5}$ Torr, was scanned at 700-900 Da s^{-1}. Data were collected and analyzed on a Mass Lynx (ver. 3.5) Windows NT PC data system using the Max Ent Electrospray software algorithm and calibrated versus an NaI calibration file. The mass accuracy of all measurements was within 0.1 *m/z* unit.

2.4 Nuclear Magnetic Resonance (NMR) Spectroscopy[1,3,4,5]

NMR data were acquired using Bruker Avance 600 MHz NMR spectrometers equipped with a triple resonance TXI (^{1}H, ^{13}C, ^{15}N) *z*-gradient cryo-probe or room temperature TXI (^{1}H, ^{13}C, ^{15}N) triple-axis (*x,y,z*) gradient probehead.

One-dimensional (1D) ^{1}H NMR data were acquired with eight transients into 32k data points over a frequency width of 9.0 kHz using either water presaturation or a double-pulsed field gradient spin-echo routine (DPFGSE) to eliminate the solvent resonance.[6]

Two-dimensional (2D) [^{1}H,^{1}H] DQFCOSY, TOCSY, and NOESY NMR data were acquired over a frequency width of 5.4 kHz in both F_2 and F_1 into 2k complex data points in F_2 (acquisition time = 190 ms) with two transients for each of 2 × 512 t_1 increments in the QF (COSY) or the States -TPPI (TOCSY and NOESY) mode. A relaxation delay of 1.4 s between transients was used for all experiments. 2D NOESY NMR data were acquired with mixing times of 100 and 400 ms, and 2D TOCSY data with a spin-lock time of 60 ms. Water suppression for COSY was achieved using water presaturation. For TOCSY and NOESY experiments, the water resonance was suppressed by means of a DPFGSE routine after the final read pulse. Data were processed using standard apodizing functions prior to Fourier transformation.

The time courses of the reactions containing ^{15}N-labelled Ru complexes were followed by NMR using a Bruker Avance NMR spectrometer operating at 800 MHz. All data were acquired on samples equilibrated at 310 K. A triple resonance (TBI: ^{1}H, ^{13}C,X) probehead equipped with a triple-axis (x,y,z) gradient coil was used for data accumulation.

1D ^{1}H NMR spectra were acquired without ^{15}N-decoupling over an 8 kHz frequency width for eight transients into 16k data points (acquisition time = 1.022 s) with a relaxation delay of 1.5 s between transients. ^{1}H pulse calibration was carried out using a presaturation pulse sequence (zgpr). Subsequently, ^{1}H NMR data were acquired either using a DPFGSE routine or its modified form in which composite inversion pulses were applied.[7] Gradients were used to select for ^{1}H-^{15}N coherences and were simultaneously responsible for eliminating the water resonance.

2D [^{1}H, ^{15}N] HSQC NMR data were acquired, with ^{15}N-decoupling during the acquisition period, over an F_2 frequency width of 8 kHz (acquisition time = 128 ms). Multiples of eight transients were accumulated for each of 128 t_1 increments over an F_1 frequency width of 80 ppm centered at -30 ppm relative to $^{15}NH_4Cl$ (reference, 0 ppm). Phase-sensitive data were acquired in a sensitivity-improved manner using an echo-antiecho acquisition mode.[8]

.

2.4.1 Water Suppression

Most of the experiments in this thesis were performed in aqueous solution (90% D_2O/10% H_2O), in which a large HOD peak is present and can be suppressed using either presaturation or 1D Double Pulse Field Gradient Spin Echo (DPFGSE; also called Shaka water suppression). Presaturation involves saturating the required signal

(in this case residual water) by irradiating the frequency of the water signal in between pulse sequences, however, this saturation is also transferred to the functional groups such as OH and NH protons which readily exchange with the protons of water. DPFGSE uses pulse field gradient spin echoes in which the refocusing pulse is the sequence soft $\pi(x)$-hard $\pi(-x)$.[6]

2.4.2 Two Dimensional Spectroscopy

2.4.2.1 COrrelation and TOtal Correlation SpectroscopY (COSY and TOCSY)

COSY is a two-dimensional homonuclear (like [^{1}H,^{1}H])-correlation NMR spectroscopy, in which the presence of an off-diagonal (or cross) peak normally indicates that the protons giving the connected resonances on the diagonal are geminally or vicinally coupled.

TOCSY is a similar technique as COSY, but in TOCSY, cross peaks are detected between all *J*-coupled members within a spin system. Magnetization is transferred successively over up to 5 or 6 bonds as long as successive protons are coupled. The number of transfer steps can be adjusted by altering the mixing time and can be tuned from 1-2 steps up to 5-7 steps.

2.4.2.2 Nuclear Overhauser Enhancement SpectroscopY (NOESY)

When the cross peaks derive from magnetization transfer through dipolar relaxation, the 2D experiment is termed NOESY. In the case of the NOESY experiment, valuable information is provided about the distance (or space) between various protons within a molecule. The NOESY experiment can provide both structural and

conformational information, and in practice, cross peaks are unobservable when the proton-proton distance exceeds about 5 Å.

2.4.2.3 2D [^{1}H, ^{15}N] Heteronuclear Single Quantum Correlation (HSQC) Spectroscopy

The HSQC experiment generates single quantum ^{15}N coherence via an INEPT (Insensitive Nuclei Enhanced by Polarization Transfer), which evolves and then is transferred back to the proton frequency by a second INEPT sequence, this time in reverse. The HSQC spectrum is 2D with one axis for ^{1}H and other for a heteronuclear (^{15}N in this thesis), which does not contain ^{1}H-^{1}H coupling in the ^{15}N dimension. A heteronucleus in NMR terminology is a nucleus other than proton. And the spectrum contains a peak for each unique proton attached to the ^{15}N being considered. If the chemical shift of a specific proton is known, the chemical shift of the coupled ^{15}N can thus be determined. The HSQC experiment is also useful for detecting interactions with ligands. By comparing the HSQC of the free ^{15}N-labelled Ru(II) arene compound, it is possible to find the changes in the chemical shifts of the peaks, which occur due to the binding of Ru(II) complex with other ligands.

2.5 Inductively Coupled Plasma Optical Emission Spectroscopy (ICP-OES)[1,2,9]

ICP-OES is a kind of emission spectroscopy in which plasma is used to produce excited atoms that emit electromagnetic radiation at a wavelength characteristic of a given element, and it is a very sensitive technique. The intensity of the emission represents the concentration of the element involved in the analyte. The principle of the technique is to excite the atoms into the higher-energy level, and atomic emission occurs when the atoms return to the ground state with the release of the additional energy, and the energy is detected as emission radiation which is characteristic to the

element emitting. This technique is used to determine the Ru or P concentrations. The analyte, if solid, is normally dissolved and then mixed with water before being fed into the plasma. Atoms in the plasma emit light (photons) with characteristic wavelengths for each element, and the light is recorded by one or more optical spectrometers and after calibrated against standards, it provides a quantitative analysis of the original analyte.

2.6 pH Measurements

pH measurements were made using a Corning 240 pH meter equipped with an Aldrich micro-combination electrode calibrated with Aldrich standard buffer solutions of pH 4, 7, and 10. For NMR samples prepared in 10% D_2O/90% H_2O, no correction has been applied for the effect of deuterium on the glass electrode and the meter reading was denoted as pH^*.

2.7 Determination of Extinction Coefficients

HPLC fractions were collected from their corresponding reactions. After lyophilization, the residue from each fraction was dissolved in 5 mL deionized water for Ru determination by ICP-OES, using a Perkin-Elmer Optima 5300 DV Optical Emission Spectrometer equipped with an AS-93plus autosampler and WinLab32 for ICP program (version 3.0.0.0103). The apparent extinction coefficient at 254 nm (ε'_{254}) for each species was calculated using eq 1.

$$\varepsilon'_{254} = [\text{peak area}]_{254}/[\text{Ru}]\ (\mu\text{mol}) \qquad (1)$$

The relative extinction coefficient ε^{R}_{254} for each species was calculated from eq 2:

$$\varepsilon^{R}_{254} = [\varepsilon'_{254}]_x/[\varepsilon'_{254}] \qquad (2)$$

where $[\varepsilon'_{254}]_x$ and $[\varepsilon'_{254}]$ represent the extinction coefficients of species *x* and Ru complex $[(\eta^6\text{-bip})Ru(en)Cl][PF_6]$(**1**; bip = biphenyl) or $[(\eta^6\text{-hmb})Ru(en)(SPh)]PF_6$ (**23**; hmb = hexamethylbenzene), respectively.

2.8 References

[1] Skoog, D. A.; Leary, J. J. *Principles of Instrumental Analysis*, Fourth ed., Saunders College Publishing, Florida, **1992**.

[2] Rouessac, F. *Chemical Analysis – Modern Instrumental Methods and Techniques*, English Ed ed., New York: Wiley, Chichester, **2000**.

[3] Harwood, L. M.; Claridge, T. D. W. *Introduction to Organic Spectroscopy*, Oxford University Press Inc, New York, **1997**.

[4] Hore, P. J. *Nuclear Magnetic Resonance*, Oxford Univeristy Press Inc, New York, **2001**.

[5] Lambert, J. B.; Mazzola, E. P. *Nuclear Magnetic Resonance Spectroscopy*: *An Introduction to Principles, Applications, and Experimental Methods* Prentice-Hall, Inc, New Jersey, **2003**.

[6] Hwang, T. L.; Shaka, A. J. *J. Magn. Reson.* **1995**, *Series A 112*, 275-279.

[7] Liu, M.; Mao, X.; Ye, C.; Huang, H.; Nicholson, J. K.; Lindon, J. C. *J. Magn. Reson.* **1998**, *132*, 125-129.

[8] (a) Palmer, A. G.; Cavanagh, J.; Wright, P. E.; Rance, M. *J. Magn. Reson.* **1991**, *93*, 151-170. (b) Kay, L. E.; Keifer, P.; Saarinen, T. *J. Am. Chem. Soc.* **1992**, *114*, 10663-10665. (c) Schleucher, J.; Schwendinger, M.; Sattler, M.; Schmidt, P.; Schedletzky, O.; Glaser, S. J.; Sørensen, O. W.; Griesinger, C. *J. Biomol. NMR* **1994**, *4*, 301-306.

[9] Harvey, D. *Modern Analytical Chemistry*, London: McGraw-Hill, Boston, **2000**.

Chapter 3

Reactions of Ruthenium(II) Arene Anticancer Complex $[(\eta^6\text{-bip})Ru(en)Cl]PF_6$ with Glutathione or Protein

3.1 Introduction

Several ruthenium(III) am(m)ine complexes such as *cis*-$[RuCl_2(NH_3)_4]Cl$ and Na[*trans*-$Ru(Im)_2Cl_4$] exhibit anticancer activity, and are thought to be activated by reduction (to Ru^{II}) in vivo which facilitates DNA binding.[1] Recently it has been shown that members of the family of Ru^{II} arene complexes $[(\eta^6\text{-arene})Ru(YZ)(X)][PF_6]$, where X is a halide and YZ is a chelating diamine, in which the presence of the arene greatly stabilizes Ru^{II} compared to Ru^{III},[2] are cytotoxic to cancer cells including cisplatin-resistant cell lines.[3] For chloro (X) ethylenediamine (YZ; en) complexes, the cytotoxicity increases with the size of coordinated arene in the order: benzene < *p*-cymene < biphenyl < dihydroanthrancene < tetrahydroanthrancene. The activity of several of the complexes against human ovarian cancer cell line A2780 is at least comparable to that of carboplatin, and some approach that of cisplatin. Activity has also been demonstrated against human xenographs in vivo.[3a]

Platinum(II) has a high affinity for sulfur-containing biological molecules.[4] Although we have demonstrated that both cysteine and methionine can form S-bound adducts with $[(\eta^6\text{-bip})Ru(en)Cl][PF_6]$(**1**; bip = biphenyl),[5] the reaction of **1** and the tripeptide glutathione (γ-L-Glu-L-Cys-Gly; GSH), an abundant (millimolar) intracellular thiol responsible for the detoxification of heavier transition metal ions, including some platinum and ruthenium anticancer complexes,[1a,6] is investigated for the first time.

As a member of the second transition series, ruthenium has seven isotopes, making the mass isotopic pattern of ion peaks of ruthenium-containing compounds characteric, yet complicated. Mass spectra obtained using electrospray ionisation mass spectrometry

(ESI-MS) with quadrupole analyser allow unambiguous assignment of singly-charged ion peaks of mono-nuclear ruthenium arene complexes as well as their adducts with amino acids, peptides and DNA[5,7-10] However, low resolution Q-ESI-MS cannot identify two multi-nuclear ruthenium cluster arising from the reaction of the ruthenium arene anticancer complex [(η^6-bip)Ru(en)Cl][PF_6] (**1**; bip=biphenyl) with the tripeptide glutathione in aqueous solution.[7]

Glutathione transferases (GSTs) are a super-family of multi-functional isoenzymes involved in the detoxication of the cell against toxic and carcinogenic compounds, cellular mechanism of drug resistance, biosynthesis of leukotrienes, and intracellular binding and transport of hydrophobic ligands.[11] A well known function of GSTs is to promote the conjugation of the sulphur atom of glutathione to an electrophilic centre of endogenous and exogenous toxic compounds, thereby increasing their solubility and excretion.[11] The GSTs are potential drug targets in cancer therapy, where resistance to chemotherapeutic drugs has been directly correlated with the overexpression of GSTs in tumor cells, and parastic diseases such as malaria and schistosomiasis.[12] Cytosolic GSTs are dimeric, and two GST isoenzymes, of 26 and 28 kDa, are found in *Schistosoma japonicum*.[13] The X-ray crystal structure of the 26 kDa GST (called 26-kDa GST) from *S. japonicum*[13] which was used for the work in this Chapter is shown in Figure 3.1, in which four free thiol groups are present.

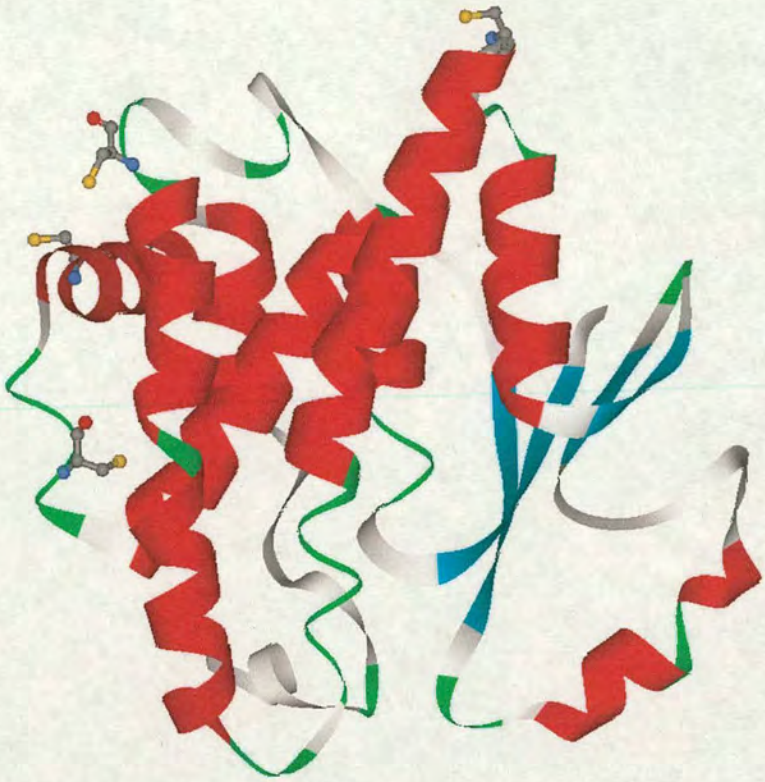

Figure 3.1 Crystal structure of Sj26GST monomer (PDB ID: 1M99).[13] Four cysteines with free thiol groups (Cys85, Cys138, Cys169 and Cys178) are labelled: yellow ball is S atom; red is O atom; purple is N atom and grey is C atom.

In this Chapter, the work is focused on reactions of the Ru^{II} anticancer complex [(η^6-bip)Ru(en)Cl][PF_6](**1**) with GSH. In particular, reactions under physiologically relevant conditions: micromolar Ru concentrations, pH 7, and millimolar GSH concentrations, were studied. Surprisingly S-bound glutathione was found to be susceptible to oxidation, and reactions carried out in water without buffering followed a different course. The findings suggest that novel redox reaction pathways could contribute to the biological activity of organometallic Ru^{II} arene complexes. And high resolution Fourier transform ion cyclotron mass spectrometry (nanoLC-FT-ICR-MS) was applied to identify the clusters separated by nanoscale liquid chromatography as the dinuclear complex {[(η^6-

bip)Ru(0)$(GSO_2)_2]_2\}^{8-}$ and tetranuclear complex $\{[(\eta^6$-bip)Ru(II)$(GSO_2)]_2[(\eta^6$-bip)Ru(I)$(GSO_2)]_2\}^{2-}$ containing glutathione sulfenate and sulfinate ligands. Use of $^{18}OH_2$ showed that the oxygen in the oxidized glutathione ligands arises from water. The reaction of **1** with GST at pH 8 was analyzed, and gave rise to a di-ruthenated GST adduct $\{[(\eta^6$-bip)Ru(en)$]_2$(GST)$\}^{2+}$.

3.2 Experimental

3.2.1 Materials

$[(\eta^6$-bip)RuCl(en)$][PF_6]$(**1**) and ^{15}N-labeled **1** (^{15}N-**1**) were synthesized by Haimei Chen as described elsewhere.[3b,14] Glutathione (GSH, reduced), sodium chloride, disodium hydrogen phosphate, 5, 5'-dithio-bis-(2-nitrobenzoic acid) (3-carboxy-4-nitrophenyl disulfide; DTNB), and Chelex resin (used for removal of impurity ions from phosphates) were purchased from Sigma; sodium dihydrogen phosphate and the ruthenium standard for atomic spectrometry (1003 μgRu/mL^{-1}) from Aldrich; sodium hydroxide and sodium chloride from Fisher; and trifluoroacetic acid (TFAH) from Acros. ^{18}O-labled water (95% $H_2{}^{18}O$) from Cambridge Isotope Laboratories. Untagged glutathione s-transferase (GST) in Tris buffer (pH 8) was synthesized and purified by Ms. Ann Marie Reid described elsewhere.[15]

3.2.2 Methods

3.2.2.1 High Performance Liquid Chromatography (HPLC)

The instrument was outlined in Chapter **2.2**. For analytical work, HPLC separations were carried out on a PLRP-S reversed-phase column (250 mm × 4.6 mm, 100 Å, 5 μm, Polymer Labs) with detection at 254 nm. And semipreparative work on a PLRP-S reversed-phase column (250 mm × 7.5 mm, 100 Å, 8 μm, Polymer Labs). Mobile phase A: water (for HPLC application, Fisher Chemicals) containing 0.1% TFAH; mobile phase B: acetonitrile (for HPLC application, Fisher Chemicals) containing 0.1% TFAH. The flow rate was 1.0 mL min^{-1}. The gradient (solvent B) was as follows: 2% to 28% within 20 min, 80% from 21 to 24 min, reset to 2% from 26 to 30 min.

3.2.2.2 Nanoscale Liquid Chromatography Fourier Transform Ion Cyclotron Mass Spectrometry

All the nano-LC-FT-ICR-MS experiments were operated by Mr. Stefan Weidt. Positive-ion electrospray ionization mass spectra were obtained with a Bruker APEX III ESI-FT-ICR mass spectrometer (Bruker Daltonics, USA) equiped with an inhouse modified heated metal transfer capillary held at a temperature of 423 K and a potential of 50V. A UltiMate 3000 series system (Diones, UK) with nanoflow splitter was coupled to the mass spectrometer using an TriVersa™ NanoMate® (Advion, USA) with spray voltage set to 1.7 kV. Mobile phase A: water (for LC-MS application, Fisher Chemicals) containing 2% CH_3CN and 0.1% TFAH; mobile phase B: acetonitrile (for LC-MS application, Fisher Chemicals) containing 20% water and 0.1% TFAH. The sample was trapped and washed for 3 min at 30 µL min^{-1} on a µ-Precolumn™ (300 µm × 5 mm, 5 µm, 100Å). The sample was eluted onto an analytical PepMap™100 column (75 µm × 15 cm, 3 µm, 100Å) held in a column-oven at 303 K. The flow rate was 300 nL min^{-1},

and gradient (solvent B) was as follows: 0% to 30% until 23 min, 30% to 100% from 23 to 24 min, 100% from 24 to 27 min, 100% to 0% from 27 to 29 min and reset to 0% until 30 min. All spectra were acquired using XMass 7.02 (Bruker Daltonics) with 512 k datapoints in the range 90 to 3000 m/z. Bruker Daltonics Data Analysis software was used for analysis and postprocessing.

3.2.2.3 Nuclear Magnetic Resonance (NMR) Spectroscopy

For HPLC-isolated glutathione products, NMR data were acquired at a temperature of 298 K. The methods were described in Chapter **2.4**.

All NMR data were processed using Xwin-nmr (version 3.5, Bruker Biospin. Ltd.).

3.2.3 Preparation of Samples

3.2.3.1 UV-Vis

The method was described in Chapter **2.1**. The UV-Vis spectra of reaction mixtures of **1** and GST at various molar ratios in Tris buffer (pH 8) at 310 K were recorded every 5 min. The reaction mixture of **1** with GST (80:20 μM) in Tris buffer (pH 8) at 310 K for 6 h was analysed by FT-ICR MS after monitoring by UV-Vis spectroscopy.

3.2.3.2 HPLC

Reaction mixtures of complex **1** with GSH at various molar ratios were prepared by mixing aliquots of 10 mM **1** and 50-500 mM GSH. For the reactions under physiologically relevant conditions (phosphate buffer pH 7.0, 22 mM NaCl), the pH values of all starting solutions were adjusted to 7 using NaOH and $HClO_4$, and the O_2

content was minimized by bubbling with N_2 before and after mixing unless otherwise stated. The mixtures were diluted to the required concentration with deionized water or with 10-50 mM phosphate buffer solution (pH 7.0, purged with N_2), bubbled with N_2 again, and then incubated at 310 K in a water bath for the required times for the subsequent HPLC and LC-MS analysis or preparative separation. The samples for semipreparative separation contained 1-10 mM complex **1** and 5-50 mM GSH.

For the reaction of complex **1** with GSH under argon, the separate reactant solutions (pH of GSH solutions adjusted to 6.8) were mixed at molar ratios of 0.02:5 mM or 1:10 mM after deoxygenation by four cycles of freeze-thawing on a vacuum line under Ar, and then incubated at 310 K for 48 h under Ar bubbling. For the same reactions under O_2, similar solutions of the starting materials were mixed in air and then incubated at 310 K for 48 h with O_2 bubbling.

The time-course of reaction of complex **1** (0.3 mM) with GSH (3 mM) in unbuffered aqueous solution in air (i.e. not purged with N_2), was followed chromatographically by injection of aliquots of the mixtures onto the HPLC column at various time intervals. Sampling at various times was done in air by briefly removing the cap to extract an aliquot.

3.2.3.3 NMR / FT- ICR MS

The HPLC fractions from the reactions of complex **1** with various molar ratios of GSH in water or in phosphate buffer (pH* 7) were collected from semipreparative HPLC separations, and immediately frozen in liquid nitrogen, and then lyophilized. The resulting solids were redissolved in 0.6 mL of 10% D_2O/90% H_2O for 1D and 2D ^1H NMR experiments. The pH* value (initially pH ca. 2 due to the presence of

trifluoroacetic acid) of the fraction containing complex **4** from the reaction of complex **1** with GSH in buffer solution (pH* 7) was immediately adjusted to 7 using NaOH and $HClO_4$. The solution was then freeze-dried and redissolved in 90% H_2O/10% D_2O, and the pH was readjusted to 7 before the NMR experiments. The samples for FT-ICR MS were diluted from NMR samples.

A 10 mM solution of ^{15}N-labeled complex **1** (^{15}N-**1**) was used to follow reactions of **1** with GSH by 1D [^{1}H] and 2D [^{1}H, ^{15}N] HSQC NMR. The reaction mixtures were prepared using the same method as that for HPLC samples.

3.2.3.4 Determination of Extinction Coefficients

HPLC fractions of complex **1**, its aqua and TFA adducts as well as the GSH adducts were collected from a 10 mM equilibrium aqueous solution of **1**, the 2-h and 24-h reaction mixtures of complex **1** with GSH in water, 24-h reaction mixture of complex **1** with GSH in buffer containing 22 mM NaCl. The method has been shown in Chapter **2.7**, and the values are listed in Table 3.1.

Table 3.1 Relative Extinction Coefficients at 254 nm of HPLC-Isolated Ru Arene Complexes

Complex	Ru[a] /μg mL^{-1}	Ru /nmol	peak area[b]	ε^{R}_{254}[c]
[(η^6-bip)Ru(en)Cl]$^+$ (**1**)	7.72	384	179358	1.00
[(η^6-bip)Ru(en)(H_2O)]$^{2+}$ (**2**)	6.30	312	161914	1.10
[(η^6-bip)Ru(en)(TFA)]$^+$ (**3**)	0.89	44.1	23722.9	1.14
[(η^6-bip)Ru(en)(GS-*S*)] (**4**)	0.74	36.8	36947.2	2.32
[(η^6-bip)Ru(en)(GS-*O*)]$^+$ (**5**)	1.06	52.6	29707.4	1.20
[(η^6-bip)Ru(en)(GS-*O*)]$^+$ (**6**)	0.89	43.8	25517.4	1.24
[((η^6-bip)Ru)$_2$(GS-*S*)$_3$]$^{2-}$ (**7**)	0.97	47.8	42539.9	1.89
[(η^6-bip)Ru(en)(GS(O)-*S*)] (**10**)	0.41	20.3	11160.2	1.17

[a] Ru concentration in 5 mL aqueous sample determined by ICP-OES.
[b] Relative peak areas of HPLC fractions with UV detection at 254 nm.
[c] Relative extinction coefficient.

3.2.3.5 Determination of Free Thiols (SH) in Proteins

DTNB is a symmetrical aryl disulfide which readily undergoes the thiol-disulfide interchange reaction in the presence of a free thiol (see Scheme 3.1):

Scheme 3.1 Reaction of DTNB with free thiol. The TNB has a relatively intense absorbance at 412 nm compared to both disulfides. Because the stoichiometry of protein thiol to TNB formed is 1:1, TNB formation can be used to assess the number of thiols present.[16]

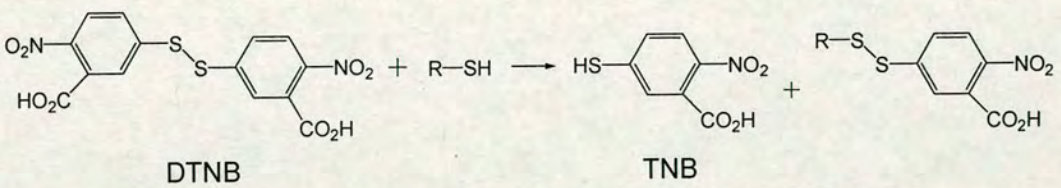

DTNB TNB

The DTNB stock solution (2 mM DTNB in 50 mM sodium acetate) and the stock solution of Tris buffer (1 M Tris buffer, pH 8) were prepared and kept refrigerated. The absorbance of DTNB solution (0.1 mM) in Tris buffer (0.1 M, pH 8) was recorded, and the reaction of DTNB (0.1 mM) with GST (15.2 μM) in Tris buffer (0.1 mM, pH 8) was followed at 412 nm, 310 K, continuously. The maximum absorbance of the reaction mixture was recorded.[16] The concentration of free thiol was calculated using eq. 1:

$$\text{Conc. (thiol)} = [\text{Abs}]_{412} / 13.6\ (\text{mM}^{-1}\ \text{cm}^{-1}) \qquad (1)$$

where 13.6 mM^{-1} $\text{cm}^{-1}$is the extinction coefficient of TNB in Tris buffer at 412 nm at 310 K.[16]

The number of free thiol groups included in GST which was used in this Chapter was calculated using eq. 2:

$$\text{No. (thiol)} = [\text{Conc. (thiol)}]\ (\mu\text{M}) \times 4 / 15.2\ (\mu\text{M}) \qquad (2)$$

where 4 is present because GST should contain 4 free thiol groups, and 15.2 μM is the concentration of GST used in the reaction mixture. It is obtained that the number of free thiols in the GST used in this Chapter is 2.

3.3 Results and Disscussion

3.3.1 Reactions of 1 with GSH in Unbuffered Aqueous Solution

The reaction of complex **1** with GSH in water without adjustment of pH was investigated using HPLC, ESI-MS, and NMR spectroscopy. Reaction of **1** (0.3 mM) with a 10-fold molar excess of GSH (pH initially ca. 3) at 310 K gave rise to two products as detected by HPLC (peaks d, e in Figure 3.2) after ca. 10 min, and then another product (peak f) after 0.5 h. After 6 h, a forth adduct (peak g) formed and increased in concentration until 24 h; meanwhile HPLC peaks d, e, and f decreased in intensity.

ESI-MS analysis of the HPLC fractions (Figure 3.2) gave a singly charged ion peak centered at *m/z* 622.1 for peaks d, e, and f, assignable to (isomers of) monoruthenium glutathione complexes **4**, **5**, and **6** (calcd *m/z* 622.1 for $\{(\eta^6\text{-bip})\text{Ru(en)(GS)} + \text{H}\}^+$).[17] A fragment ion peak at *m/z* 561.9 resulting from release of en (calcd *m/z* 562.1 for $\{(\eta^6\text{-bip})\text{-Ru(GS)} + \text{H}\}^+$) was detectable only for fraction f (adduct **4**), which suggests that the Ru-N bonds in this complex are weakened as might be the case for an S-bound thiolato complex [(η^6-bip)Ru(en)(GS-*S*)] (**4**). The trans-labilizing effect of sulfur is well-known in Pt^{II} chemistry.[18] At low pH (ca. 3.0), the amino group of GSH is protonated and unlikely to coordinate to Ru. Therefore, fractions d and e are more likely to correspond to Glu or Gly carboxylate-bound species $[((\eta^6\text{-bip})\text{Ru})(\text{en})(\text{Glu-Cys-Gly-}O)]^+$ (**5**) and $[((\eta^6\text{-bip})\text{-Ru})(\text{en})(O\text{-Glu-Cys-Gly})]^+$ (**6**). The mass spectrum (Figure 3.3) of peak g indicated that this fraction contained a diruthenium glutathione adduct $[((\eta^6\text{-bip})\text{-Ru})_2(\text{GS})_3]^{2-}$ (**7**) (calcd *m/z* 715.6 for $\{((\eta^6\text{-bip})\text{Ru})_2(\text{GS})_3 + 4\text{H}\}^{2+}$).

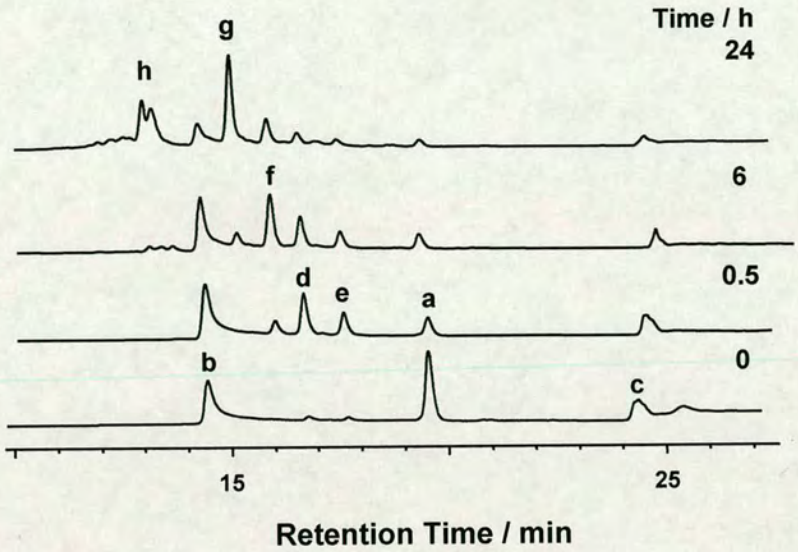

Figure 3.2 HPLC time-course for the reaction of 1 (0.3 mM) with 10 mol equiv GSH in aqueous solution (pH ca. 3) at 310 K. Peak assignments: (a) 1; (b) $[(\eta^6\text{-bip})Ru(en)(H_2O)]^{2+}$ (**2**); (c) $[(\eta^6\text{-bip})Ru(en)(TFA)]^{+}$ (**3**); (d, e, f, g, and h) GSH adducts. Peak h appears to be due to tetranuclear clusters (discussed later).

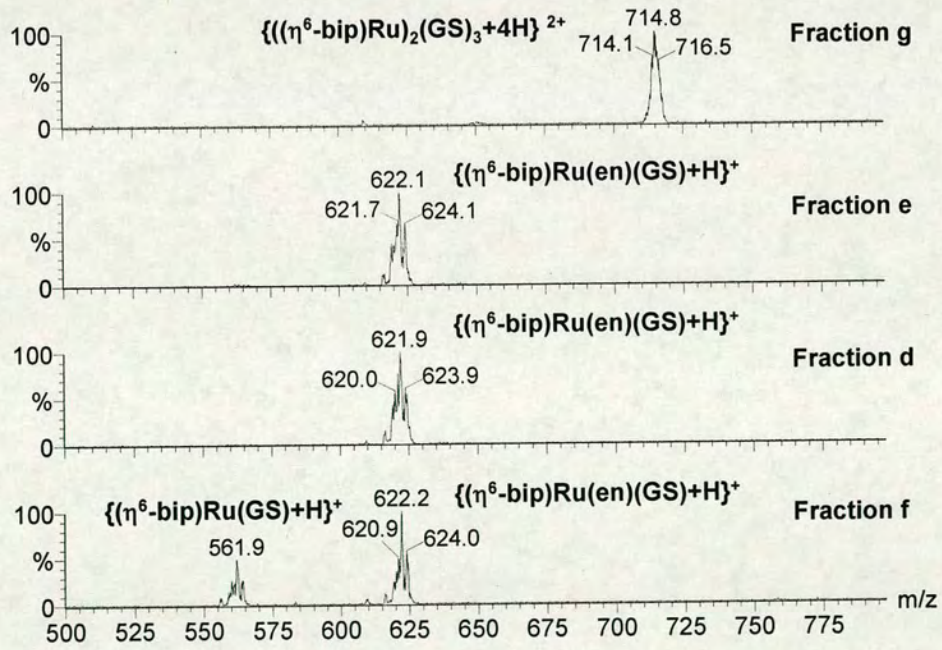

Figure 3.3 Mass spectra for HPLC fractions d, e, f and g (see Figure 3.2) from the reaction of complex **1** with GSH (0.3: 3 mM) in aqueous solution (pH ca. 3).

Fraction g in Figure 3.2 was also collected from a reaction mixture of complex **1** (5 mM) with GSH (25 mM) incubated at 310 K for 48 h and was characterized by 1D ^{1}H and 2D [^{1}H,^{1}H] NMR spectroscopy (Figures 3.4, 3.5, and 3.6). Only one set of proton resonances was observed for the two biphenyl ligands (Figure 3.6, Table 3.3) and one set for the three glutathione ligands (Figure 3.4, Table 3.2), which indicates that the two biphenyl and three glutathione ligands in this adduct are magnetically equivalent, and that adduct **7** $[((\eta^6\text{-bip})Ru)_2\text{-}(GS)_3]^{2-}$ is formed via the substitution of en in $[(\eta^6\text{-bip})Ru\text{-}(en)(GS\text{-}S)]$ (**4**) by two glutathione ligands. No peaks for en protons (en-NH_2 or enCH_2) were detectable. For the biphenyl groups, five well-separated resonances are observed for the ortho (δ 7.46, 7.26), meta (δ 5.72, 5.83), and para (δ 5.97) protons of the coordinated phenyl ring (A), and four peaks for the ortho (δ 7.57), meta (δ 7.65, 7.51), and para (δ 7.45) protons of the noncoordinated phenyl ring (B). At pH 2.9, compared with free GSH at the same pH value (Table 3.2), the β-CH_2 and α-CH proton resonances of the cysteine residues in adduct **7** are shifted to high field by 0.51, 0.58, and 0.42 ppm, respectively, as expected for an S-bound glutathione ligand. The 2D [^{1}H,^{1}H] NOESY NMR spectrum (Figure 3.5) shows that there are strong NOEs between the aromatic protons of the coordinated biphenyl ring (A) and the α-CH and β-CH_2 protons of the cysteine residues in **7** (the assignments for the NMR spectra were carried out with the assistance of Dr. Fuyi Wang).

ICP-OES calibration of HPLC peak areas (Table 3.1) showed that after 2 h of the reaction 9% of the Ru was present as **4** and 31% as **5** + **6**. After 24 h, the dinuclear complex **7** was the main product (35%).

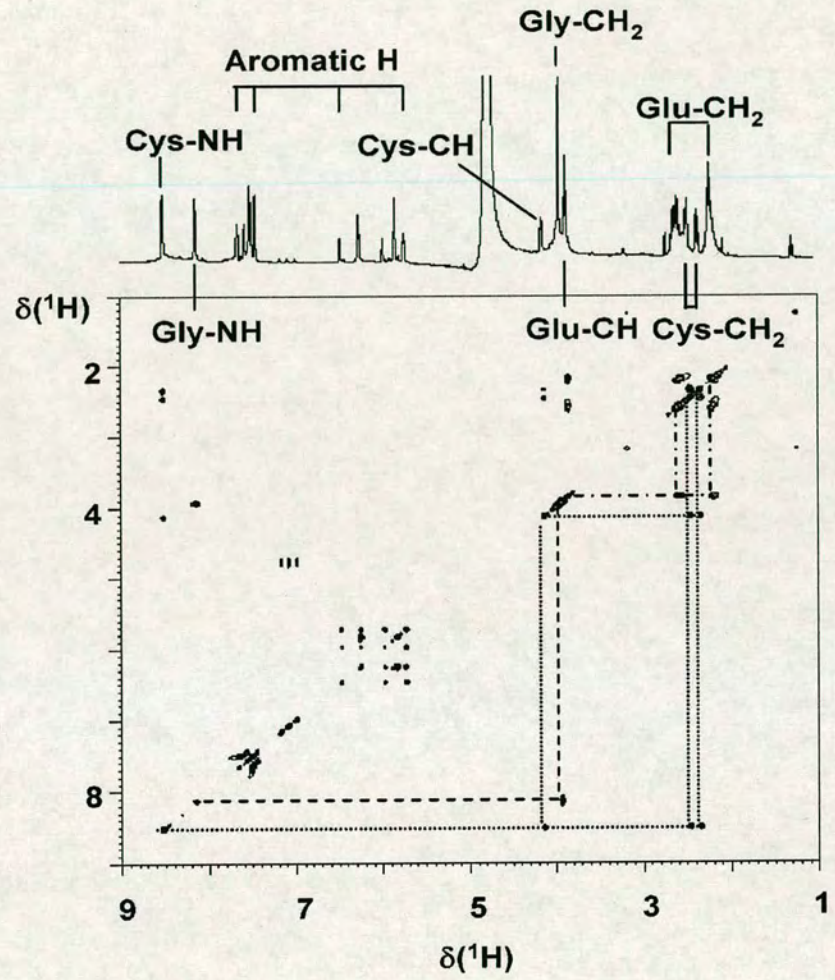

Figure 3.4 1D ^{1}H and 2D [^{1}H,^{1}H] TOCSY NMR spectra for HPLC fraction (g) (see Figure 3.2) from the reaction of complex **1** with GSH (5:25 mM) in aqueous solution for 48 h at 310 K.

Table 3.2 ^{1}H NMR chemical shifts (δ) for GSH and GSH ligands in the adduct [((η^6-bip)Ru)$_2$(GS-μ-S)$_3$]$^{2-}$ (**7**) in 90% H_2O/10% D_2O at pH* 3(298 K)

proton	δ (^{1}H) ($\Delta\delta$) [a]	
	GSH	**7**
		Glu
γ-CH_2	2.52	2.59 (0.07)
β-CH_2	2.13	2.19 (0.06)
α-CH	3.79	3.88 (0.09)
α-NH_3^+	- [b]	- [b]
		Cys
β-CH_2	2.95	2.44 (-0.51)
	2.90	2.32 (-0.58)
α-CH	4.54	4.12 (-0.42)
α-NH	8.44	8.51 (0.07)
		Gly
α-CH_2	3.94	3.93 (-0.01)
α-NH	8.48	8.16 (-0.32)

[a] $\Delta\delta$ = δ (**7**) - δ (GSH). [b] Not observed (fast exchange).

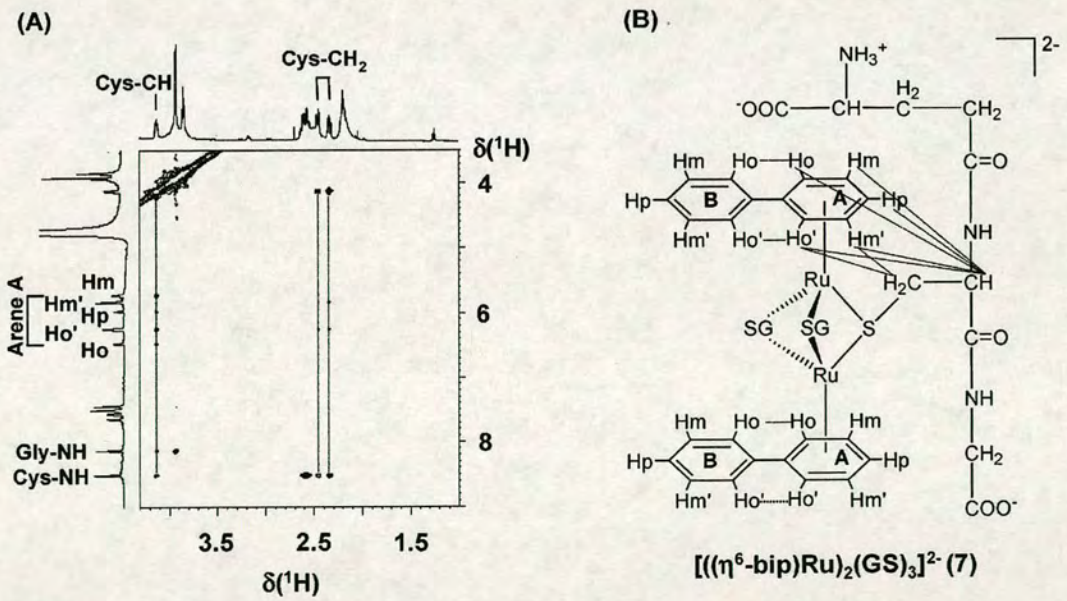

Figure 3.5 (A) NOEs between the protons of the biphenyl ligand and cysteine α-CH, β-CH_2 protons of **7**, indicating their proximity. (B) Structure of **7** with NOEs indicated by dotted lines; the side chains of two of the GS ligands are omitted for clarity. For NOEs between protons of the two phenyl rings, see Figure 3.6.

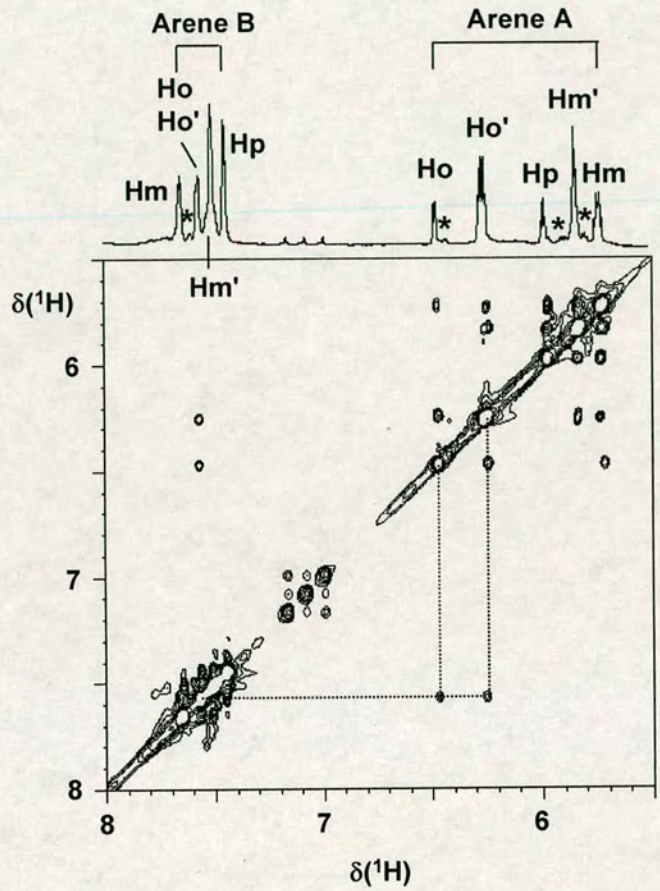

Figure 3.6 NOEs between the phenyl rings of the biphenyl ligands in the thiolato adduct $[((\eta^6\text{-bip})Ru)_2(GS)_3]^{2-}$ (**7**), allowing assignments for resonances of aromatic protons. The ortho proton from arene A is correlated with the ortho proton from arene B, and the ortho' proton from arene A is correlated with the ortho' proton from arene B (see Figure 3.5(B)). Resonances labelled with an asterisk (*) arise from impurity species such as the aqua adduct (**2**), mono thiolato adduct (**4**), see Figure 3.2. Some of the impurity resonances are overlapped with those of **7**, which leads to distortion of the signal intensities. For proton labelling, see Figure 3.5.

Table 3.3 ^{1}H NMR chemical shifts for biphenyl ligands in complex **1** and the adduct [((η^6-bip)Ru)$_2$(GS-μ-*S*)$_3$]$^{2-}$ (**7**) in 90% H_2O / 10% D_2O (298 K)

Proton[a]	Complex (pH*)	
	1 (5.5)[b]	**7** (2.9)
	δ	
Phenyl ring A		
Ho	5.98	7.46
Ho′	5.98	7.26
Hm	6.26	5.72
Hm′	6.26	5.83
Hp	5.91	5.97
Phenyl ring B		
Ho	7.83	7.57
Ho′	7.83	7.57
Hm	7.64	7.65
Hm′	7.64	7.51
Hp	7.64	7.45

[a] For proton labels, see Figures 3.5. [b] Wang, F. Y.; Chen, H. M.; Parkinson, J. A.; Murdoch, P. D.; Sadler, P. J. *Inorg. Chem.* 2002, *41*, 4509-4523.

The reaction of complex **1** with GSH in unbuffered solution was also studied at millimolar concentrations (**1**:GSH 2:20 mM) at 310 K by 2D [^{1}H,^{15}N] HSQC NMR using ^{15}N-labeled **1** (^{15}N-**1**). The spectra are shown in Figure 3.7, and the ^{1}H and ^{15}N chemical shifts are listed in Table 3.4. The results are consistent with those obtained by HPLC. During the early stages (<1 h), three pairs of new cross-peaks appeared which are assignable to the ^{15}N-en ligands in adducts **4**, **5**, and **6**. Cross-peaks 5a/b and 6a/b (Figure 3.7) decreased in intensity after ca. 4 h and disappeared after ca. 10, and cross-peaks 4a/b increased in intensity up to 6 h, and then decreased and disappeared after 13 h. Because the diruthenium adduct **7** does not contain bound ^{15}N-en, it does not give rise to ^{1}H,^{15}N cross-peaks, and therefore no ^{1}H/^{15}N signals were detectable during the late stages (>13 h) of the reaction when adduct **7** was the main product (the assignments were made with the help of Dr. Fuyi Wang). The two intermediates **5** and **6** were not stable long enough in aqueous solution to allow sufficient NMR data to be recorded to provide an unambiguous identification of the binding sites. However, the 2D HSQC NMR spectra showed two pairs of cross-peaks corresponding to the formation of the intermediates **5** and **6** (Figure 3.7), and their ^{15}N-en ^{1}H/^{15}N chemical shifts (Table 3.4; δ 5a 6.24/-24.9, 5b 4.23/-24.9; 6a 6.14/-24.6, 6b 4.18/-24.6) are in a similar range to those for ^{15}N-en groups in carboxylate-bound adducts of cystine $[(\eta^{6}\text{-bip})Ru(en)(Cys_2H_2\text{-}O)]^{2+}$ (δ 6.07/-24.7, 4.12/-24.7), cysteine $[(\eta^{6}\text{-bip})Ru(en)(L\text{-}CysH\text{-}O)]^{+}$ (δ 6.08/-24.1, 4.08/-24.1)[19] and acetate (δ 6.06/-25.6, 4.13/-25.6).[20]

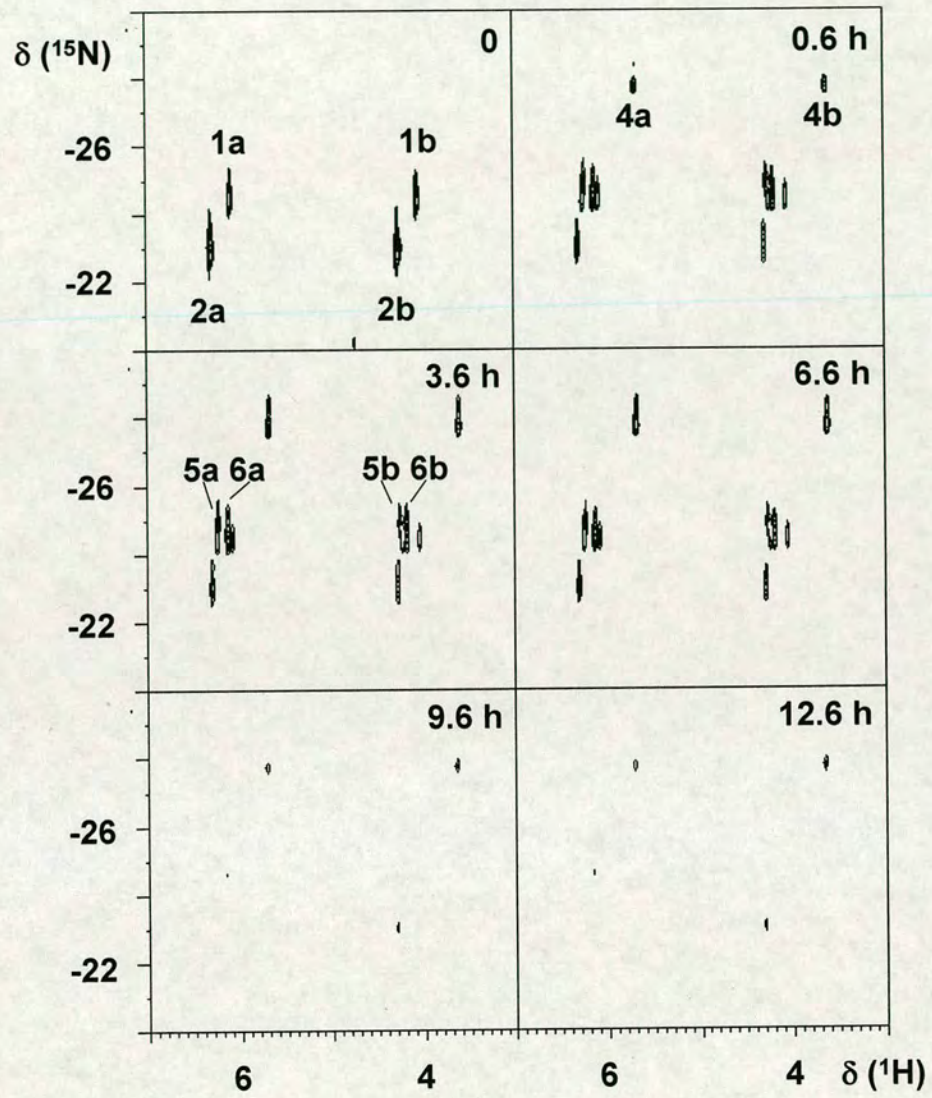

Figure 3.7 2D [^{1}H, ^{15}N] HSQC NMR time course for the reaction of ^{15}N-1 (2 mM) with GSH (10 mM) in 90% H_2O / 10% D_2O at 310 K over 24 h. After 13 h reaction, no cross-peaks were detectable. Assignments: 1a/b complex **1** ([(η^6-bip)Ru(^{15}N-en)Cl]$^{+}$, 2a/b aqua complex **2** ([(η^6-bip)Ru(^{15}N-en)(H_2O)]$^{2+}$), 4a/b, 5a/b and 6a/b GSH adducts **4**, **5** and **6** ([(η^6-bip)Ru(^{15}N-en)(GS)]). No cross-peaks are observed for the diruthenium adduct **7** ([((η^6-bip)Ru)$_2$(GS)$_3$]$^{2-}$) which is a product of the reaction.

Table 3.4 $^{1}H,^{15}N$ NMR Peaks Observed for Reactions of ^{15}N-**1** (2 mM) with GSH (20 mM) in 90% H_2O/10% D_2O (pH* ca. 2.9, Figure 3.7) at 310 K

complex	(peak) δ 1H/15N	
1	(1a) 6.09/-24.62	(1b) 4.05/-24.62
2	(2a) 6.30/-23.06	(2b) 4.26/-23.06
4	(4a) 5.68/-27.74	(4b) 3.60/-27.74
5[a]	(5a) 6.24/-24.92	(5b) 4.23/-24.92
6[a]	(6a) 6.14/-24.60	(6b) 4.18/-24.60

[a] Assignments for **5** and **6** are ambiguous.

Chloro Ru^{II} arene complexes such as complex **1** undergo rapid hydrolysis with half-lives ranging from 5 to 10 min.[21] In aqueous solution, in the presence of nucleophiles such as acetate, the aqua ligand is readily displaced.[20,21] Hence, the carboxylate-bound intermediates $[(\eta^6\text{-bip})Ru(en)(Glu\text{-}Cys\text{-}Gly\text{-}O)]^+$ (**5**) and $[(\eta^6\text{-bip})Ru(en)(O\text{-}Glu\text{-}Cys\text{-}Gly)]^+$ (**6**) are kinetically favored products from reaction of **1** with 10 mol equiv of GSH and are formed via displacement of the aqua ligand in $[(\eta^6\text{-bip})Ru(en)\text{-}(H_2O)]^{2+}$ (**2**) (Scheme 3.2). However, sulfur-coordination of thiolate to $\{(\eta^6\text{-bip})Ru(en)\}^{2+}$ appeared to be thermodynamically favored, and the thiolato adduct $[(\eta^6\text{-bip})Ru(en)(GS\text{-}S)]$ (**4**) became the dominant product after 6 h. Subsequently, the en ligand of **4** was readily released assisted by en protonation, by the trans-labilizing effect of S-bound glutathione and binding of two other S-bound glutathione ligands, giving the triply S-bridged diruthenium thiolato complex $[((\eta^6\text{-bip})Ru)_2(GS\text{-}\mu\text{-}S)_3]^{2-}$ (**7**). This reaction pathway is similar to that observed previously for reaction of L-cysteine with **1**.[19]

Scheme 3.2 Pathways for Reactions of Complex **1** with GSH for 24 h at pH 3

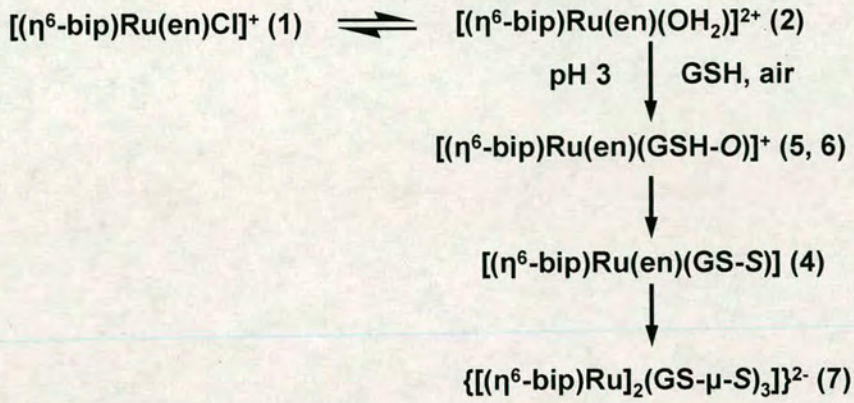

In unbuffered solution (pH ca. 3) and at 310 K, ruthenium arene anticancer complex **1** reacted with 10 mol equiv GSH for 48 h, giving rise to two di-ruthenium glutathione complexes as main products (Figure 3.8) of which the diruthenium triply-S bridged product has been identified by conventional LC-ESI MS and NMR.

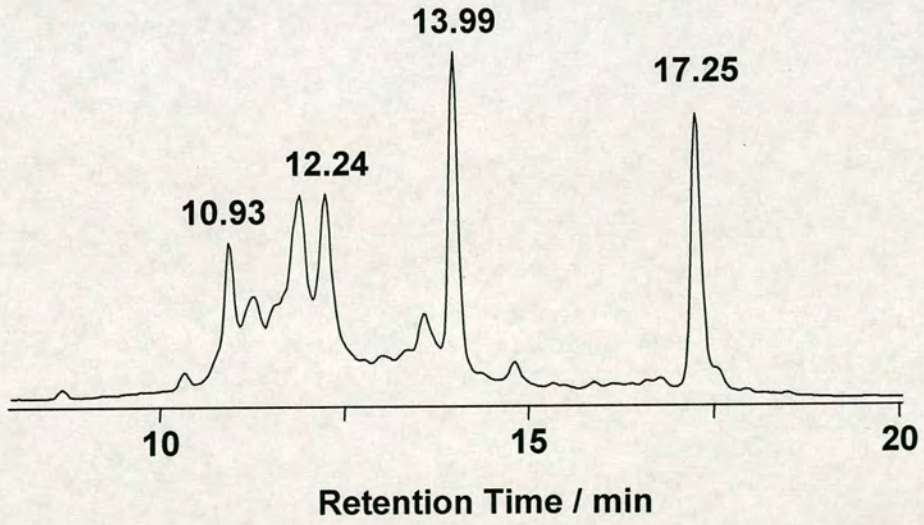

Figure 3.8 HPLC chromatogram with UV detection at 254 nm for the reaction of **1** and GSH (2:20 mM) in unbuffered solution (pH ~3) at 310 K for 43 h. The peak centred at 13.99 min corresponds to the S-bridged di-ruthenium glutathione adduct $[((\eta^6\text{-bip})Ru)_2(S\text{-GS})_3]^{2-}$ (**7**).

The fraction centred at 17.25 min was collected and concentrated for ESI-MS (Figure 3.9) and 1D ^{1}H, 2D [^{1}H,^{1}H] NMR (Figure 3.11 and 3.12) experiments. A singly-charged ion peak centred at *m/z* 1824.2 and a doubly-charged ion peak centred at *m/z* 913.2 were assigned to a di-ruthenated adduct **8** according to the patterns of the ion peaks (Figure 3.10). Two singly-charged fragment ions at *m/z* 1485.2 and 1146.3 appear to correspond to release of one and two sulfinate (GSO_2^{2-}) ligands, from the di-ruthenated adduct, respectively (Figure 3.9), which indicates that at least two GSO_2^{2-} ligands are involved in this adduct. Due to the pH value for the reaction of **1** with GSH in water was ca. 3, the sulfinato ligand GSO_2^{2-} could be protonated as GSO_2H^-.[22]

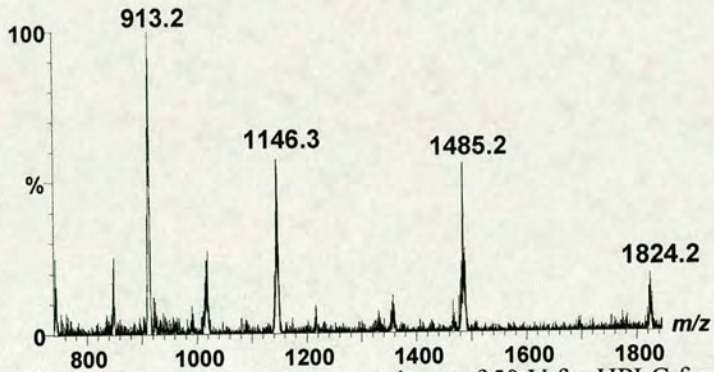

Figure 3.9 ESI mass spectrum with a cone voltage of 50 V for HPLC fraction centred at 17.25 min (see Figure 3.8).

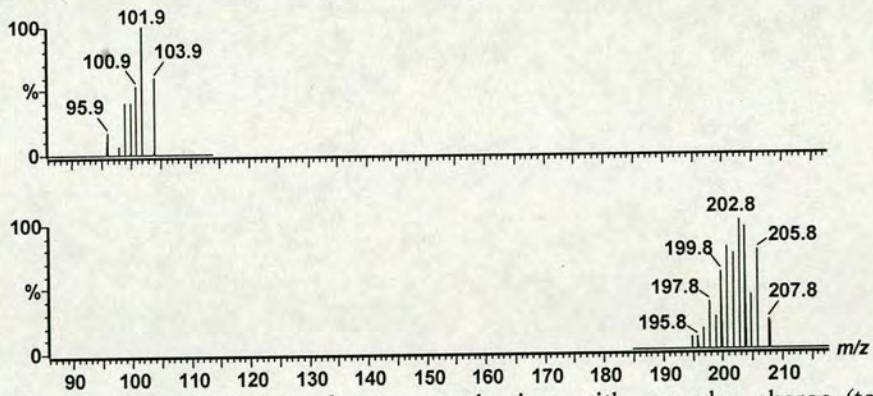

Figure 3.10 Isotopic simulations for mono-ruthenium with one plus charge (top) and di-ruthenium with one plus charge (bottom).

Only one set of proton resonances was observed for the two biphenyl ligands (Figure 3.12, Table 3.6), and one set for the glutathione ligands (Figure 3.11, Table 3.5). Due to the oxidation of sulfur in the Cys, the proton resonances for Cys-CH and Cys-CH_2 could not observed (Figure 3.11), and the signals for these two proton resonances probably shift and are covered by the water signal. The significantly different chemical shifts of α-CH and β-CH_2 in the cysteine part of GSH between **8** and unbound GSH (Table 3.6) indicated that Ru(II) arene anticancer complex **1** binds to GSOH and GSO_2H both via Ru-S. Because it is a di-ruthenated complex, the pattern of the proton resonances for the biphenyl ligand was not very clear, but they were still assigned according to the correlations shown in the NOESY spectrum (Figure 3.12). Therefore, the ESI-MS and NMR results showed that the two ruthenium centres are equivalent and that the ethylenediamine chelate ligand has gone. The HPLC fraction eluted from 10.93 to 12.24 min could not be separated although the gradient was changed to improve the separation, and the concentration of multinuclear ruthenium clusters in the fraction eluted from 10.93 to 12.24 min was too low to allow good ESI MS analysis. Therefore, ESI-FT-ICR MS experiments were performed to identify the structures of two multinuclear Ru complexes.

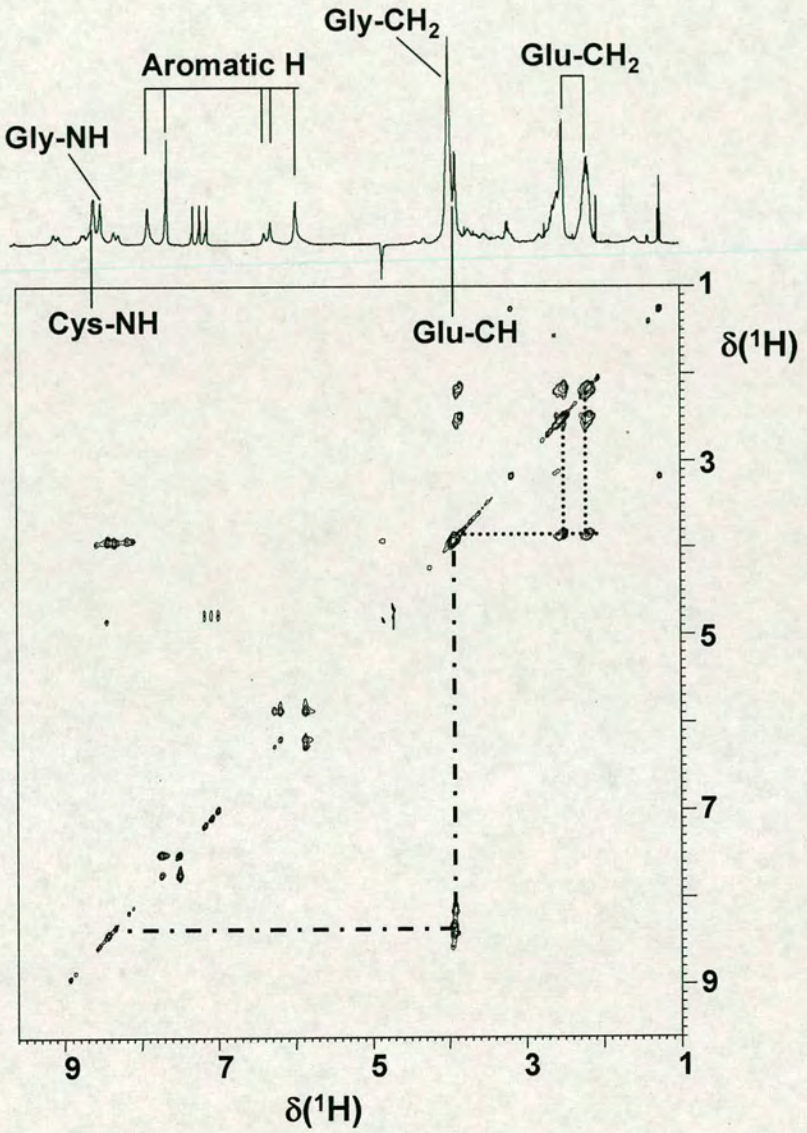

Figure 3.11 1D ^{1}H and 2D [^{1}H,^{1}H] TOCSY NMR spectra for HPLC fraction centred at 17.25 min (see Figure 3.8) from the reaction of **1** with GSH (2:20 mM) in unbuffered solution (pH ~3) at 310 K for 43 h.

Table 3.5 ^{1}H NMR chemical shifts (δ) for GSH and GSH ligands in the di-ruthenated adduct **8** in 90% H_2O/10% D_2O (298 K, pH 2.9).

	δ (^{1}H) ($\Delta\delta$) [a]	
Proton	GSH	**8**
		Glu
γ-CH_2	2.52	2.48 (-0.04)
β-CH_2	2.13	2.17 (0.04)
α-CH	3.79	3.84 (0.05)
α-NH_3^+	- [b]	- [b]
		Cys
β-CH_2	2.95	- [c]
	2.90	- [c]
α-CH	4.54	- [c]
α-NH	8.44	8.42 (-0.02)
		Gly
α-CH_2	3.94	3.92 (-0.02)
α-NH	8.48	8.33 (-0.15)

[a] $\Delta\delta$ = δ (**8**) - δ (GSH). [b] Not observed (fast exchange). [c] Not observed (probably covered by water signal).

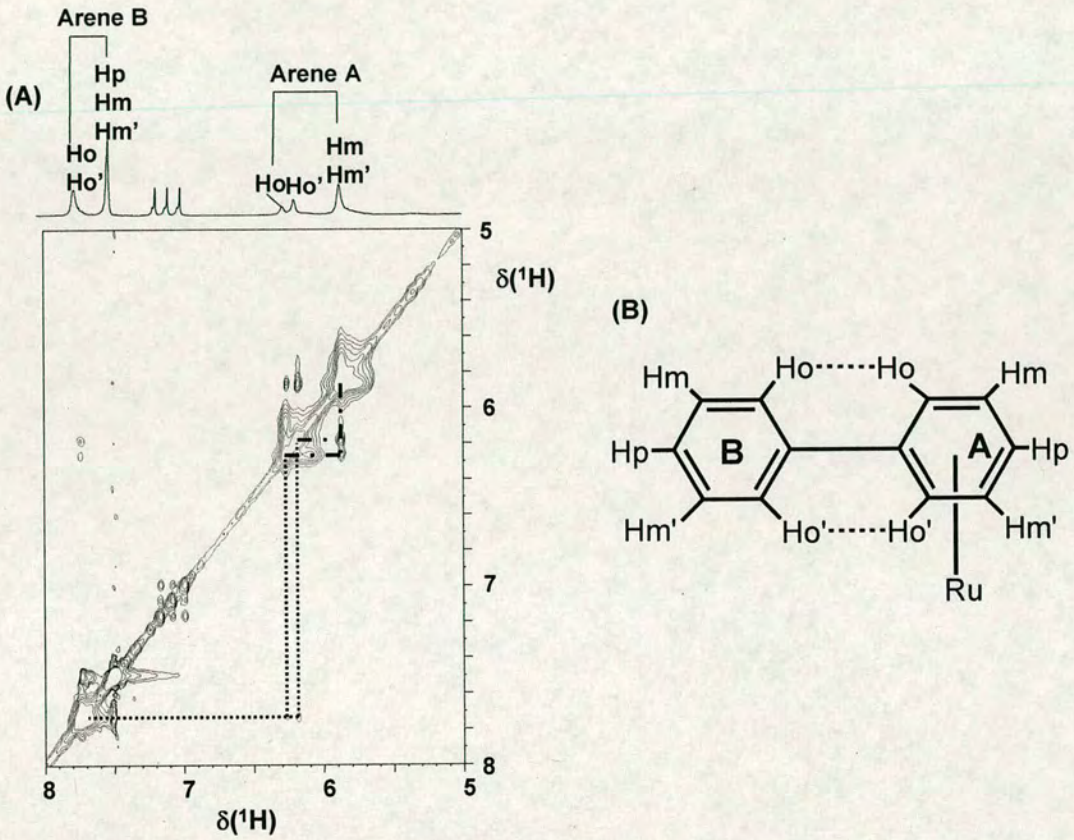

Figure 3.12 (A) NOEs between the phenyl rings of the biphenyl ligands in the di-ruthenated adduct **8**, allowing assignments for resonances of aromatic protons; (B) Structure of biphenyl ligand with NOEs indicated by dotted lines. The ortho proton from arene A is correlated with the ortho proton from arene B, and the ortho' proton from arene A is correlated with the ortho' proton from arene B.

Table 3.6 ^{1}H NMR chemical shifts for biphenyl ligands in complex 1 and the di-ruthenated adduct **8** in 90% H_2O / 10% D_2O (298 K)

Proton[a]	Complex (pH)	
	1 (5.5)[b]	**8** 2.9)
	δ	
Phenyl ring A		
Ho	5.98	6.26
Ho′	5.98	6.18
Hm	6.26	5.86
Hm′	6.26	5.86
Hp	5.91	-[c]
Phenyl ring B		
Ho	7.83	7.73
Ho′	7.83	7.73
Hm	7.64	7.49
Hm′	7.64	7.49
Hp	7.64	7.49

[a] For proton labels, see Figures 3.12. [b] Wang, F. Y.; Chen, H. M.; Parkinson, J. A.; Murdoch, P. D.; Sadler, P. J. *Inorg. Chem.* **2002,** *41*, 4509-4523. [c] Not observed

The HPLC fraction eluted from 10.90 to 12.50 min (see Figure 3.8) was collected for the analysis using ^{1}H NMR spectroscopy. Compared to the ^{1}H NMR spectra for a di-ruthenated tri-glutathione adduct $\{[(\eta^6\text{-bip})Ru]_2(GS\text{-}\mu\text{-}S)_3\}^{2-}$ (**7**) involved in the HPLC fraction eluted centered at 13.99 min in Figure 3.8 and the di-ruthenated adduct **8** obtained from the HPLC fraction eluted centered at 17.25 min in Figure 3.8, the biphenyl proton signals obtained from the ^{1}H NMR spectrum for the HPLC fraction eluted from 10.90 to 12.50 min in Figure 3.8 were too broad to observe (Figure 3.13), which may illustrated that the oxidation states for two ruthenium atoms in complex **8** are +2 or 0, and oxidation states for some Ru atoms in the complex of which spectrum is shown in Figure 3.13(C) may be +1 or +3, because Ru(I) and Ru(III) are paramagnetic[23] which causes the signals for protons close to Ru to become very broad..

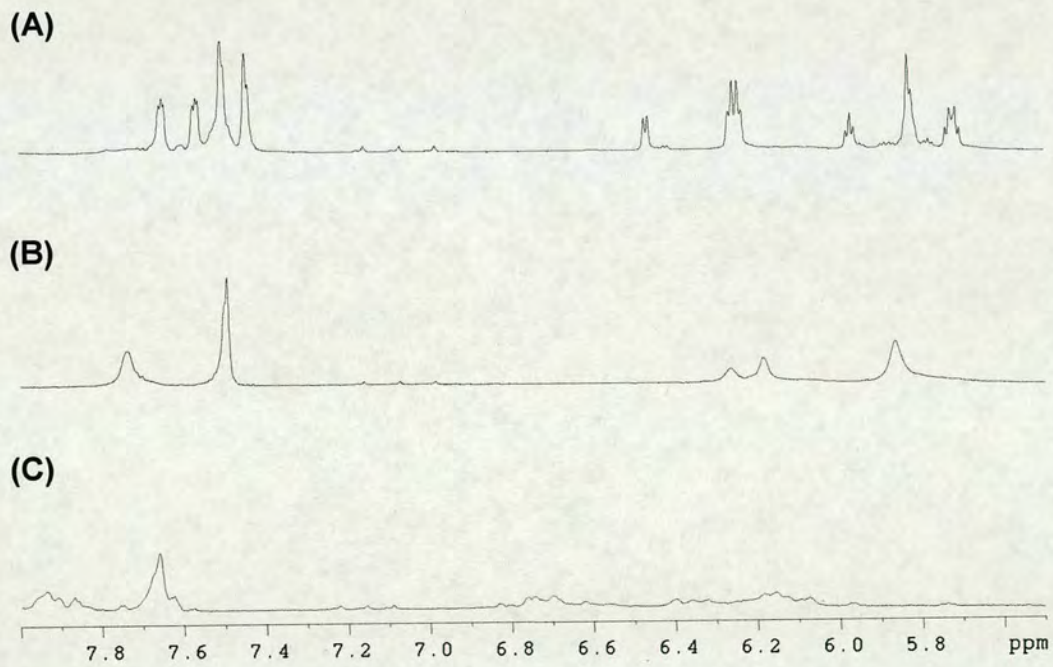

Figure 3.13 ^{1}H NMR spectra for a di-ruthenated tri-glutathione adduct **7** (A), the di-ruthenated adduct **8** (B) and the HPLC fraction eluted from 10.90 to 12.50 min in Figure 3.8 (C).

In order to identify the multinuclear ruthenium glutathione product unambiguously by MS, the NMR sample of the di-ruthenated complex **8** was analysed by FT-ICR MS, and a range of doubly-charged ion peaks and two triply-charged ion peaks were observed (Figure 3.14(A), Table 3.7). A doubly-charged ion peak centered at *m/z* 921.1 was assigned to $\{[(\eta^6\text{-bip})Ru(GSO_2)]_2 - 2O + 10\ H\}^{2+}$, corresponding to a di-ruthenated glutathione adduct $\{[(\eta^6\text{-bip})Ru(GSO_2)]_2\}^{8-}$ (**8**) according to the MS isotopic simulation (see Figure 3.14(B)). A doubly-charged ion peak centered at *m/z* 848.2 and a triply-charged ion peak centered at *m/z* 565.8 are assignable to release one glutamate acid part and three oxygen atoms from the adduct **8**. Also the HPLC fraction eluted from 10.93 to 12.24 min was collected for FT-ICR MS analysis. A series of doubly-charged and triply-charged ion peaks were obtained (see Figure 3.15(A) and (B)). The doubly-charged ion peak centered at *m/z* 1189.2 was assigned to $\{[(\eta^6\text{-bip})Ru(GSO_2)]_4 + 4\ H\}^{2+}$ (corresponding to a tetranuclear complex $\{[(\eta^6\text{-bip})Ru(GSO_2)]_4\}^{2-}$ (**9**)) based on the isotopic simulation (Figure 3.15(C)). The assignments of all the MS ion peaks in Figure 3.14(A), 3.15(A) and (B) were listed in Table 3.7. The proposed structures of complexes **8** and **9** were shown in Chart 3.1.

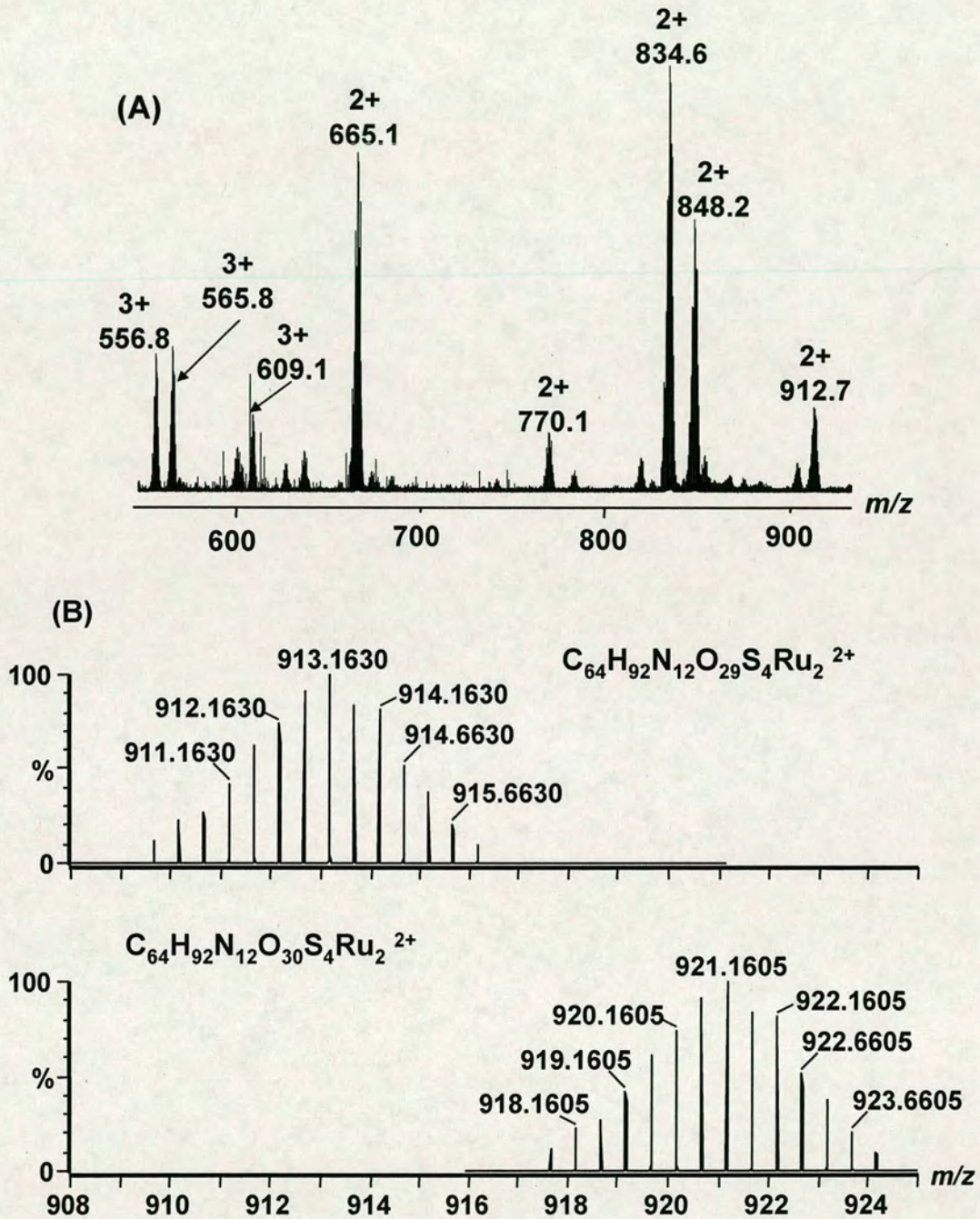

Figure 3.14 (A) FT-ICR mass spectrum for the di-ruthenated complex **8**; (B) MS isotopic simulations for ion peaks centered at *m/z* 921.1 and 912.7.

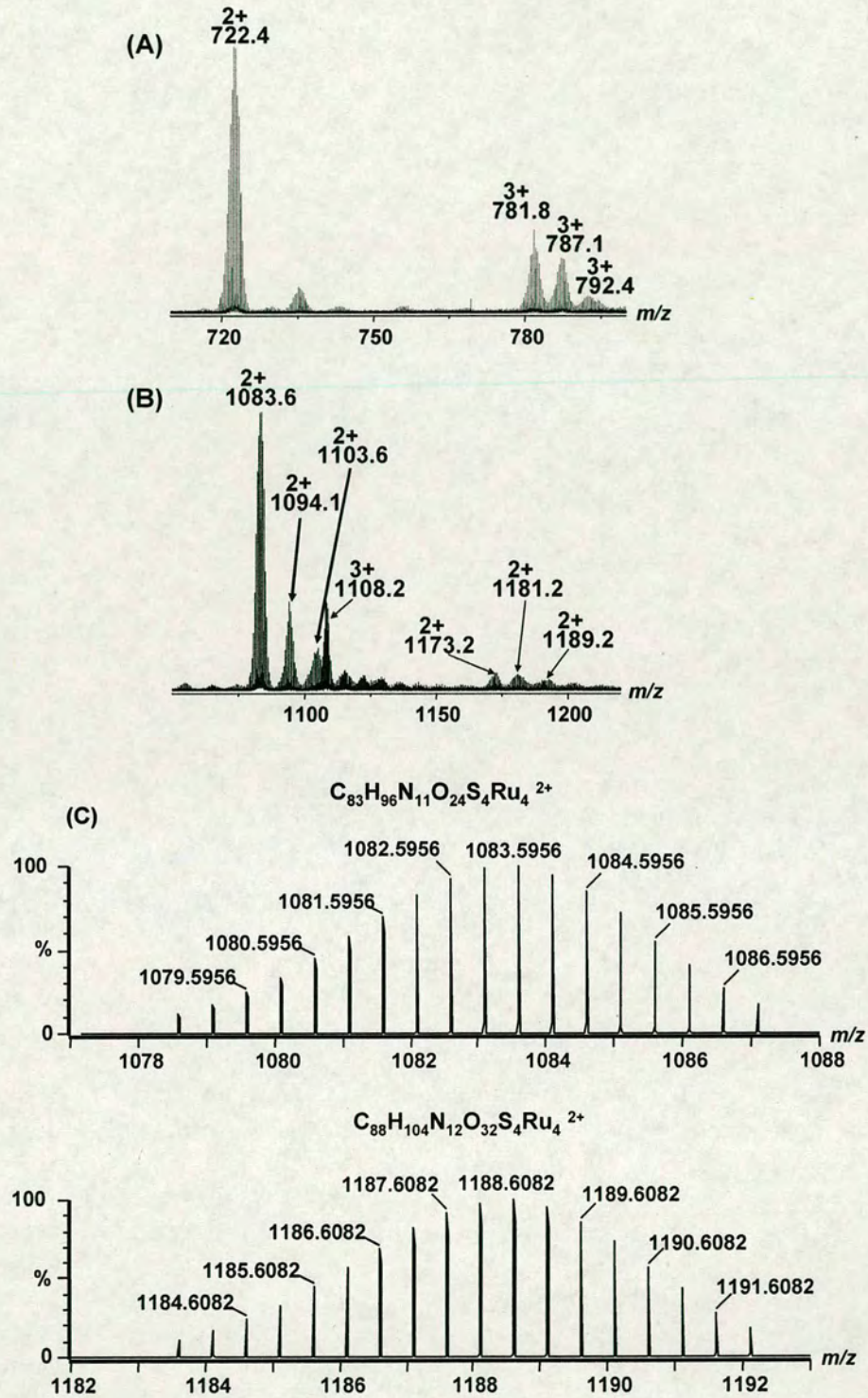

Figure 3.15 (A) and (B) FT-ICR MS for the HPLC fraction eluted from 10.93 to 12.24 min as shown in Figure 3.8; (C) Isotopic simulations for the ion peaks centered at *m/z* 1189.2 and 1083.6.

Table 3.7 The mass-to-charge ratios of the most abundant isotopomer of the ion fragments from the ruthenium sulfinate/sulfenate glutathione adducts $\{[(\eta^6\text{-bip})Ru(GSO_2)_2]_2\}^{8-}$ (**8**) and $\{[(\eta^6\text{-bip})Ru(GSO_2)]_4\}^{2-}$ (**9**) detected by direct infusion ESI-FT-ICR MS.

Adduct	m/z	Ion
8	556.7662	$\{\mathbf{8} - Glu^a - Gly^b + 11H^c\}^{3+}$
	565.7668	$\{\mathbf{8} - Glu - 3O + 11H\}^{3+}$
	609.1334	$\{\mathbf{8} - 3O + 11H\}^{3+}$
	665.0882	$\{\mathbf{8} - Glu - Gly - GSO_2 + 10H\}^{2+}$
	834.6312	$\{\mathbf{8} - Glu - Gly + 10H\}^{2+}$
	848.1573	$\{\mathbf{8} - Glu - 3O + 10H\}^{2+}$
	912.6801	$\{\mathbf{8} - 3O + 10H\}^{2+}$
9	722.4247	$\{\mathbf{9} - Glu - 5O + 5H\}^{3+}$
	781.7766	$\{\mathbf{9} - 2O + 5H^b\}^{3+}$
	787.1078	$\{\mathbf{9} - O + 5H\}^{3+}$
	792.4406	$\{\mathbf{9} + \mathbf{5}H\}^{3+}$
	1083.6502	$\{\mathbf{9} - Glu - 5O + 4H\}^{2+}$
	1094.1453	$\{\mathbf{9} - Glu - 4O + 4H\}^{2+}$
	1103.6351	$\{\mathbf{9} - Glu - 3O + 4H\}^{2+}$
	1173.1748	$\{\mathbf{9} - 2O + 4H\}^{2+}$
	1181.1743	$\{\mathbf{9} - O + 4H\}^{2+}$
	1189.1709	$\{\mathbf{9} + 4H\}^{2+}$

[a] Indicates loss of a Glu residue $HO_2CCH(NH_2)CH_2CH_2CO$ ($C_5H_8O_3N$). [b] Indicates loss of a Gly residue $NHCH_2CO_2H$ ($C_2H_4O_2N$). [c] H indicates gain of a proton.

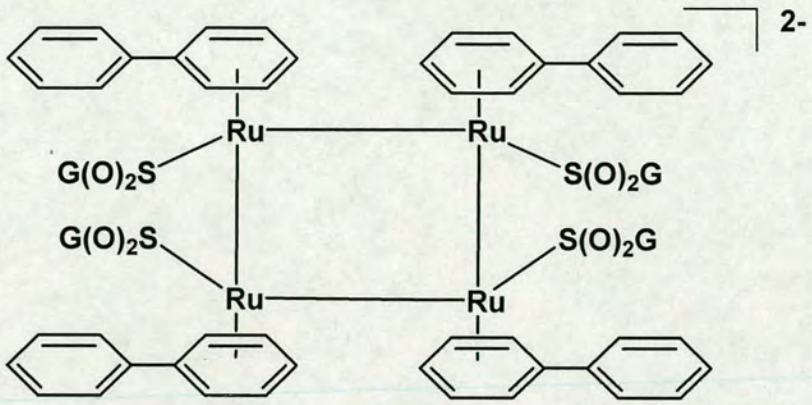

9

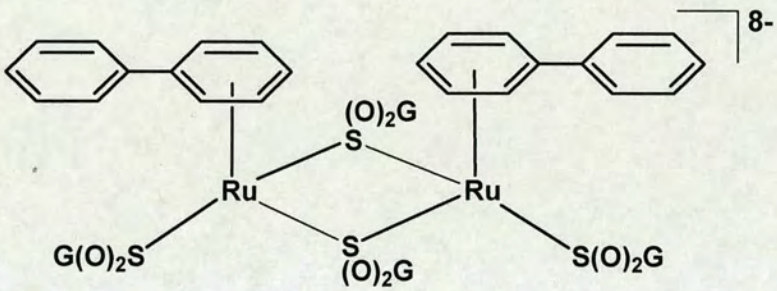

8

Chart 3.1 Proposed structures of tetra- and di- ruthenium glutathione sulfinate adducts. The exact nature of the bridges between the ruthenium atoms in these clusters is unknown.

A reaction mixture of complex **1** with GSH (2:20 mM) in unbuffered 66.6% ^{18}O-labelled water incubated at 310 K for 48 h was analysed using nanoLC-nanoESI-FT-ICR MS method described above. Two peaks appeared in the TIC chromatogram (Figure 3.16) and the mass spectra for the fractions eluting at 18.2 and 22.6 min are shown in Figure 3.17. The isotopic simulations (Figure 3.18) indicate that the fractions contain a tetra- and a di-ruthenium sulfinate/sulfenate glutathione complexes, respectively, of which the

oxygen atoms in sulfinate and sulfenate ligand were ^{18}O. FT-ICR MS was applied to the unambiguous determination of iron atom oxidation in a metalloprotein by matching experimental and theoretical isotopic abundance mass distribution.[24] The good fit between the experimental mass isotopic peaks and theoretical isotopic simulations (Figure 3.18) showed the oxidation states for the two Ru atoms in **8** may be zero, and the oxidation states for two Ru atoms in **9** may be +1 and the other two may be still +2.

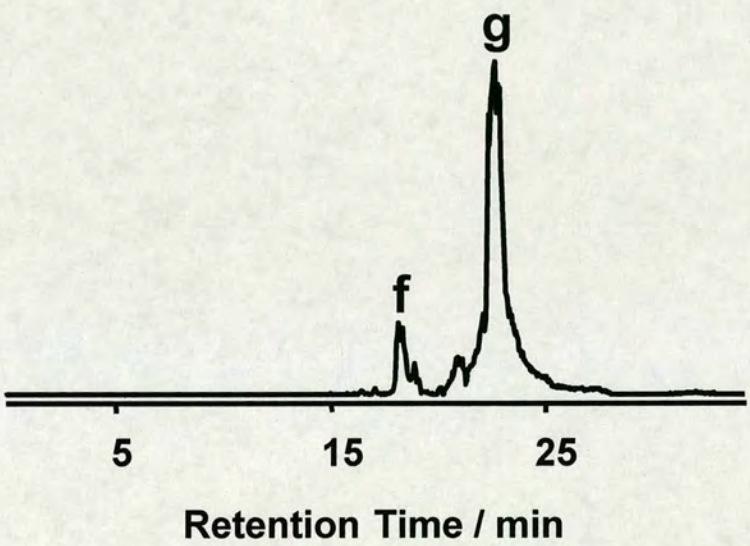

Figure 3.16 TIC chromatogram for the reaction of **1** with GSH (2:20 mM) in unbuffered 66.6% ^{18}O-labelled water incubated at 310 K for 48 h.

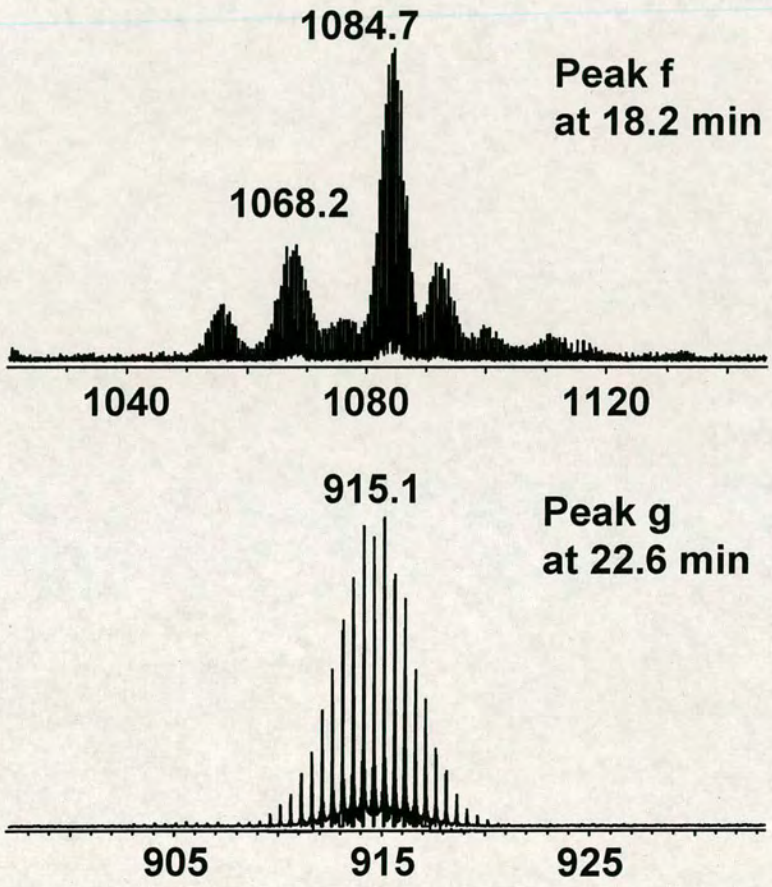

Figure 3.17 FT-ICR mass spectra for fractions at specific retention time (RT) of LC peaks f and g from the reactions of **1** and GSH 2:20 mM in 66.6% ^{18}O-labeled water (pH ~3) at 310 for 48 h as shown in Figure 3.16.

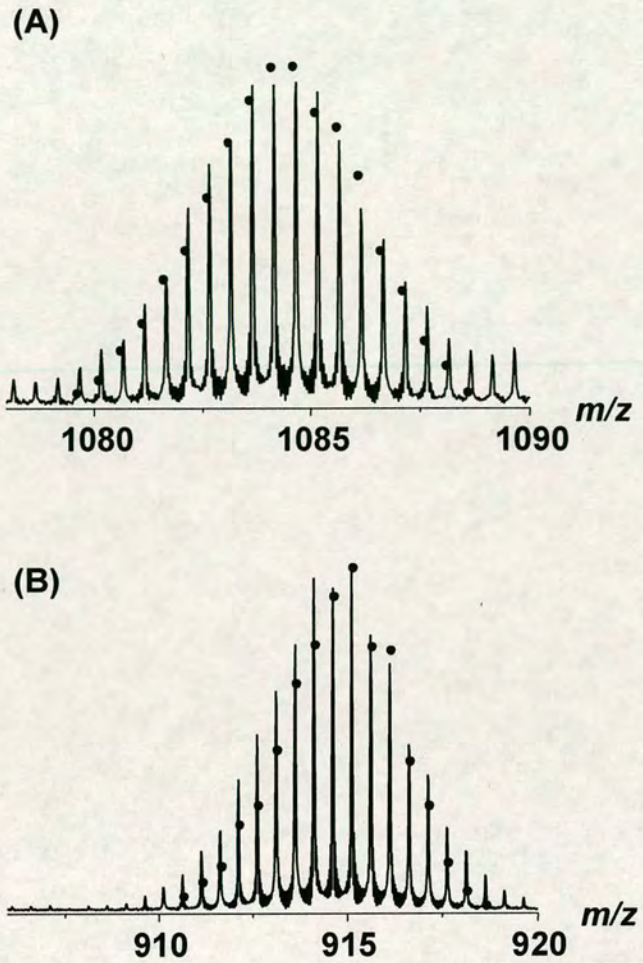

Figure 3.18 Isotopic model (dots, of which the values of X and Y correspond to the m/z and intensity of the respective isotopic ion peak) and mass spectral (lines) for fragmented ions of arene ruthenium ^{18}O-labelled sulfinate/sulfenate glutathione adducts (A) $\{[(\eta^6\text{-bip})Ru(S\text{-}GS^{18}O_2)]_4 - Glu - 5^{18}O + 4H\}^{2+}$ ($[C_{83}H_{96}O_{21}{}^{18}O_3S_4N_{11}Ru(II)_2Ru(I)_2]^{2+}$) and (B) $\{[(\eta^6\text{-bip})Ru(S\text{-}GS^{18}O_2)]_2 - 3^{18}O + 10H\}^{2+}$ ($[C_{64}H_{92}O_{24}{}^{18}O_5S_4N_{12}Ru(0)_2]^{2+}$). The simulation was carried out by Mr. Stefan Weidt.

Also under argon, the reaction of **1** with GSH under physiologically-relevant conditions (the result is shown in Figure 3.25 in **3.3.2**) gave rise to the di-ruthenated glutathione sulfenato/sulfinato adduct **8**, which illustrates that the oxygen atoms in sulfinate and sulfenate ligands of the di-ruthenated adduct **8** arise from solvent water. Water cannot act as an oxidant, so the function of water is only providing oxygen atoms in this

reaction. A similar contribution of water has been found in the oxidation of NHase by Cpx.[25] The thiol group in GSH is proposed to reduce the Ru(II) complex to Ru(0), and the redox reaction occurred between ruthenium atoms and sulphur atoms, in which Ru(+2) was reduced to Ru(0) while S(-2) was oxidized to S(0) and S(+2). Such similar redox reaction has been observed in the reactions of *trans*, *cis*-[Pt(en)$(OH)_2I_2$] with rHA.[26] Similarly, for complex **9**, when GS(-2)H was oxidized to GS(+2)O_2H by Ru(II) (Ru(+2) is reduced to Ru(+1)), oxygen atoms are provided from the solvent H_2O as shown by FT-ICR MS combined with ^{18}O-labelling experiments. The oxidation states of the sulfurs is given in Scheme 3.3.[26] The formation of Ru-Ru bonds, Ru-S bonds and Ru-S-Ru bonds as well as determination of the oxidation states of Ru atoms require the use of other technologies such as EXAFS for identification.

Scheme 3.3 Major pathways for thiol oxidation with oxidation states of sulfhur, reproduced from the literature 26.

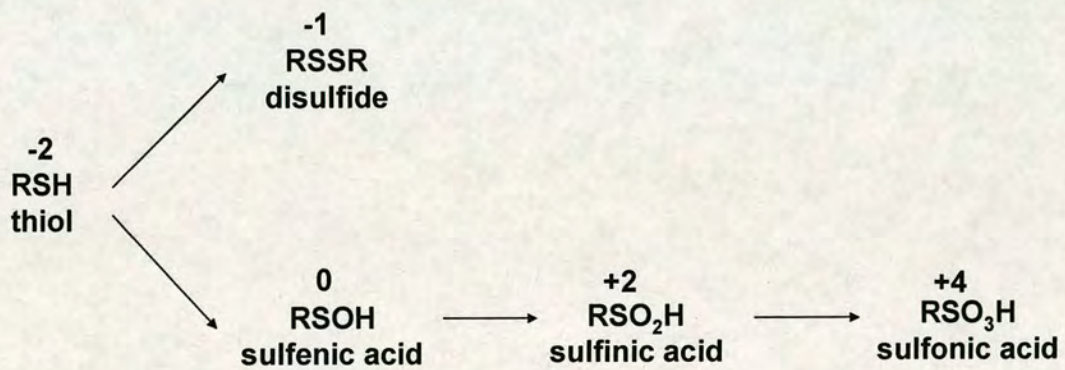

Ruthenium(0) arene complexes are usually useful catalysts for hydrogenation,[27,28] isomerization,[29] and dimerization[30] reactions of alkenes. The dinuclear Ru(0) arene complex with sulfenate (SO) bridges is reported here for the first time; whereas some multinuclear Ru(II) complexes with sulfur monoxide (SO) or sulfur dioxide (SO_2)

bridges, like $Ru_6C(CO)_{15}(SO)$ and $Ru_6C(CO)_{17}(SO_2)$, have been demonstrated before.[31] The diruthenium complex **8** may play a similar role to that of the mono-ruthenated sulfenate glutathione adduct [(η^6-bip)Ru(en)(GS(O)-*S*)] in the competitive reactions of **1** with GSH and guanine in DNA (see Chapter 4).

Few investigations of ruthenium(I) complexes have been reported.[32] Ru(I) complexes have shown very promising catalytic activities in hydrogenation and carbonylation of organic substrates,[33-36] and dinuclear Ru(I) complexes have unusual edge-sharing bioctahedral structures which stretch to other bridging anionic groups like pyrazolato or thiolato ligands.[37-39]

3.3.2 Reactions of 1 with GSH under Physiologically-relevant Conditions

The reaction of complex **1** (20 μM) with 250 mol equiv of GSH was studied in at physiologically-relevant conditions (the conditions similar to those which might be present in cells: micromolar Ru concentrations, in pH 7 phosphate buffer containing 22 mM NaCl (the cytoplasmic concentration of chloride)[40]) at 310 K.[41] To minimize the content of O_2, all starting solutions were purged of air by bubbling with N_2 before and after mixing.

The reaction course was different from that described above for unbuffered reactions. During the early stages (<12 h), HPLC peak i was dominant, but later (48 h) peak j increased in relative intensity (Figure 3.19). The mass spectrum of fraction i (Figure

3.20(A)) is identical to that of fraction f from the reaction of **1** with GSH in unbuffered aqueous solution (Figures 3.2 and 3.19), and corresponds to the thiolato adduct [(η^6-bip)Ru(en)(GS)] (**4**). A fragment ion MS peak at *m/z* 562.3 corresponding to release of the en ligand from this complex is observed, suggesting that S-bound glutathione can labilize the en ligand in **4**. For fraction j, a singly charged ion peak at *m/z* 638.3 was observed, corresponding unexpectedly to the sulfenato complex [(η^6-bip)-Ru(en)(GS(O))] (**10**) (calcd *m/z* 638.1 for {(η^6-bip)Ru(en)-(GS(O)) + H}$^+$), accompanied by a singly charged ion peak at *m/z* 324.0 corresponding to the release of the fragment {GSOH + 2H}$^+$ (calcd *m/z* 324.1; Figure 3.20). The amount of **10** in the reaction mixture increased from 11% (of the total Ru) after 12 h to 19% after 48 h.

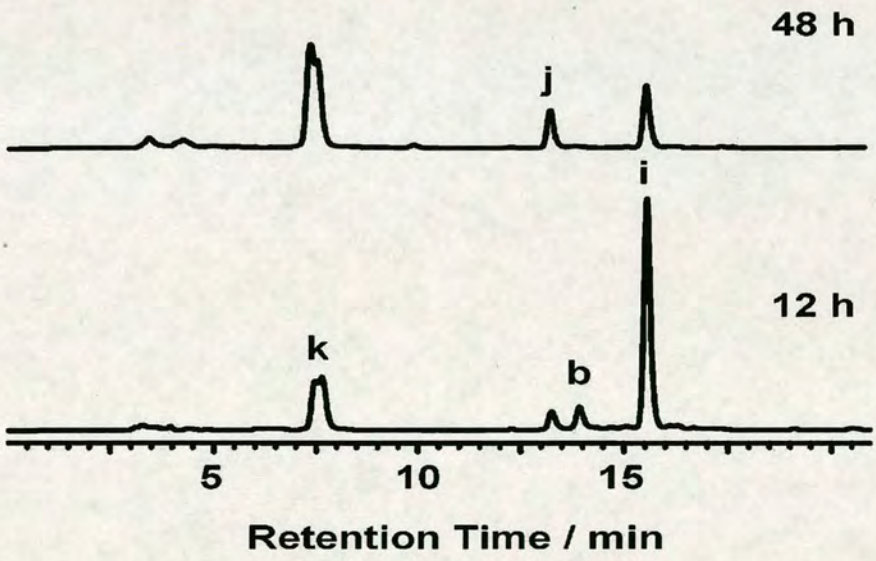

Figure 3.19 HPLC chromatograms recorded 12 and 48 h after the start of the reaction of complex **1** (20 μM) with a 250-fold molar excess of GSH in phosphate buffer (pH 7) containing 22 mM NaCl at 310 K. Peak assignments: (b) aqua adduct [(η^6-bip)Ru(en)(H_2O)]$^{2+}$ (**2**); (i) thiolato adduct **4**; (j) sulfenato adduct **10**; (k) GSH/GSSG (overlapped).

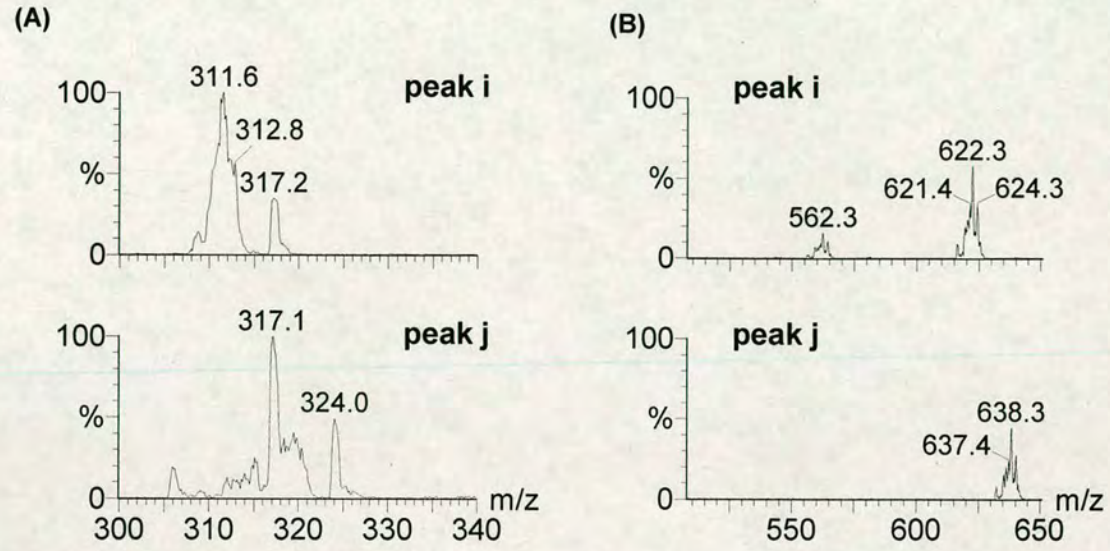

Figure 3.20 Mass spectra for HPLC fractions i and j (see Figure 3.19) in different *m/z* regions. It is notable that the mass spectrum for fraction i is the same as that for fraction f obtained from the reaction of **1** with a 10-fold molar excess of GSH at pH ca. 3 (see Figures 3.2 and 3.3).

From a reaction mixture containing complex **1** (1 mM) and GSH (25 mM) which had been incubated at 310 K for 24 h, the thiolato adduct [(η^6-bip)Ru(en)(GS)] (**4**) was isolated by preparative HPLC and characterized by 1D and 2D ^{1}H NMR spectroscopy. The pH* of the HPLC fraction was adjusted to 7, and after lyophilization the sample was dissolved in 90% H_2O/10% D_2O for NMR study. In the 2D [^{1}H, ^{1}H] COSY (Figure 3.21) and NOESY (Figure 3.22) NMR spectra, three sets of proton resonances are observed, assignable to the glutathione, biphenyl, and en groups. The chemical shifts for the former two groups are listed in Tables 3.8 and 3.9, respectively. It can be seen that ruthenium coordination induces large changes in the chemical shifts of the Cys β-CH_2, α-CH, and α-NH protons of the thiolate ligand. The signals of two CH_2 protons separate into two quartets (δ 2.96, 2.81), and the resonances of α-CH and α-NH protons are shifted to high field by 0.16 and 0.14 ppm, respectively, compared with those of the free

peptide. Strong NOEs signals are observed (Figure 3.23), corresponding to the interaction of the β-CH_2 protons with the protons of the coordinated phenyl ring (A) (the NMR assignments were made with the help of Dr. Fuyi Wang).

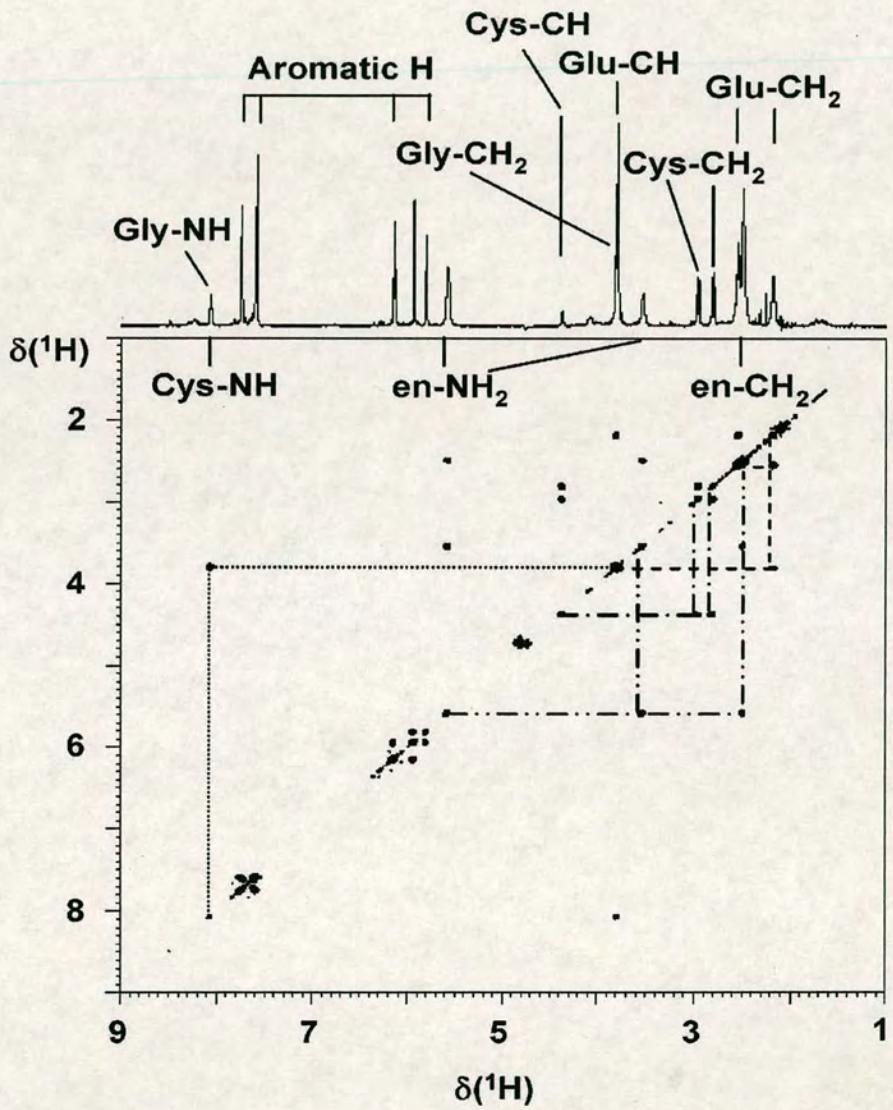

Figure 3.21 1D ^{1}H and 2D [^{1}H,^{1}H] COSY NMR spectra for HPLC fraction (i) (see Figure 3.19) from the reaction of **1** with GSH (5:25 mM) in phosphate buffer (pH 7) containing 22 mM NaCl at 310 K for 24 h.

Table 3.8 ^{1}H NMR chemical shifts (δ) for GSH and GSH ligands in the adduct [(η^6-bip)Ru(en)(GS-S)] (**4**) in 90% H_2O/10% D_2O at pH* 7 (298 K)

proton	δ (^{1}H) ($\Delta\delta$) [a]	
	GSH	**4**
		Glu
γ-CH_2	2.52	2.54 (0.02)
β-CH_2	2.13	2.20 (0.07)
α-CH	3.74	3.82 (0.08)
α-NH_3^+	- [b]	- [b]
		Cys
β-CH_2	2.95	2.96 (0.01)
	2.90	2.81 (-0.09)
α-CH	4.54	4.38 (-0.16)
α-NH	8.21	8.07 (-0.14)
		Gly
α-CH_2	3.94	3.81 (-0.13)
α-NH	8.25	8.31 (0.06)

[a] $\Delta\delta = \delta$ (**4**) - δ (GSH). [b] Not observed (fast exchange).

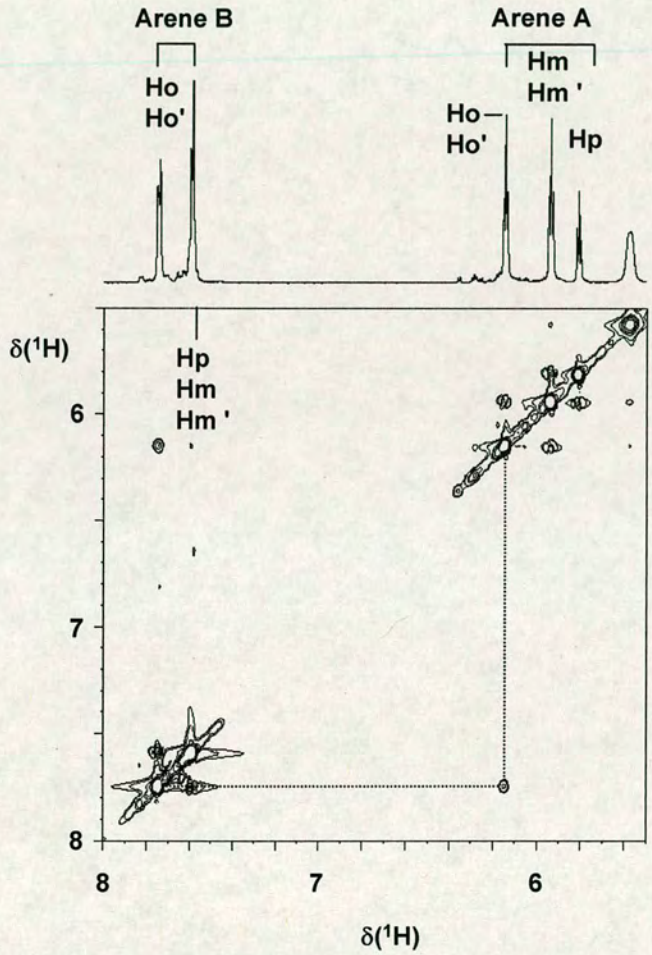

Figure 3.22 NOEs between the phenyl rings of the biphenyl ligand in the thiolato adduct [(η^6-bip)Ru(en)(GS-*S*)] (**4**), allowing assignments of peaks for aromatic protons. For proton labelling, see Figure 3.23.

Table 3.9 ^{1}H NMR chemical shifts for biphenyl ligands in complex **1** and the adduct [(η^6-bip)Ru(en)(GS-*S*)] (**4**) in 90% H_2O / 10% D_2O (298 K)

Proton[a]	Complex (pH*)	
	1 (5.5)[b]	**4** (7.3)
	δ	
Phenyl ring A		
Ho	5.98	5.95
Ho′	5.98	5.95
Hm	6.26	6.16
Hm′	6.26	6.16
Hp	5.91	5.81
Phenyl ring B		
Ho	7.83	7.75
Ho′	7.83	7.75
Hm	7.64	7.61
Hm′	7.64	7.61
Hp	7.64	7.61

[a] For proton labels, see Figures 3.23. [b] Wang, F. Y.; Chen, H. M.; Parkinson, J. A.; Murdoch, P. D.; Sadler, P. J. *Inorg. Chem.* **2002,** *41*, 4509-4523.

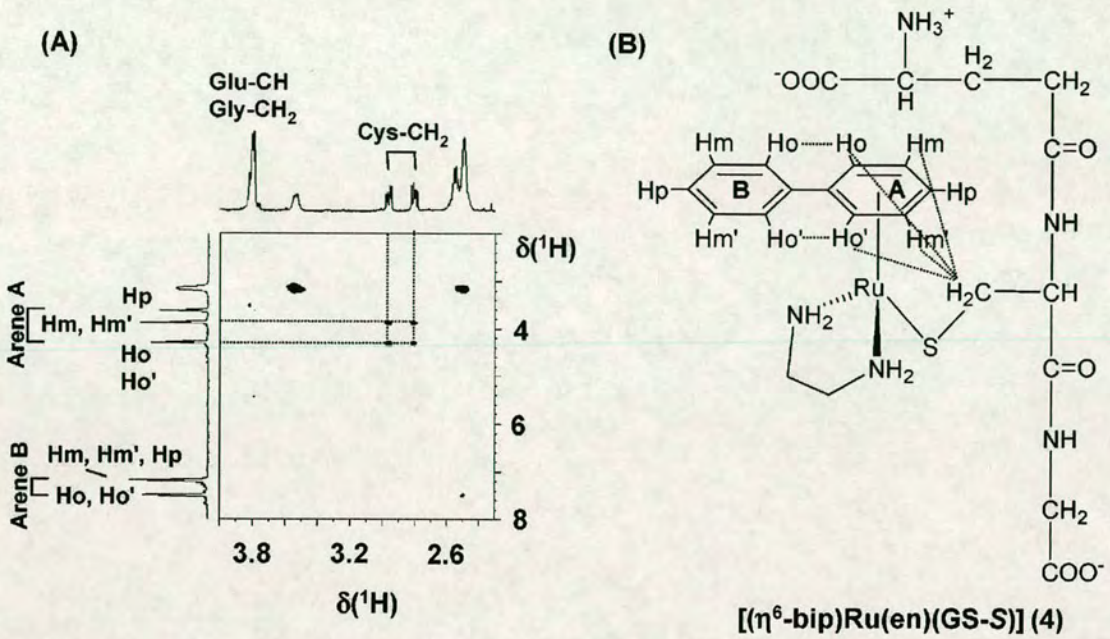

Figure 3.23 (A) NOEs between the biphenyl and Cys β-CH_2 protons in complex **4**, indicating their proximity (<ca. 5 Å apart). (B) Structure for **4** with NOEs indicated by dotted lines. For NOEs between protons of the two phenyl rings, see Figure 3.22.

HPLC and MS studies (Figures 3.24 and 3.25) showed that the thiolato adduct **4** is not stable in air at pH 7, but is converted to the sulfenato complex **10**, instead of into the diruthenium thiolato complex $[((\eta^6\text{-bip})Ru)_2(GS)_3]^{2-}$ (**7**) as at pH 3. This instability was first observed over a period of 3 d while NMR spectra of an HPLC-isolated sample of **4** (pH* 7) were being recorded; during that time 52%[42] of **4** transformed into **10** (Figure 3.24), supporting the proposed pathway (Scheme 3.4) to **10** by oxygenation of **4**.

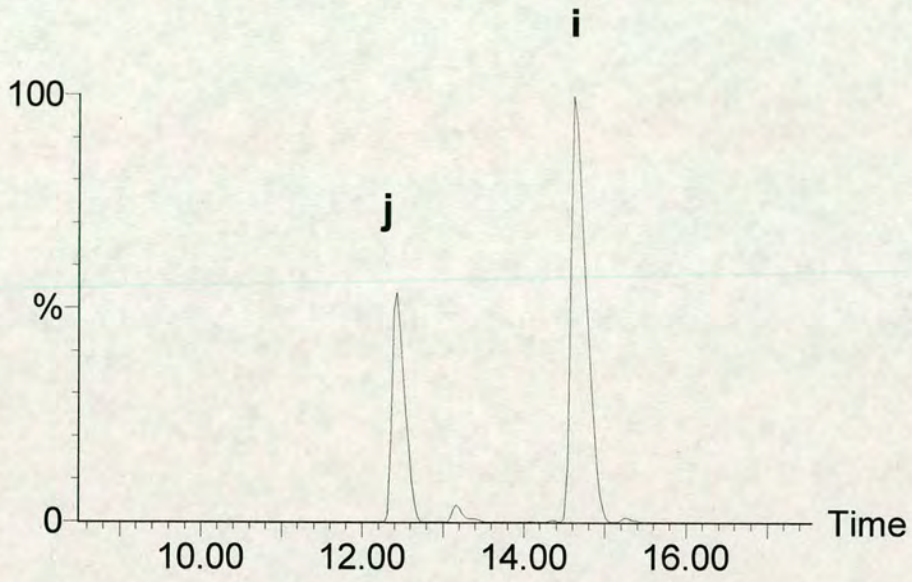

Figure 3.24 HPLC chromatogram with UV detection at 254 nm for an HPLC-isolated sample of the thiolato adduct [(η^6-bip)Ru(en)(GS-*S*)] (**4**), obtained from the reaction of complex **1** with GSH (1:10 mM) in phosphate buffer (pH 7) containing 22 mM NaCl at 310 K for 24 h, after standing for 3 d whilst NMR spectra were recorded. The partial oxidation of the thiolato complex **4** (peak i) to the sulfenato complex [(η^6-bip)Ru(en)(GS(O)-*S*)] (**10**) (peak j) is evident.

A comparison was also made between the HPLC profiles for reactions carried out under O_2 and under argon (Figure 3.25(A)). For reactions under O_2, the sulfenato product **8** was dominant, and little of **4** remained after 48 h reaction; however, under Ar the thiolato adduct **4** was dominant, and little of **10** was formed, which strongly suggests that the sulfenate arises from oxidation of the thiolato complex and that the oxygen atom in the sulfenate originates from O_2. For the reaction under Ar, two new HPLC peaks with retention times of 16.60 and 17.04 min were observed, labeled l in Figure 3.25. The mass spectrum of fraction l (Figure 3.25(B)), separated from a mixture of 1 mM **1** and 10 mM GSH in pH 7 buffer containing 22 mM NaCl at 310 K which had reacted for 48

h under Ar, suggested that it may contain a novel diruthenium thiolato/ sulfinato adduct (**8**; see Figure 3.25).

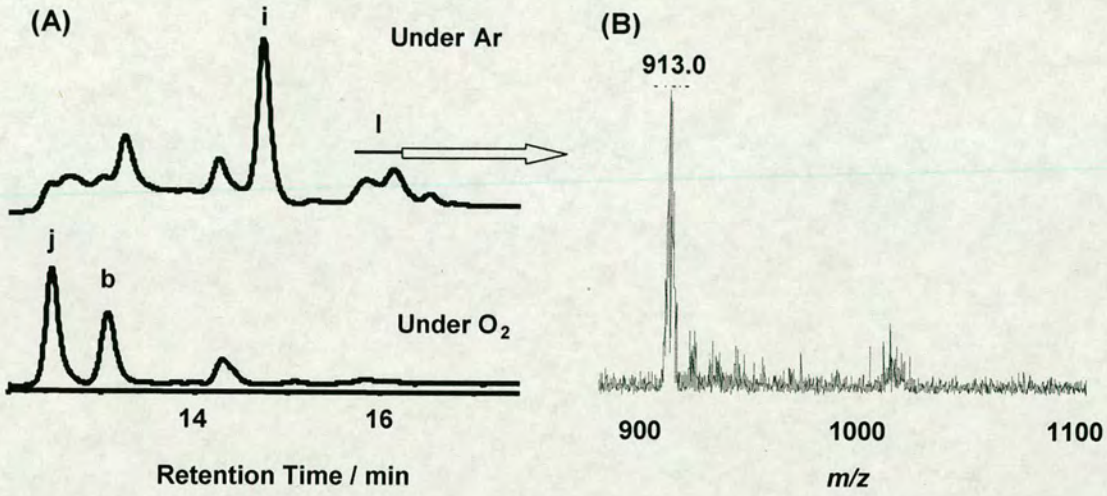

Figure 3.25 (A) HPLC chromatograms for reactions of complex **1** (20 μM) with a 250-fold molar excess of GSH in phosphate buffer (10 mM, pH 7) containing 22 mM NaCl under O_2 (bottom) or Ar (top) at 310 K for 48 h. Peak assignments: (b) $[(\eta^6\text{-bip})Ru(en)(H_2O)]^{2+}$ (**2**); (i) thiolato adduct **4**; (j) sulfenato adduct **10**; (l) dinuclear adduct **8**. (B) Mass spectrum for HPLC fraction l containing the adduct **8**.

Scheme 3.4 Pathways for Reactions of Complex **1** with GSH at pH 7

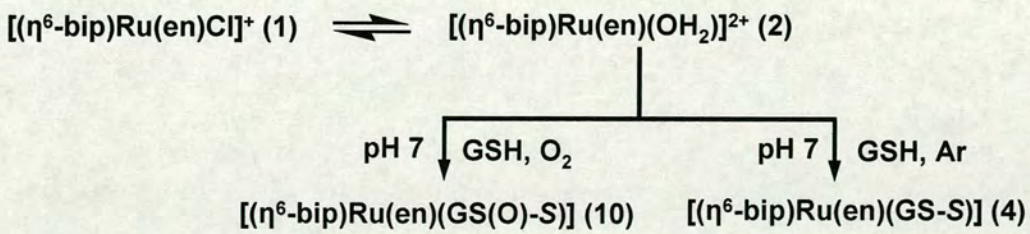

Sulfenic acids are generally too reactive to isolate,[43] but a few examples are known in which they are stabilized by binding to transition metal ions such as Co^{III},[44] Ni^{II},[45] $Ru^{II/III}$,[46] Rh^{III},[47] and Ir^{III}.[48] The sulfenato complex **10** obtained here is a new example of the stabilization of a sulfenate by coordination to a transition metal. In principle binding of the sulfenate to Ru^{II} could occur through sulfur or oxygen. In the reported X-ray structures of Ru^{II} and Ru^{III} sulfenate complexes, the sulfenate is S-bonded.[46] A similar situation exists for sulfoxides, for which S-bonding is common, although both modes of binding are known.[49] It seems likely that the preferred mode of binding of glutathione sulfenate in [(η^6-bip)Ru(en)-(GS(O))] (**10**) is also through sulfur, as suggested by the SO stretching frequency (vide infra).

A characteristic infrared S=O stretching frequency of 1018 cm^{-1} was observed for **10** by Dr. Fuyi Wang (data not shown), a frequency similar to those reported for the S-bonded sulfenates in $[IrCl_2(CO)(PPh)_3(S(O)Me)]$ (1013 cm^{-1})[48] and $[CpW(CO)_3(CH_2S(O)Me)]$ (1017 cm^{-1})[50] and not nearly so low as the 855 cm^{-1} found for the *O*-sulfinates (ν_{as}(SOIr)) in complex Ir(*O*-O_2S-*p*-tolyl)(CO)(PPh_3)$_2$,[48] evidence for S coordination in the sulfenate **10**.

In the process of oxidation of thiolate, sulfenate can be further oxidized to sulfinate (Scheme 3.5).[51] However, in the reaction of **1** with GSH at pH 7, the oxidation of thiolate stays at sulfenate due to the presence of GSH which acted as reductant.

Scheme 3.5 Oxidation pathway for metal-binding thiols.

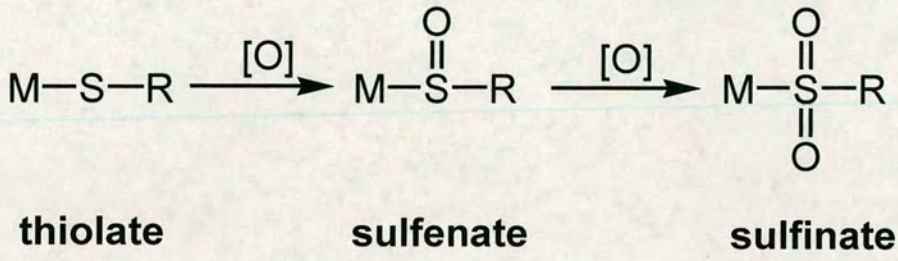

3.3.3 Reactions of 1 with GST in Tris Buffer

The reaction of complex **1** with GST in Tris buffer (pH 8) was investigated using UV-Vis and FT-ICR MS. Compared to the spectrum of GST (blue trace in Figure 3.26), the spectra for the reaction of **1** (80 μM) with GST (20 μM) in Tris buffer (pH 8) at 310 K showed that the absorption for the band of 278 nm decreased as the time passed (see Figure 3.26). The band is due to the effects of conjugation of adjacent benzene chromophores, the spectrum of biphenyl above 185 nm consists of two broad and intense bands at 202 nm and 248 nm.[52] CT transitions Ru → C_6H_6 (transitions from the metal into π* orbital) are found around 250 nm in $[Ru(C_6H_6)Cl_2]_2$.[53]

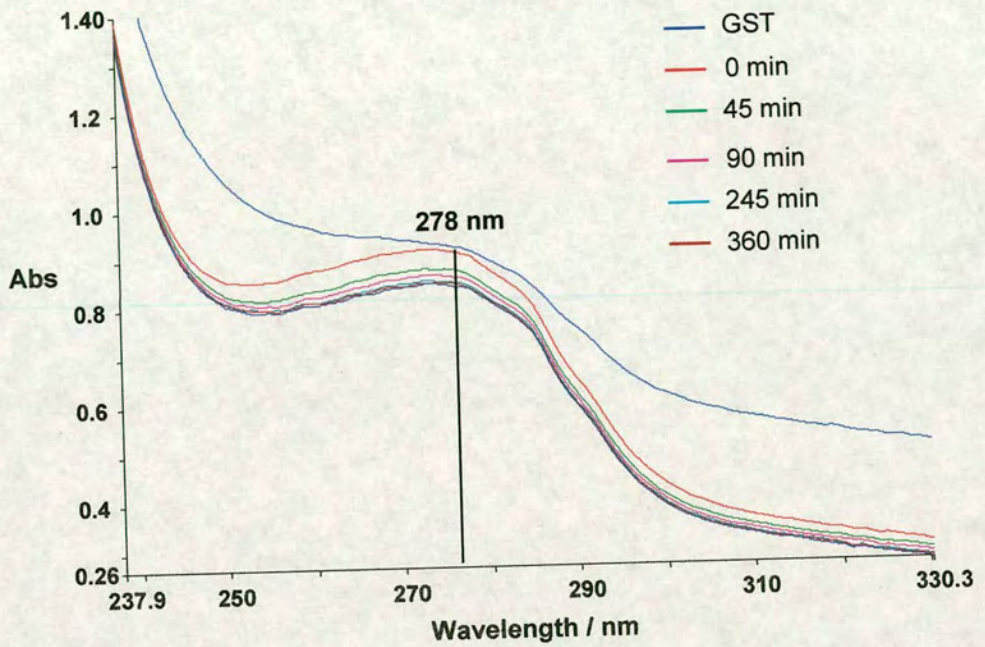

Figure 3.26 UV-Vis time course for the reaction of **1** (80 μM) with GST (20 μM) in Tris buffer (pH 8) at 310 K except for the blue trace (see the labels in the Figure).

The GST protein was synthesized, purified and identified by Ms. Ann Marie Reid using FT-ICR MS (data not shown), and the molecular weight for the GST used in this work was confirmed as 27482 Da.[15] The reaction mixture of **1** (80 μM) and GST (20 μM) in Tris buffer (pH 8) at 310 K for 6 h was analysed by Mr. Stefan Weidt using FT-ICR MS, and an ion peak centred at *m/z* 1172.31 with 24 positive charges was detected, assignable to a di-ruthenated GST adduct **11** $\{[(\eta^6\text{-bip})Ru(en)]_2(GST)+22H\}^{24+}$ (Figure 3.27), and no sulfenate or sulfinate products were observed in the reaction.

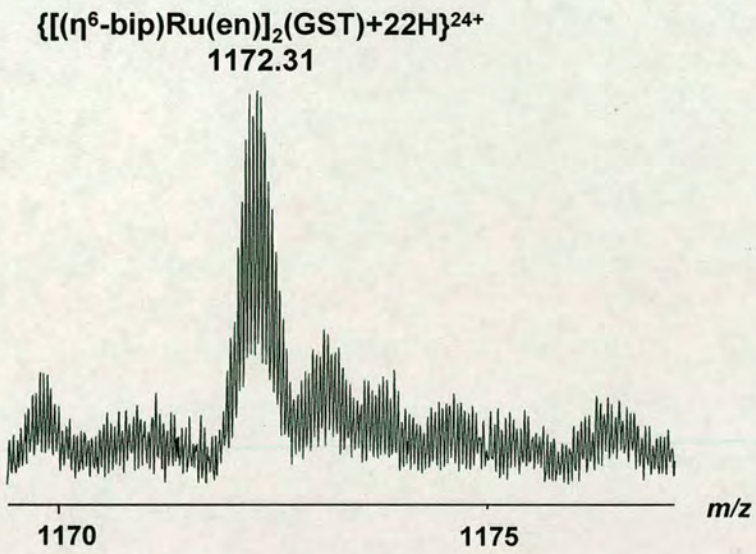

Figure 3.27 FT-ICR mass spectrum for the reactions mixture of **1** (80 μM) and GST (20 μM) in Tris buffer (pH 8) at 310 K for 6 h.

There has been a rapidly growing interest in the redox behaviour of cysteine residues in peptides and proteins in recent years. Sulfur has several different oxidation states (as shown in Scheme 3.3) in biological systems, and it takes part in many diverse redox reactions.[54,55] Previous work has shown that after ruthenium complex **1** binds to GSH, an oxygen atom is easily added to oxidize the thiolato adduct to the sulfenato adduct which provides a facile route for displacement of S-bound glutathione by guanine N7.[7] Therefore, in the presence of air, the ruthenated GST adduct **11** is probably oxidized to the corresponding sulfenato adduct by O_2 or H_2O_2 (mild oxidant), which will change the function of GST. Even if the sulfenato adduct is easily substituted by guanine bases in DNA and RNA, formation of sulfenic acids in protein plays a role in enzyme catalysed oxidations due to protein sulfenic acids are good electrophilic centres which are well suited for participation in oxidative catalysis,[56] redox regulation,[57] and redox signalling.[58]

3.4 Summary

Cells contain high (millimolar) concentrations of the tripeptide glutathione which has several binding sites for metal ions: the amino and carboxylate groups at the Glu terminus, carboxylate at the Gly terminus, and thiolate sulfur of the central Cys residue. Binding to the deprotonated amide nitrogen of Cys is possible when a N/S chelate ring can be formed, as has been observed for platinum amine complexes.[59] For heavier, "soft" transition metal ions, thiolate sulfur is a particularly strong site, and for Pt^{II}, such bonds are essentially formed irreversibly. Elevation of GSH levels therefore provides cells with detoxification and resistance mechanisms. The aim of this work was therefore to investigate reactions of the organometallic Ru^{II} arene anticancer complex $[(\eta^6\text{-bip})Ru(en)Cl]^+$ with GSH. The strategy involved separation of the products by HPLC and identification by ESI-MS, and after preparative HPLC, characterization by NMR spectroscopy. ^{15}N-labeling of the chelated ethylenediamine ligand and use of 2D [^1H, ^{15}N] HSQC NMR spectroscopy was helpful for elucidation of some of the complicated reaction pathways.

First reactions were studied at 310 K (body temperature) in unbuffered aqueous solution, since buffers themselves usually contain potential ligands. Hydrolysis of **1** was followed by initial binding to the carboxylate sites and then to the thiolate sulfur (Scheme 3.2), but at this acidic pH (3) displacement of en by further S-bound GSH ligands was favorable, and, after 24 h, the major product was the dinuclear S-bridged complex $[((\eta^6\text{-bip})Ru)_2(GS\text{-}\mu\text{-}S)_3]^{2-}$ (**7**). Ruthenium arene complexes induce oxidation of coordinated glutathione to give rise to two multinuclear complexes as the main products which were unambiguously identified as a diruthenium sulfinate/sulfenate complex **8** and a tetraruthenium sulfinate complex **9**, respectively, though the metal oxidation state and coordination model will need to be confirmed by further experiments. With ^{18}O-labelled water as solvent, FT-ICR MS analysis indicated that

all oxygen atoms in sulfenate and sulfinate products arise from water, implying that water may be involved in the oxygenation of cysteine-sulfur in biological signalling processes. The developed method will be helpful to investigate the oxygenation of cysteinyl groups in thiol-containing proteins resulting from coordination of ruthenium anticancer complexes. Although ruthenium(0) complexes have been widely used as catalysts,[27-30] the di-ruthenated complex **8** studied in this work may play an important role in the biological reactions of Ru(II) arene anticancer complexes.

Subsequent reactions were studied at pH 7 using phosphate buffer in the presence of a typical cytoplasmic concentration of chloride (22 mM) and at Ru concentrations relevant to cytotoxicity (micromolar). Here, in N_2-purged solutions, the S-bound adduct [(η^6-bip)Ru(en)(GS-*S*)] (**4**) was the major product, and there was little tendency for loss of the en ligand. However, unexpectedly, complex **4** was very sensitive to the presence of air and underwent oxidation to the sulfenato complex [(η^6-bip)Ru(en)(GS(O)-*S*)] (**10**).

When reactions were carried out in an atmosphere of O_2, the sulfenato complex **10** was the main product, suggesting that the oxygen atom in the sulfenate ligand arises from O_2. Intriguingly, reactions carried out under strictly anaerobic conditions under Ar gave rise not only to the expected thiolato adduct **4** but also to an apparent dinuclear complex **8** as well as obtained in the reaction in unbuffered water.

Preliminary studies on reactions of **1** with GST protein in Tris buffer (pH 8) were undertaken. The reaction of **1** with GST (80:20 μM) in Tris buffer (pH 8) gave rise to a di-ruthenated GST adduct **11**, and further investigation of the oxidation of **11** to a

sulfenate/sulfinate adduct and effect on the biological functions of GST will need, such as detoxication of the cell against toxic and carcinogenic compounds, and cellular mechanism of drug resistance.

Due to the formation of sulfenato/sulfinato adducts for these ruthenium arene complexes which is not observed for Pt anticancer complexes in the reactions of **1** with GSH under the physiologically-relevant conditions (phosphate buffer, pH 7, 22 mM NaCl) at 310 K, further investigations on the competitive reactions of **1** with GSH and cGMP/DNA oligonucleotides under physiologically-relevant conditions will be described in Chapter 4.

3.5 References

[1] (a) Frasca, D. R.; Clarke, M. J. *J. Am. Chem. Soc.* **1999**, *121*, 8523-8532. (b) Clarke, M. J.; Zhu, F.; Frasca, D. R. *Chem. ReV.* **1999**, *99*, 2511-2533 and references therein. (c) Sava, G.; Alessio, E.; Bergamo, E.; Mestroni, G. *Top. Biol. Inorg. Chem.* **1999**, *1*, 143-170. (d) Frasca, D.; Ciampa, J.; Emerson, J.; Umans, R. S.; Clarke, M. J. *Metal-Based Drugs* **1996**, *3*, 197209.

[2] Bennett, M. A.; Byrnes, M. J.; Kovacik, I. *J. Organomet. Chem.* **2004**, *689*, 4463-4474 and references therein.

[3] (a) Aird, R. E.; Cummings, J.; Ritchie, A. A.; Muir, M.; Morris, R. E.; Chen, H.; Sadler, P. J.; Jodrell, D. I. *Br. J. Cancer* **2002**, *86*, 1652-1657. (b) Morris, R. E.; Aird, R. E.; Murdoch, P. D.; Chen, H. M.; Cummings, J.; Hughes, N. D.; Parsons, S.; Parkin, A.; Boyd, G.; Jodrell, D. I.; Sadler, P. J. *J. Med. Chem.* **2001**, *44*, 3616-3621.

[4] (a) Barnham, K. J.; Guo, Z. J.; Sadler, P. J. *J. Chem. Soc., Dalton Trans.* **1996**, 2867-2876. (b) Barnham, K. J.; Djuran, M. I.; Murdoch, P. D.; Sadler, P. J. *J. Chem. Soc., Chem. Commun.* **1994**, 721-722. (c) Barnham, K. J.; Djuran, M. I.; Murdoch, P. D.; Ranford, J. D.; Sadler, P. J. *J. Chem. Soc., Dalton Trans.* **1995**, 3721-3726. (d) Teuben, J. M.; Reedijk, J. *J. Biol. Inorg. Chem.* **2000**, *5*, 463-468. (e) Bugarcic, Z. D.; Soldatovic, T.; Jelic, R.; Alguero, B.; Grandas, A. *Dalton Trans.* **2004**, 3869-3877.

[5] Wang, F. Y.; Chen, H. M.; Parkinson, J. A.; Murdoch, P. D.; Sadler, P. J. *Inorg. Chem.* **2002**, *41*, 4509-4523.

[6] Reedijk, J. *Chem. Rev.* **1999**, *99*, 2499-2510.

[7] Wang, F. Y.; Xu, J.; Habtemariam, A.; Bella, J.; Sadler, P. J. *J. Am. Chem. Soc.* **2005,** *127*, 17734-17743.

[8] Dyson P. J.; Johnson, B. F. G.; McIndoe, J. S.; Langridge-Smith, P. R. R. *Inorg. Chem.* **2000**, *39*, 2430-2431.

[9] Butcher, C. P. G.; Dinca, A.; Dyson, P. J.; Johnson, J. S.; Langridge-Smith, P. R. R.; McIndoe, J. S. *Angew. Chem. Int. Ed.* **2003**, *42*, 5752-5755.

[10] Dyson, P. J.; Hearley, A. K.; Johnson, B. F. G.; Khimyak, T.; McIndoe, J. S.; Langridge-Smith, P. R. R *Organometallics* **2001**, *20*, 3970-3974.

[11] Hayes, J. D.; Pulford, D. J. *Crit. Rev. Biochem. Mol. Biol.* **1995**, *30*, 445-600.

[12] Mahajan, S.; Atkins, W. M. *Cell. Mol. Life Sci.* **2005**, *62*, 1221-1233.

[13] Cardoso, R. M. F.; Daniels, D. S.; Bruns, C. M.; Tainer, J. A. *Proteins: Structure, Function, and Genetics* **2003**, *51*, 137-146.

[14] Chen, H.; Parkinson, J. A.; Parsons, S.; Coxall, R. A.; Gould, R. O.; Sadler, P.J. *J. Am. Chem. Soc.* **2002**, *124*, 3064-3082.

[15] Shi, B.; Stevenson, R. Campopiano, D. J.; Greaney, M. F. *J. Am. Chem. Soc.* **2006**, *128*, 8459-8467.

[16] Ellman, G. L. *Arch. Biochem. Biophys.* **1959**, *82*, 70-77.

[17] Under the conditions used in this work, coordinated GS has an overall charge of -2. Similarly coordinated GSO and GSO2 are assumed to have charges of -2 in the formulae.

[18] Rau, T.; Alsfasser, R.; Zahl, A.; van Eldik, R. *Inorg. Chem.* **1998**, *37*,4223-4230.

[19] Wang, F. Y.; Chen, H.; Parkinson, J. A.; Murdoch, P. D.; Sadler, P. J. *Inorg. Chem.* **2002**, *41*, 4509-4523.

[20] Wang, F. Y.; Bella, J.; Parkinson, J. A.; Sadler, P. J. *J. Biol. Inorg. Chem.* **2005**, *10*, 147-155.

[21] Wang, F. Y.; Chen, H. M.; Parsons, S.; Oswald, L. D. H.; Davidson, J. E.;

Sadler, P. J. *Chem.sEur. J.* **2003**, *9*, 5810-5820.

[22] Burkhard, R. K.; Seliers, D. E.; DeCou, F.; Lambert, J. L. *J. Org. Chem.* **1959**, *24*, 767-769.

[23] Cox, P. A.; Anthony, P. *Inorganic Chemistry* Oxiford University Press **2000**.

[24] He, F.; Hendrickson, C. L.; Marshall, A. G. *J. Am. Soc. Mass Spectr.*, **2000**, *11*, 120-126.

[25] Tsujimura, M.; Odaka, M.; Nakayama, H.; Dohmae, N.; Koshino, H.; Asami, T.; Hoshino, M.; Takio, K.; Yoshida, S.; Maeda, M.; Endo, I. *J. Am. Chem. Soc.* **2003**, *125*, 11532-11538.

[26] Kratochwil, N. A.; Ivanov, A. I.; Patriarca, M.; Parkinson, J. A.; Gouldsworthy, A. M.; Murdoch, P. del S.; Sadler, P. J. *J. Am. Chem. Soc.* **1999**, *121*, 8193-8203.

[27] Pertici, P.; Vitulli, G.; Bigelli, C.; Lazaron, R. *J. Organomet. Chem.* **1984**, *275*, 113-117.

[28] Bennett, M. A.; Neumann, H.; Thomas, M.; Wang, X.; Vitulli, G.; Pertici, P.; Salvadori, P. *Organometallics* **1991**, *10*, 3237-3245.

[29] Pertici, P.; Barretta, G. U.; Burzagli, F.; Salvadori, P.; Bennett, M. A. *J. Organomet. Chem.* **1991**, *413*, 303-311.

[30] Pertici, P.; Ballantini, V.; Salvadori, P.; Bennett, M. A. *Organometallics* **1995**, *14*, 2565-2569.

[31] Chihara, T.; Kubota, H.; Fukumoto, M.; Ogawa, H.; Yamamoto Y.; Wakatsuki, Y. *Inorg. Chem.* **1997**, *36*, 5488-5497.

[32] Cabeza, J. A.; Fernandez-Colinas, J. M. *Coord. Chem. Rev.* **1993**, *126*, 319-336.

[33] Jenck, J.; Kalck, P.; Pinelli, E.; Siani, M.; Thorez, A. *J. Chem. Soc., Chem. Commun.* **1988**, 1428-1430.

[34] Matteoli, U.; Menchi, G.; Bianchi, M.; Piacenti, F. *J. Mol. Catal.* **1991**, *64*, 257-267.

[35] Frediani, P.; Bianchi, M.; Salvini, A.; Carluccio, L.; Rosi, L. *J. Organomet. Chem.* **1997**, *547*, 35-40.

[36] Salvini, A.; Frediani, P.; Rivalta, E. *Inorg. Chim. Acta* **2003**, *351*, 225-234.

[37] Frediani, P. Bianchi, M.; Salvini, A.; Guarducci, R.; Carluccio, L. C.; Piacenti, F.; Ianelli, S.; Nardelli, M. *J. Organomet. Chem.* **1993**, *463*, 187-198.

[38] Sherlock, S. J.; Cowie, M.; Singleton, E.; Steyn, M. M. de V. *Organometallics* **1988**, *7*, 1663-1666.

[39] Shiu, K. B.; Chen, J. Y.; Lee, G. H.; Liao, F. L.; Ko, B. T.; Wang, Y.; Wang, S. L.; Lin, C. C. *J. Organomet. Chem.* **2002**, *658*, 117-125.

[40] Jennerwein, M.; Andrews, P. A. *Drug Metab. Dispos.* **1995**, *23*, 178-184.

[41] The concentrations of **1**, GSH, and NaCl were chosen so as to be within the ranges present in the cell cytoplasm.

[42] Calculated on the basis of HPLC peak areas for adducts **4** and **8**, calibrated by ICP-OES (Table 3.1).

[43] (a) Claiborne, A.; Yeh, J. I.; Mallett, T. C.; Luba, J.; Crane, E. J.; Charrier, V.; Parsonage, D. *Biochemistry* **1999**, *38*, 15407-15416. (b) O'Donnell, J. S.; Schwan, A. L. *J. Sulfur Chem.* **2004**, *25*, 183-211.

[44] (a) Weigand, W.; Wu¨nsch, R. *Chem. Ber.* **1996**, *129*, 1409-1419. (b) Jackson, W. G.; Sargeson, A. M.; Whimp, P. O. *J. Chem. Soc., Chem. Commun.* **1976**, 934-935. (c) Adzamli, I. K.; Libson, K.; Lydon, J. D.; Elder, R. C.; Deutsch, E. *Inorg. Chem.* **1979**, *18*, 303-311. (d) Kung, I.; Schweitzer, D.;

Shearer, J.; Taylor, W. D.; Jackson, H. L.; Lovell, S.; Kovacs, J. A. *J. Am. Chem. Soc.* **2000**, *122*, 8299-8300.

[45] Buonomo, R. M.; Font, I.; Maguire, M. J.; Reibenspies, J. H.; Tuntulani, T.; Darensbourg, M. Y. *J. Am. Chem. Soc.* **1995**, *117*, 963-973.

[46] (a) Shiu, K.-B.; Chen, J.-Y.; Yu, S.-J.; Wang, S.-L.; Liao, F.-L.; Wang, Y.; Lee, G.-H. *J. Organomet. Chem.* **2002**, *648*, 193-203. (b) Sellmann, D.; Hein, K.; Heinemann, F. W. *Eur. J. Inorg. Chem.* **2004**, 3136-3146. (c) Dilworth, J. R.; Zheng, Y.; Lu, S.; Wu, Q. *Transition Met. Chem.* **1992**, *17*, 364-368.

[47] Kita, M.; Yamanari, K.; Shimura, Y. *Bull Chem. Soc. Jpn* **1983**, *56*, 32723275.

[48] (a) George, T. A.; Watkins, D. D. *Inorg. Chem.* **1973**, *12*, 398-402. (b) Reed, C. A.; Roper, W. R. *Chem. Commun.* **1971**, 1556-1557.

[49] (a) Alessio, E.; Balducci, G.; Calligaris, M.; Costa, G.; Attia, W. M.; Mestroni, G. *Inorg. Chem.* **1991**, *30*, 609-618. (b) Iengo, E.; Mestroni, G.; Geremia, S.; Calligaris, M.; Alessio, E. *J. Chem. Soc., Dalton Trans.* **1999**, 3361-3371. (c) Tanase, T.; Aiko, T.; Yamamoto, Y. *Chem. Commun.* **1996**, 2341-2342. (d) Geremia, S.; Mestroni, S.; Calligaris, M.; Alessio, E. *J. Chem. Soc., Dalton Trans.* **1998**, 2447-2448.

[50] Schenk, W. A.; Frisch, J.; Adam, W.; Prechtl, F. *Inorg. Chem.* **1992**, *31*, 3329-3331.

[51] Weigand, W.; Wunsch, R. *Chem. Ber.* **1996**, *129*, 1409-1419.

[52] Lambert, J. B.; Shurvell, H. F.; Lightner, D. A.; Cooks, R. G. *Organic Structural Spectroscopy* Prentice-Hall Inc., New Jersey **1998**.

[53] Tom Dieck, H.; Kollvitz, W.; Kleinwachter, I. *Organometallics* **1986**, *5*, 1449-1457.

[54] Giles, N. M.; Watts, A. B.; Giles, G. I.; Fry, F. H.; Littlechild, J. A.; Jacob, C. *Chem. Biol.* **2003**, *10*, 677-693.

[55] Jacob, C.; Giles, G. I.; Giles, M. N.; Sies, H. *Angew. Chem. Int. Ed. Engl.* **2003**, *42*, 4742-4758.

[56] Allison, W. S. *Acc. Cheml. Res.* **1976**, *9*, 293-299.

[57] Claiborne, A.; Yeh, J. I.; Mallett, T. C.; Luba, J.; Crane, E. J.; Charrier, V.; Parsonage, D. *Biochemistry* **1999**, *38*, 15407-15416.

[58] Poole, L. B.; Karplus, P. A.; Claiborne, A. *Annu. Rev. Pharmacol. Toxicol.* **2004**, *44*, 325-347.

[59] Murdoch, P. del S.; Kratochwil, N. A.; Parkinson, J. A.; Patriarca, M.; Sadler, P. J. *Angew. Chem., Int. Ed.* **1999**, *38*, 2949-2951.

Chapter 4

Competition between Glutathione and cGMP/oligonucleotides for a Ru(II) Arene Anticancer Complex

4.1 Introduction

DNA is a potential target for organometallic Ru(II) arene anticancer complexes of the type $[(\eta^6\text{-arene})Ru(II)(en)Cl][PF_6]$ (en = ethylenediamine), which exhibit a high selectivity for binding to N7 of guanine (G) bases on DNA oligomers.[1] DNA platination is thought to be a key event in the mechanism of action of platinum anticancer drugs such as cisplatin,[2] whereas the interaction of platinum species with sulfur-containing biomolecules has been associated both with negative phenomena (such as toxic side effects and the development of resistance) and with positive effects (such as delivery of active species to cells and/or serving as a drug reservoir for ultimate platination of DNA).[3] The competitive reactions of N-donor (G^{N7}-DNA) and S-donor (thiol/thioether) ligands for Pt^{II} have been widely studied.[4] However, those between Ru^{II} arene anticancer complexes, N-donor nucleotides, and S-donor amino acids and peptides are largely unexplored, although it has been shown that both cysteine and methionine can form S-bound adducts with $[(\eta^6\text{-bip})RuCl(en)][PF_6]$ (**1**; bip = biphenyl).[5] In this work, cGMP was chosen as a model nucleotide for investigating competitive reactions with glutathione and complex **1** because it is a diester as are the nucleotides in DNA and RNA.

The aim of this Chapter is to gain insight into the competition between the glutathione and guanine for these Ru(II) arene anticancer complexes under physiologically-relevant conditions. This will involve for cGMP work: micromolar Ru concentrations, millimolar GSH concentration, pH 7, 22 mM NaCl; for DNA oligonucleotide work: micromolar Ru concentrations, millimolar GSH concentration, pH 7, 4 mM NaCl. The glutathione (γ-L-Glu-L-Cys-Gly; GSH) is an abundant (millimolar) intracellular thiol responsible for the detoxification of heavier transition metal ions, including some platinum and ruthenium

anticancer complexes.[3,6]Guanosine-3′,5′-cyclic monophosphate (cGMP; structure is shown in Figure 4.1) is a phosphate diester, as are the nucleotides in DNA and RNA. In this work, two Ru(II) arene anticancer complexes with different η^6-arenes ([(η^6-bip)RuCl(en)][PF_6] (**1**) and [(η^6-tha)RuCl(en)][PF_6] (**12**; tha = tetrahydroanthracene)) were studied. Interestingly, it is shown that the Ru-S bond can be substituted by a Ru-N 7 bond via an intermediate-sulfenate adduct which has been observed and discussed in Chapter 3.

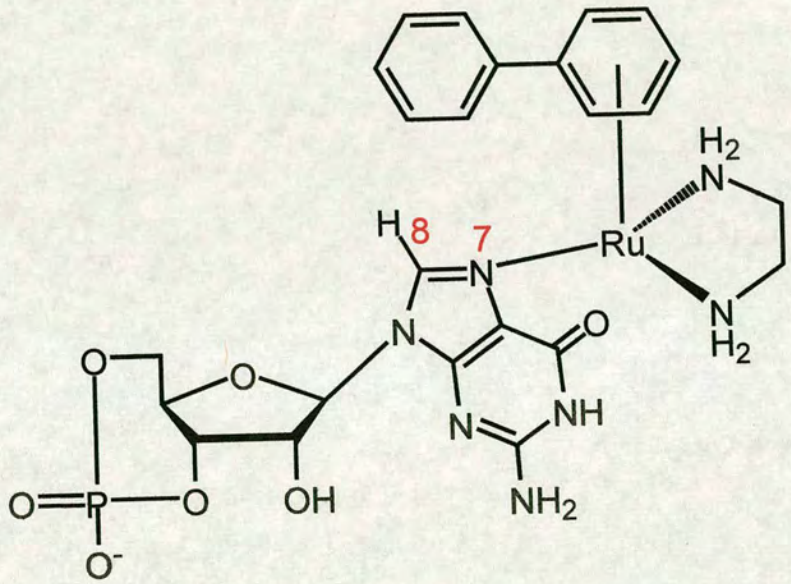

Figure 4.1 Chemical structure and atom numbering of cGMP.

4.2 Experimental

4.2.1 Materials

[(η^6-bip)RuCl(en)][PF_6] (**1**), ^{15}N-labeled **1** (^{15}N-**1**) and [(η^6-tha)RuCl(en)][PF_6] (**12**) were synthesized by Dr. Haimei Chen as described elsewhere.[1,7a] Glutathione (GSH, reduced), guanosine 3′,5′-cyclic monophosphate (cGMP), sodium salt, disodium hydrogen phosphate, and Chelex resin (used for removal of impurity ions from phosphates) were purchased from Sigma; sodium dihydrogen phosphate, sodium perchlorate, the ruthenium standard for atomic spectrometry (1003 μgRu/mL^{-1}) and the phosphorus standard for atomic spectrometry (1030 μgP/mL^{-1}) from Aldrich; sodium hydroxide and sodium chloride from Fisher; trifluoroacetic acid (TFAH) from Acros; triethylammonium acetate buffer (TEAA) and ammonium acetate (AA) from Fluka, and the aqua solutions of two 14-mer DNA oligonucleotides (sequences as shown below), which are HPLC purified Na^+ salts ($\varepsilon_{260\ nm}$ = 149.8 L·mmol^{-1}·cm^{-1} for **I**, $\varepsilon_{260\ nm}$ = 139.4 L·mmol^{-1}·cm^{-1} for **II**), were purchased from DNA Technology A/S.

$A_1\ T_2\ A_3\ C_4\ A_5\ T_6\ G_7\ G_8\ T_9\ A_{10}\ C_{11}\ A_{12}\ T_{13}\ A_{14}$ **(I)**

$T_{28}\ A_{27}\ T_{26}\ G_{25}\ T_{24}\ A_{23}\ C_{22}\ C_{21}\ A_{20}\ T_{19}\ G_{18}\ T_{17}\ A_{16}\ T_{15}$ **(II)**

4.2.2 Methods

4.2.2.1 High Performance Liquid Chromatography (HPLC)

For DNA oligonucleotide work, HPLC separations were carried out on a PLRP-s reversed-phase column (250 mm × 4.6 mm, 300 Å, 5 μm, Polymer Labs) with detection at 260 nm. Mobile phase A: water (for HPLC application, Fisher Chemicals) containing

20 mM TEAA; mobile phase B: acetonitrile (for HPLC application, Fisher Chemicals) containing 20 mM TEAA. The flow rate was 1.0 mL min^{-1}. The gradient (solvent B) was as follows: 11.5% to 80% within 16 min, reset to 11.5% within 1 min, and kept at 11.5% from 17 to 22 min.

4.2.2.2 Nanoscale Liquid Chromatography Fourier Transform Ion Cyclotron Mass Spectrometry (Operated by Mr. Stefan Weidt)

Negative-ion electrospray ionization mass spectra were obtained with a Bruker APEX III ESI-FT-ICR mass spectrometer (Bruker Daltonics, USA) equipped with a 9.4 T superconducting magnet (Magnes, UK). An UltiMate 3000 series system (Diones, UK), with a nanoflow splitter, was coupled to the mass spectrometer using an TriVersa™ NanoMate® (Advion, USA) with spray voltage set to 1.7 kV. Mobile phase: water (for LC-MS application, Fisher Chemicals) containing 20 mM AA. The sample was eluted onto a TSK-Gel® Super SW2000 column (4.6 mm ID × 30 cm, 4 μm) with a guardcolumn (4.6 mm × 3.5 cm). The flow rate was 300 nL min^{-1}. A modified heated metal capillary was used with temperature set to 423 K held at a potential of 50 V. All Spectra were acquired using XMass 7.02 (Bruker Daltonics) with 512 k datapoints in the range 90 to 3000 m/z. Bruker Daltonics Data Analysis software was used for analysis and postprocessing.

4.2.3 Preparation of Samples

4.2.3.1 Preparation of the 14-mer DNA duplex

The 14-mer DNA duplex **III** (Scheme 4.1) was prepared by mixing the single-stranded DNA oligonucleotide **I** (0.5 mM) with the complementary single-stranded DNA

oligonucleotide **II** (0.5 mM) in $NaClO_4$ (100 mM) to maintain duplex stability in a 10 mm path length quartz cuvette, and the solution was incubated in a temperature controller at 288 K at the beginning. Then the temperature was increased from 288 K to 353 K within 2 min, and finally decreased from 353 K to 288 K within 3 h. The presence of duplex **III** was confirmed by ^1H NMR.

Scheme 4.1 Preparation of **III**.

$A_1\ T_2\ A_3\ C_4\ A_5\ T_6\ G_7\ G_8\ T_9\ A_{10}\ C_{11}\ A_{12}\ T_{13}\ A_{14}$ **(I)**

$T_{28}\ A_{27}\ T_{26}\ G_{25}\ T_{24}\ A_{23}\ C_{22}\ C_{21}\ A_{20}\ T_{19}\ G_{18}\ T_{17}\ A_{16}\ T_{15}$ **(II)**

I + II = III

4.2.3.2 HPLC

Reaction mixtures of complex **1** with GSH and cGMP at various molar ratios under physiologically relevant conditions (phosphate buffer pH 7.0, 22 mM NaCl) were prepared by mixing aliquots of 10 mM **1**, 50-500 mM GSH, and 20-100 mM cGMP, and the pH values of all starting solutions were adjusted to 7 using NaOH and $HClO_4$, and the O_2 content was minimized by bubbling with N_2 before and after mixing unless otherwise stated. The mixtures were diluted to the required concentration with deionized water or with 10-50 mM phosphate buffer solution (pH 7.0, purged with N_2), bubbled with N_2 again, and then incubated at 310 K in a water bath for the required times for the subsequent HPLC and LC-MS analysis or preparative separation. The reaction mixtures of complexes **1** or **12** with GSH and DNA oligonucleotides at different molar ratios under physiologically-relevant conditions (TEAA buffer, pH 7.0, 4 mM NaCl) were prepared by mixing aliquots of 1 mM **1** or **12**, 50 mM GSH and 0.5-1 mM DNA

oligonucleotides, and the pH value of GSH solution was adjusted to 7 using NaOH and $HClO_4$. All the reactions were carried out in the presence of air.

The time-courses of reactions of **1** (20 μM) with GSH (5 mM) and cGMP (0.5 mM) under N_2 (all starting solutions purged by N_2 bubbling) at 310 K were followed chromatographically by injection of aliquots of the mixtures onto the HPLC column at various time intervals. Sampling at various times was done in air by briefly removing the lid to extract an aliquot with no further N_2 bubbling.

4.2.3.3 NMR

A 10 mM solution of ^{15}N-labeled complex **1** (^{15}N-**1**) was used to follow reactions of **1** with GSH and cGMP by 1D [^{1}H] and 2D [^{1}H, ^{15}N] HSQC NMR. The reaction mixtures were prepared using the same method as that for HPLC samples.

4.2.3.4 Determination of Extinction Coefficients

HPLC fraction of cGMP adducts were collected from 30-h reaction mixture of complex **1** with GSH and cGMP in buffer. The value of Relative Extinction Coefficients at 254 nm for $[(\eta^6\text{-bip})Ru(en)(cGMP\text{-}N7)]^+$ (**13**) is 2.62 ($\varepsilon_{[(\eta^6\text{-bip})Ru(en)Cl]^+(1)}^{R} = 1$).

4.2.3.5 Measurement of DNA oligonucleotides concentrations

The aqueous solution of two 14-mer DNA oligonucleotides (**I** and **II**) was diluted in 5 mL deionized water for P determination by ICP-OES, using a Perkin-Elmer Optima 5300 DV Optical Emission Spectrometer equipped with an AS-93plus autosampler and WinLab32 for ICP program (version 3.0.0.0103). The concentrations of the DNA oligonucleotides were calculated using eq 3, and the values are listed in Table 4.1.

$$[\text{DNA olig.}]\ (\text{mM}) = [\text{P}]\ (\text{mg/L}) \times \text{fold (diluted)} / (31 \times 13) \qquad (3)$$

where 13 arises from the 13 phosphates in both of the DNA oligonucleotides, respectively, 31 is the molecular weight of the P atom.

Table 4.1 Concentrations of 14-mer DNA oligonucleotides purchased from DNA Technology A/S.

DNA oligonucleotides	P /mg mL^{-1}	DNA olig. /mM
I	3.063	1.510
II	3.845	1.793

4.3 Results and Discussion

4.3.1 Competitive Reactions of GSH and cGMP with Complex 1 under physiologically relevant conditions

The competitive binding of cGMP and GSH to complex **1** was investigated. Incubation of 20 μM **1** with 250 mol equiv of GSH and 25 mol equiv of cGMP in phosphate buffer (pH 7) containing 22 mM NaCl at 310 K for 30 h gave rise to both GSH-and cGMP containing products (Figure 4.2). All initial solutions at neutral pH were purged with N_2 before and after mixing to minimize their O_2 content. HPLC fractions a and b (Figure 4.2) contained the thiolato adduct **4** and sulfenato adduct **10**, respectively. The mass spectrum of fraction c (Figure 4.3) contained a singly-charged ion peak at *m/z* 774.2 and a doubly-charged ion peak at *m/z* 659.9, assignable to the TFA ion-paired adduct of the cGMP complex [(η^6-bip)Ru(en)(cGMP)][TFA] (calcd *m/z* 774.1 for {[(η^6-

bip)Ru(en)(cGMP)][TFA] + H}$^+$) and the dimer {[(η^6-bip)Ru(en)(cGMP)]$_2$}$^{2+}$ (calcd *m/z* 660.1), respectively, confirming the formation of the cGMP adduct [(η^6-bip)Ru(en)-(cGMP)]$^+$ (**13**). After 30 h of reaction, the ratios of **4**:**10**:**13** were 18:15:13. The presence of N7-bound cGMP in **13** was confirmed by the ^{1}H NMR time course of a 24-h reaction mixture of 1 mM **1** with 5 mM GSH and 1 mM cGMP, which showed a peak at δ 8.28 assignable to H8 f bound cGMP in **13**, shifted downfield by 0.31 ppm relative to free cGMP.[7b]

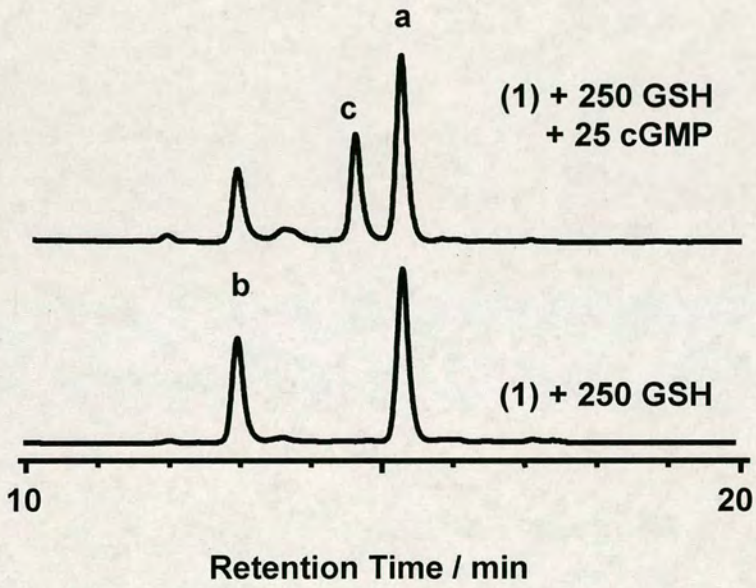

Figure 4.2 HPLC chromatograms for reactions of **1** (20 μM) with 250 mol equiv GSH (bottom), and with 250 mol equiv GSH and 25 mol equiv cGMP (top) in phosphate buffer (pH 7) containing 22 mM NaCl at 310 K for 30 h. Peak assignments: (a) thiolato adduct **4**; (b) sulfenato adduct **10**; (c) cGMP adduct **13**. The nucleotide adduct is still formed even in the presence of a 10-fold excess of GSH.

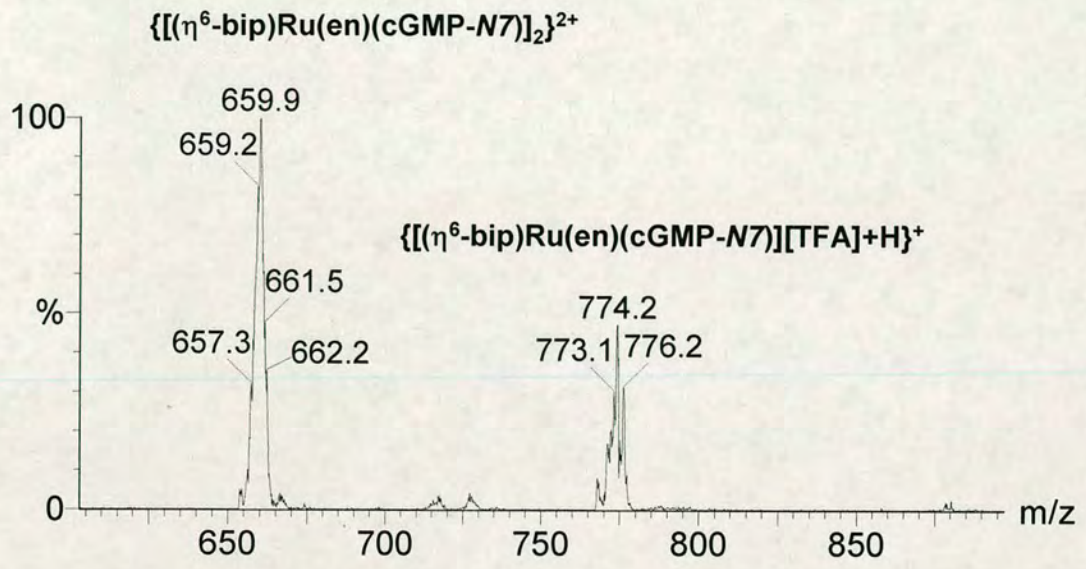

Figure 4.3 Mass spectrum for HPLC fraction m from the reaction of complex **1** with GSH and cGMP (1 : 10 : 25 mM) in phosphate buffer (pH 7.0) containing 22 mM NaCl at 310 K for 30 h, showing the detection of the cGMP adduct $[(\eta^6\text{-bip})Ru(en)(cGMP\text{-}N7)]^+$ (**13**) (calc *m/z* 660.1 and 774.1 for $\{[(\eta^6\text{-bip})Ru(en)(cGMP)]_2\}^{2+}$ and $\{[(\eta^6\text{-bip})Ru(en)(cGMP)][TFA] + H\}^+$, respectively). The TFA anion is from the ion-pairing reagent TFAH used in the HPLC separation.

A similar reaction mixture was prepared and sampled in air at various time intervals over 3 d for HPLC assays (Figure 4.4). In this case, conversion of the thiolato adduct **4** to the sulfenato complex **10** began after only 6 h, and by 24 h all the thiolato adduct had disappeared. After 72 h, the major product (ca. 62% of the total Ru) was the cGMP adduct **13** (Figure 4.4).

cGMP (25 mol equiv) was added to a solution of **1** (20 μM) which had been allowed to react with 250 mol equiv GSH for 6 h at 310 K. After 24 h, the cGMP product **13** accounted for 12% of the Ru present, the thiolato adduct **4**, 49%, and sulfenato adduct **10**, 34% (Figure 4.5). Addition of only 5 mol equiv of cGMP to a similar solution of 20

μM **1**, which had reacted with 250 mol equiv of GSH for 6 h, still gave rise to a detectable amount (5%) of the cGMP product **13** after 24 h (Figure 4.5).

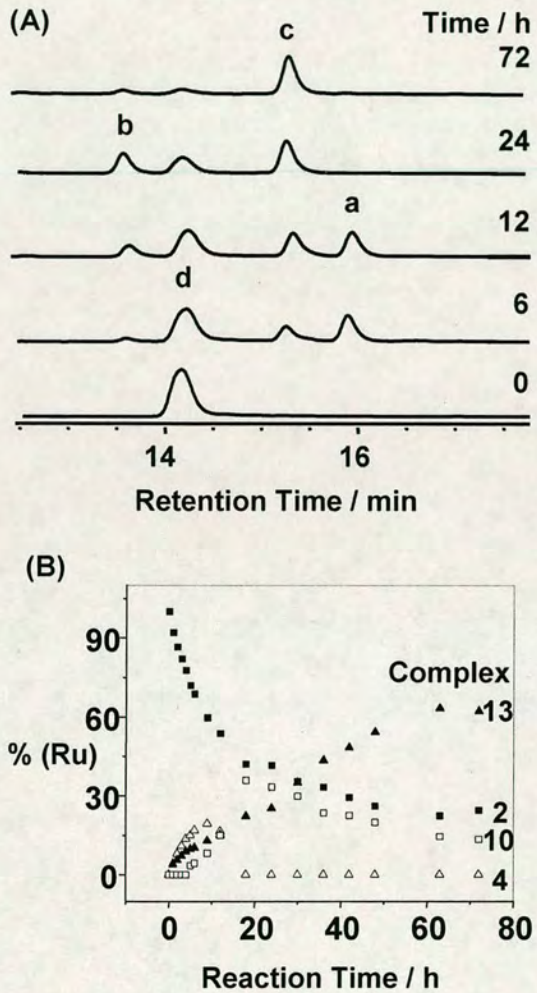

Figure 4.1 (A) HPLC time-course for the competitive reaction of **1** (20 μM) with 250 mol equiv of GSH and 25 mol equiv of cGMP in phosphate buffer (pH 7) containing 22 mM NaCl at 310 K. Peak assignments: (d) $[(\eta^6\text{-bip})Ru(en)(H_2O)]^{2+}$ (**2**); (a) thiolato adduct $[(\eta^6\text{-bip})Ru(en)(GS)]$ (**4**); (b) sulfenato adduct $[(\eta^6\text{-bip})Ru(en)(GS(O))]$ (**10**); (c) $[(\eta^6\text{-bip})Ru(en)\text{-}(cGMP)]^{+}$ (**13**). (B) Variation of the relative Ru concentrations of species detected during the reaction in (A) with time (processed by Dr. Fuyi Wang). The HPLC areas were calibrated by ICP-OES; the relative extinction coefficients for complexes **2**, **4**, **10**, and **13** are listed in Table 5.1. The thiolato adduct appears to be converted to the sulfenato adduct after 6 h that, in turn, appears to be converted to the cGMP adduct after 24 h. Some formation of **13** by direct reaction of cGMP with **2** may also occur.

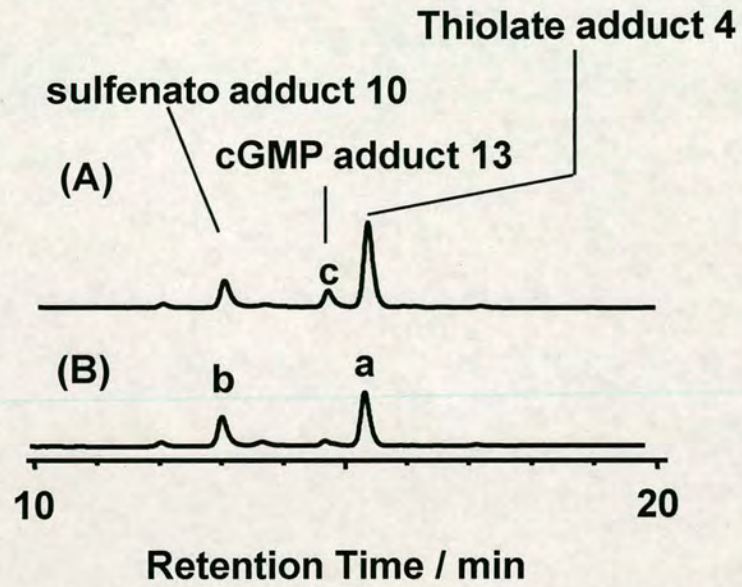

Figure 4.2 HPLC chromatograms for the 24-h reaction mixtures of (A) 0.5 mM and (B) 0.1 mM cGMP with 20 μM complex **1** which had first reacted with 5 mM GSH for 6 h at 310 K.

The competitive reaction of GSH and cGMP at millimolar concentrations (**1**:GSH:cGMP 1:5:1 mM) was also followed by 2D [^{1}H,^{15}N] HSQC NMR at 310 K using ^{15}N-labeled **1** (^{15}N-**1**). The spectra are shown in Figure 4.6 and the ^{1}H and ^{15}N NMR chemical shifts are listed in Table 4.2. During the early stages (<1 h), a pair of new cross-peaks (4a, 4b) was observed for the ^{15}N-en ligand in thiolato adduct **4**, and after 2 h, cross-peak 13a appeared, assignable to the cGMP adduct [(η^6-bip)Ru-(^{15}N-en)(cGMP)]$^{+}$ (**13**). This increased in intensity until 72 h. After 12 h, two pairs of cross-peaks (10a/b and 10c/d) were detectable and can be assigned to the sulfenato complex [(η^6-bip)Ru(^{15}N-en)(S(O)G)] (**10**) in accordance with the HPLC results (Figure 4.4). Cross-peaks 4a/b and 10a/b/c/d slowly decreased in intensity after ca. 50 h. It is notable that a pair of cross-peaks (14a/b) assignable to the phosphate adduct [(η^6-bip)Ru(^{15}N-en)-(PO_4)]$^{-}$ (**14**)[6,8] is observed for the equilibrium solution of complex **1** in 50 mM

phosphate buffer (pH 7). After ca. 36 h, cross-peak 15a corresponding to the release of ^{15}N-en from glutathione-coordinated Ru complexes appeared.

Table 4.2 ^{1}H, ^{15}N NMR peaks observed for reactions of ^{15}N-**1** (1 mM) with GSH (5 mM) and cGMP (1 mM) in 50 mM phosphate buffer (pH 7) and 22 mM NaCl (Figure 4.6) at 310 K.

complex	(peak) δ 1H/15N	
1	(1a) 6.09/-24.62	(1b) 4.05/-24.62
2	(2a) 5.64/-19.50	(2b) 4.49/-19.50
4	(4a) 5.68/-27.74	(4b) 3.60/-27.74
10	(10a) 3.85/-35.26	(10b) 2.91/-35.26
	(10c) 3.53/-32.55	(10d) 2.79/-32.55
13	(13a) 6.59/-28.96	(13b) -[a]
14[b]	(14a) 6.04/-21.89	(14b) 4.35/-21.89

[a] Too broad to observe. [b] Phosphate adduct $[(\eta^6\text{-bip})Ru(en)(PO_4)]^-$.

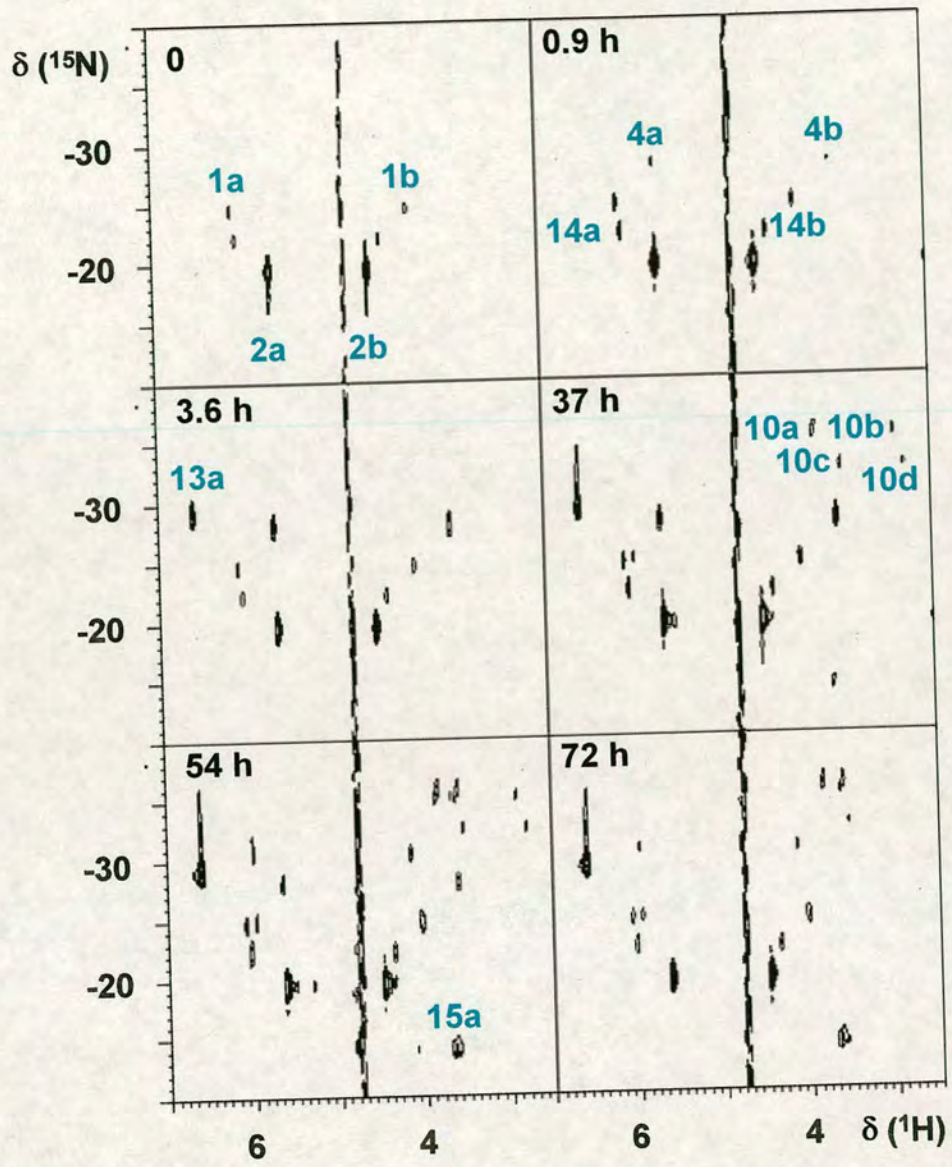

Figure 4.3 2D [^{1}H, ^{15}N] HSQC NMR time course for the reaction of ^{15}N-**1** (1 mM) with GSH (5 mM) and cGMP (1 mM) in 90% H_2O / 10% D_2O over a period of 72 h. Assignments: 1a/b complex **1** [(η^6-bip)Ru(^{15}N-en)Cl]$^+$, 2a/b complex **2** [(η^6-bip)Ru(^{15}N-en)(H_2O)]$^{2+}$, 4a/b thiolato adduct **4** [(η^6-bip)Ru(^{15}N-en)(GS)], 10a/b and 10c/d sulfenato adduct **10** [(η^6-bip)Ru(^{15}N-en)(S(O)G)], 13a cGMP product **13** [(η^6-bip)Ru(^{15}N-en)(cGMP)]$^+$. As for the guanosine complex [(η^6-bip)Ru(^{15}N-en)(Guo-*N7*)]$^{2+}$ (Chen, H.; Parkinson, J. A.; Parsons, S.; Coxall, R. A.; Gould, R. O.; Sadler, P. J. *J. Am. Chem. Soc.*, **2002**, *124*, 3064), resonances for the en NH_d protons of **13**, which are oriented away from the biphenyl ligand, are too broad to observe. One set of cross-peaks (14a/b) corresponds to ^{15}N-en in the phosphate adduct **14**, [(η^6-bip)Ru(^{15}N-en)(PO_4-*O*)]$^-$. Note the appearance of cross-peak 15a after ca. 36 h, assignable to ^{15}N-en, and indicative of some release of en. The non-equivalence of the nitrogens and the protons of the ^{15}N-en ligand in **10** is also evident, perhaps strongly influenced by the adjacent chiral S atom.

Previous work in our laboratory has shown that en Ru^{II} arene complexes exhibit a high selectivity for N7 of guanine in reactions with DNA[1,7c] and show little binding to the phosphate group of diesters.[7] The en NH_2 protons in $[(\eta^6\text{-arene})Ru(en)Cl]^+$ can form a strong H-bond with the exocyclic C6 carbonyl oxygen of G but are repulsive toward exocyclic amino groups of nucleobases, and this appears to contribute to the high base-selectivity. Arene ligands which contain an extended γ-electron system, as in the biphenyl group of **1**, can provide additional stabilization for the interaction between the Ru^{II} arene complexes and nucleosides or nucleotides by hydrophobic π-π stacking with the purine ring of G.[7a,b]

No peaks with ^{15}N-en chemical shifts similar to those of *O*-bound adducts $[(\eta^6\text{-bip})Ru(en)(GS\text{-}O)]$ (Chapter 3) were observed, again suggesting that **10** contains an S-bound sulfenate. In the process of oxidation of thiolate, sulfenate can be further oxidized to sulfinate.[9] However, in the reaction of **1** with GSH with cGMP at pH 7, the oxidized thiolate remains as sulfenate due to the presence of GSH which acted as reductant and the –S(O)G was substituted by cGMP before it was further oxidized to $-S(O_2)G$.

The sulfenato complex **10** was protonated at pH ca. 2[10] to form sulfenic acid $[(\eta^6\text{-bip})Ru(en)(S(OH)G\text{-}S)]^+$ (**15**) which is very highly reactive.[9] Even at pH 7, a small amount of sufenate **10** was protonated to form the sulfenic acid which appeared to be readily displaced by cGMP giving the cGMP adduct **13** $[(\eta^6\text{-bip})Ru(en)(cGMP\text{-}N7)]^+$ as the dominant product of the reaction (Figure 4.4, Scheme 4.2). This implies that the sulfenato ligand is readily substituted by cGMP, but the thiolato ligand is not. Cisplatin and related Pt^{II} anticancer complexes can catalyze the breaking of disulfide bonds,[11] but thiolates bound to Pt^{II} are not readily displaced by N7-donor ligands, guanine or

adenine.[4c,12] However, S-donor thioether ligands such as L-methionine[4b,c] and S-methylated glutathione (GSMe)[4d,13] bound to Pt^{II} are readily substituted by N7-donor nucleosides or nucleotides and oligonucleotides. On the other hand, GSH facilitates the binding of $[Ru^{III}Cl(NH_3)_5]^{2+}$ to DNA through reduction to $[Ru^{II}(H_2O)(NH_3)_5]^{2+}$. However, at [GSH]/[Ru] > 1, GSH inhibits the binding of $[Ru^{III}Cl(NH_3)_5]^{2+}$ to DNA by forming $[Ru^{III}(GS)(NH_3)_5]^{2+}$, and a high [GSH]/[Ru] even eliminates G N7 coordination.[6] But in the competition between GSH and cGMP for Ru(II) arene complex $[(\eta^6\text{-bip})Ru(en)Cl]^+$, GSH can not block the binding of **1** to cGMP even in the presence of excess GSH (Figure 4.4 and 4.6) due to the formations of sulfenato adduct **10** and the sulfenic acid which appear to provide a facile route for displacement of S-bound glutathione by G N7.

Scheme 4.2 Pathway for reaction of complex **1** with cGMP and GSH at pH 7.

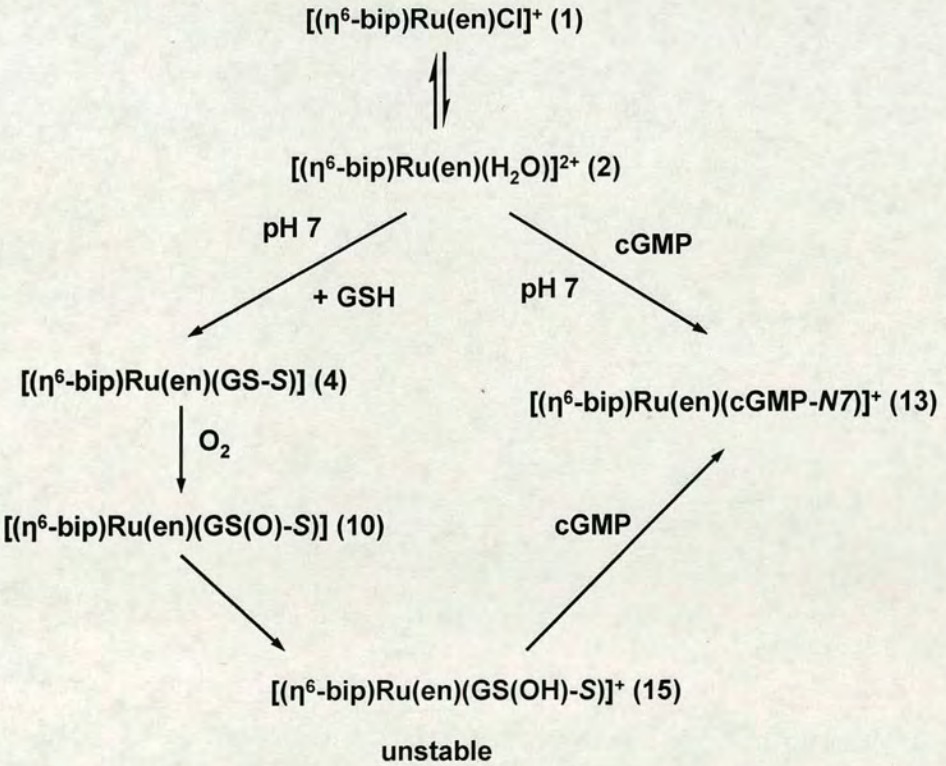

4.3.2 Competition between GSH and DNA oligonucleotides for Ru(II) Arene Anticancer Complexes under physiologically-relevant conditions

4.3.2.1 Competitive reaction of complex 1 with GSH and single strand II

Reactions of **1**, GSH (pH 7) and single strand **II** in different ratios, incubated under physiologically-relevant condition (pH 7, 4 mM NaCl) for 48 h, gave rise to one monoruthenated oligonuleotide product, as separated and identified by HPLC-ESI-MS (Figures 4.7 and 4.8). The fraction e (Figure 4.7) corresponds to the mass spectrum (B), in which the triply-charged ion peak centred at *m/z* 1416.7 and the quadruply-charged ion peak centred at *m/z* 1062.4 (Figure 4.8(B)) were both assigned to free single strand **II** according to the simulation (Figure 4.8(D)). ESI-MS analysis of the HPLC fraction f (Figure 4.7) gave one triply-charged ion peak centred at *m/z* 1521.3 and one quadruply-charged ion peak centred at *m/z* 1140.9 (Figure 4.8(A)), both assignable to monoruthenated single strand **II** adduct **16** on the basis of the simulation (Figure 4.8(C)). No ruthenated GSH product was detected, which indicated that the Ru complexes are not inactivated by GSH. Similar result was obtained in the competitive reaction of **1** with histidine and **II** at pH 7, in which no histidine adducts of complex **1** were formed in the presence of the oligonucleotide.[14] In this reaction, G18 and G25 are two potential targets, but specific assignment of monoruthenation site to G18 or G25 was not made.[15] For the reactions of **1** and duplex **III**, the NMR studies identified five mono-ruthenated oligonucleotides (two conformers were identified for the G18-ruthenated adducts), suggesting that all the four guanine residues (G7, G8, G18 and G25) could be ruthenated.[15]

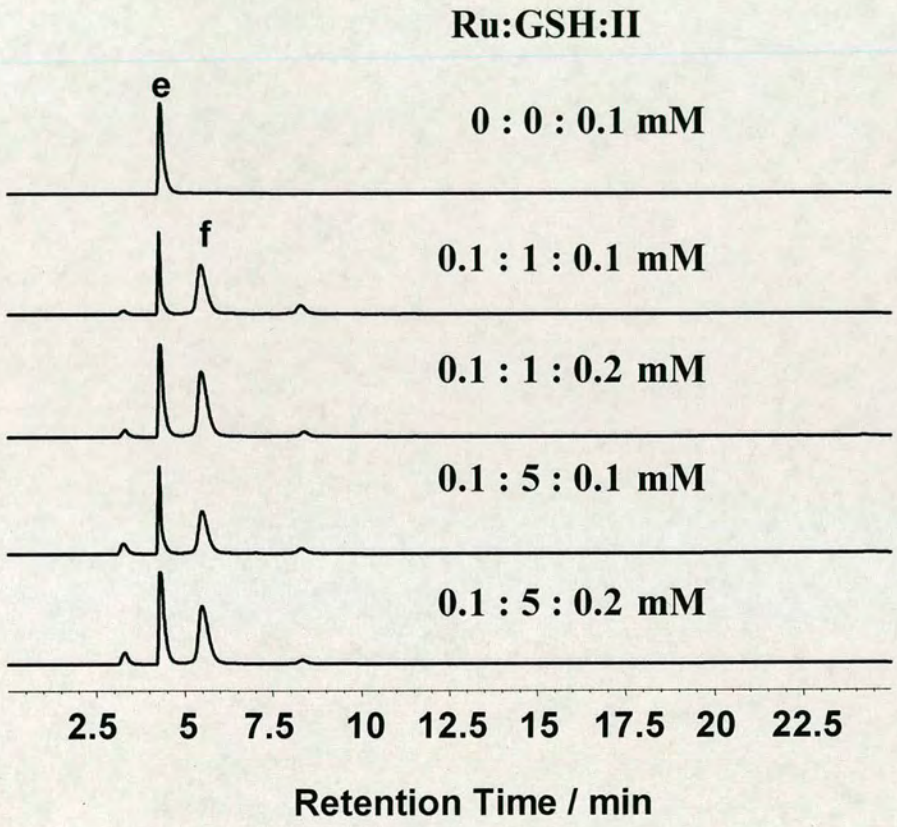

Figure 4.4 HPLC separations for reactions of **1**, GSH and single strand **II** in different ratios (as shown above) at 310 K for 48h.

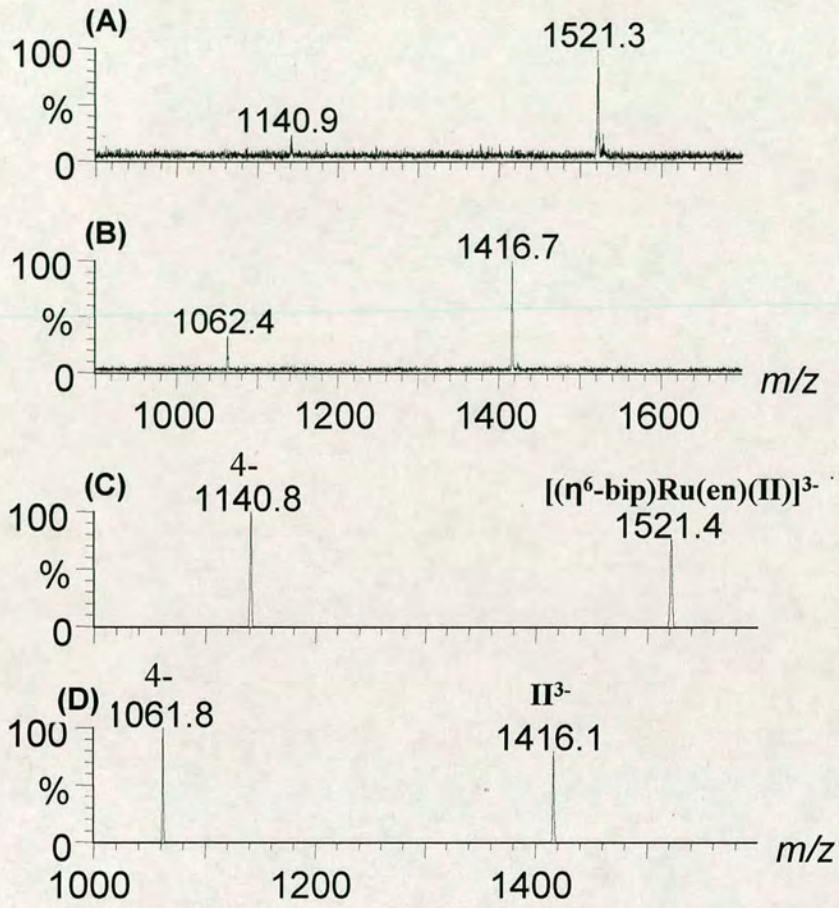

Figure 4.5 (A) ESI mass spectrum for HPLC fraction e (Figure 4.7); (B) ESI mass spectrum for HPLC fraction f (Figure 4.7); (C) Simulation for species f which is a monoruthenated single strand **II** adduct **16**; (D) Simulation for species e which is free single strand **II**.

4.3.2.2 Competition of 1 with GSH and 14-mer duplex

The 14-mer duplex **III** was prepared from the two single strands **I** and **II** (**I** + **II** = **III**; Scheme 4.1), and the annealing was confirmed by NMR (Figure 4.9). The pattern of ^{1}H chemical shifts for the imino region arising from hydrogen bonds forming of duplex **III** was similar to that shown in the literature (^{1}H chemical shifts are listed in Table 4.3).[16]

Products from reactions of **1** (0.1 mM) and duplex **III** (0.1 mM) with GSH (1 mM, pH 7) and without GSH for 48 h, were separated and analysed by conventional LC-ESI-MS (Figure 4.10 and 4.11). The HPLC assays gave identical chromatograms (Figure 4.10) for the two reaction mixtures, but the MS analysis of the fractions (Figure 4.11) was not able to give unambiguous identifications for the ruthenated duplex **III** products due to the low resolution. Therefore, nano-HPLC-FT-ICR-MS was applied to analyse the reaction mixture in the presence of GSH. A series of triply-charged and penta-charged ion peaks was detected for the fraction eluting from 4 to 6 min (Figure 4.10). The ion peaks centred at m/z 1416.2 and 1422.2 (Figure 4.12(A)) were assigned to free single strand **II** and **I**, respectively, due to the fragmentation of duplex **III** during the ionisation, and the two ion peaks centred at m/z 1521.3 and 1527.3 (Figure 4.12(A)) were assignable to mono-ruthenated single strand **II** and **I** adducts **16** and **17**, respectively. The two penta-charged ion peaks centred at m/z 1703.4 and 1766.2 are assignable to free duplex **III** and mono-ruthenated duplex **III** adduct **18** (Figure 4.12(B)), respectively. When the molar ratio of Ru:**III**:GSH was changed to 2:1:20 (0.1:0.05:1 mM), besides the mono-ruthenated duplex **III** adduct **18**, a di-ruthenated duplex **III** adduct **19** was identified by nano-HPLC-FT-ICR-MS (Figure 4.13 and 4.14) for the reaction mixture incubated for 48 h. Interestingly, two ruthenium glutathione complexes were detected by conventional LC-MS (Figure 4.15 and 4.16) for the reaction mixture of **1** (0.1 mM), GSH (5 mM) and duplex **III** (0.05 mM) incubated for 16 h. The ion peak centred at m/z 562.45 corresponds to a mono-ruthenated glutathione adduct **4** [(η^6-bip)Ru(en)(SG)], and the other ion peak centred at m/z 638.02 is assignable to a mono-ruthenated glutathione sulfenate adduct **10** [(η^6-bip)Ru(en)(SOG)], which indicates that the pathway for competitive reaction of **1** with GSH and DNA oligonucleotides (Scheme 4.3) is similar to that for reaction of **1** with GSH and cGMP

(Scheme 4.2). Therefore, in the reaction of **1** with duplex **III**, sulfenato complex **10** plays the same role as that in the reaction of **1** with cGMP.

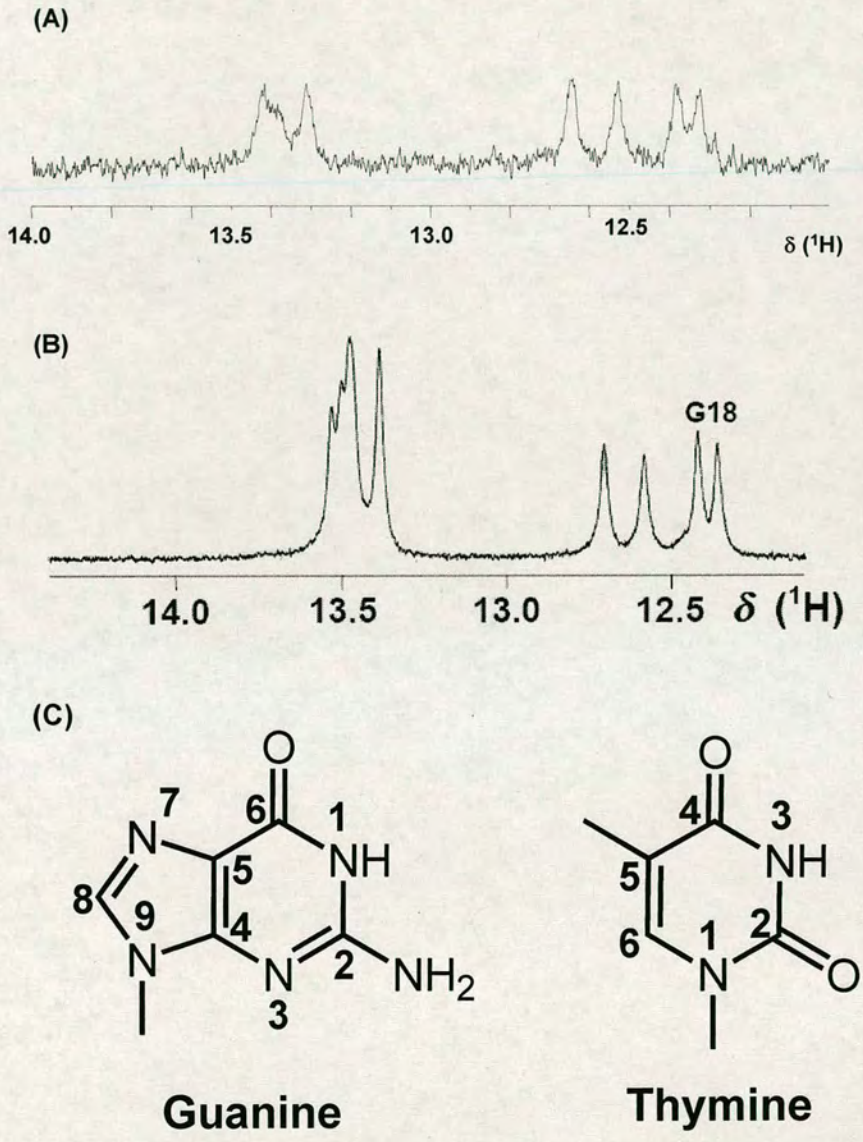

Figure 4.6 (A) The imino region of the ^{1}H NMR spectrum of **III** obtained at 288 K. (B) The same region of ^{1}H NMR spectrum of **III** at 278 K as published previously in the literature.[11] (C) The chemical structures and numbering for the guanine and thymine bases.

Table 4.3 ^{1}H chemical shift assignments (ppm) observed for the imino region of duplex **III** compared to published values.[16]

Base[a]	GH1/TH3[b]	GH1/TH3 ([11])
T6	-[c]	13.54
G7	12.52	12.55
G8	12.64	12.69
T17	13.31	13.40
G18	12.38	12.42
T19	-[c]	13.48
T24	-[c]	13.51
G25	12.32	12.37
T26	13.31	13.40

[a] The numbering for duplex **III** is shown in Scheme 5.1; [b] The numbering is shown in Figure 6.9(C); [c] The signals are weak and the three peaks are overlapped.

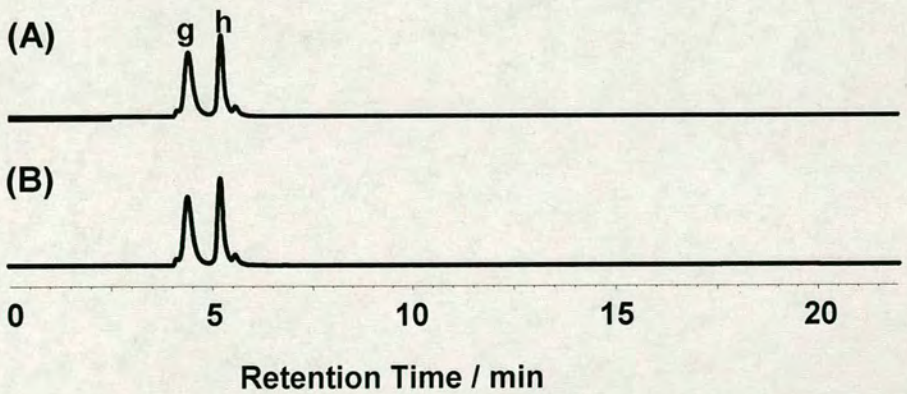

Figure 4.7 (A) HPLC separation for the reaction of **1** (0.1 mM) and 14-mer duplex **III** (0.1 mM) under physiologically-relevant conditions for 48 h; (B) HPLC chromatogram for the reaction of **1** (0.1 mM), GSH (1 mM) and 14-mer duplex **III** (0.1 mM) under physiologically-relevant conditions for 48 h. The two reactions gave rise to the same two species.

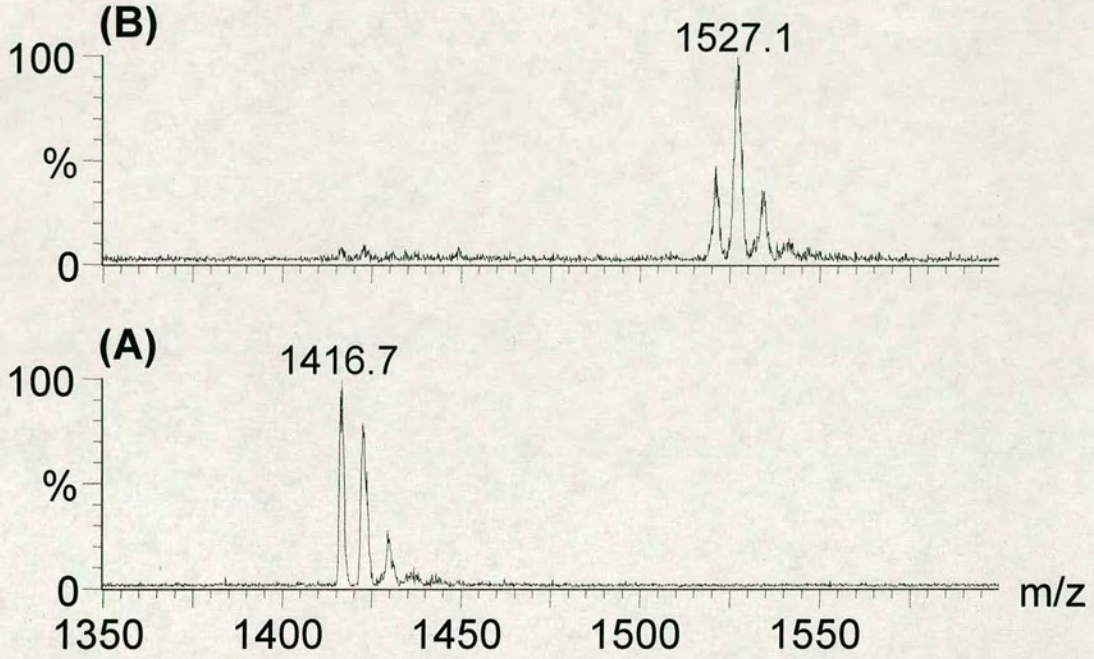

Figure 4.8 (A) ESI mass spectrum for the fraction g (Figure 4.10); (B) ESI mass spectrum of the HPLC fraction h (Figure 4.10).

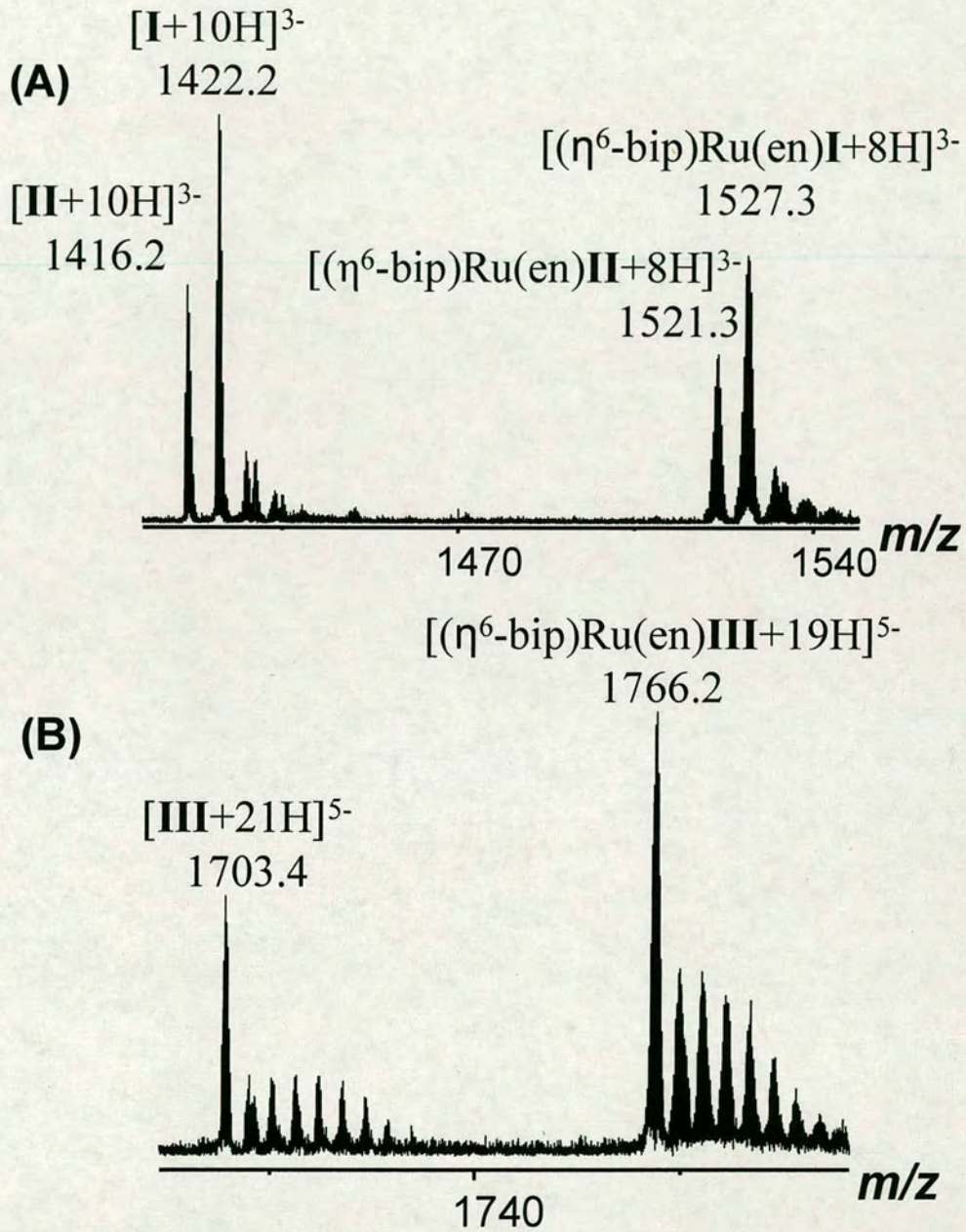

Figure 4.9 FT-ICR mass spectra for the fraction eluting from 4 to 6 min (Figure 4.10).

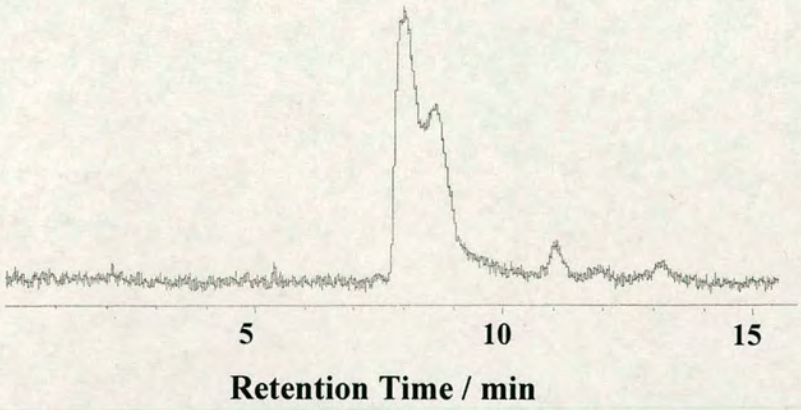

Figure 4.10 Nano HPLC separation for the reaction mixture of **1** (0.1 mM) with GSH (1 mM, pH 7) and duplex **III** (0.05 mM) after incubation for 48 h.

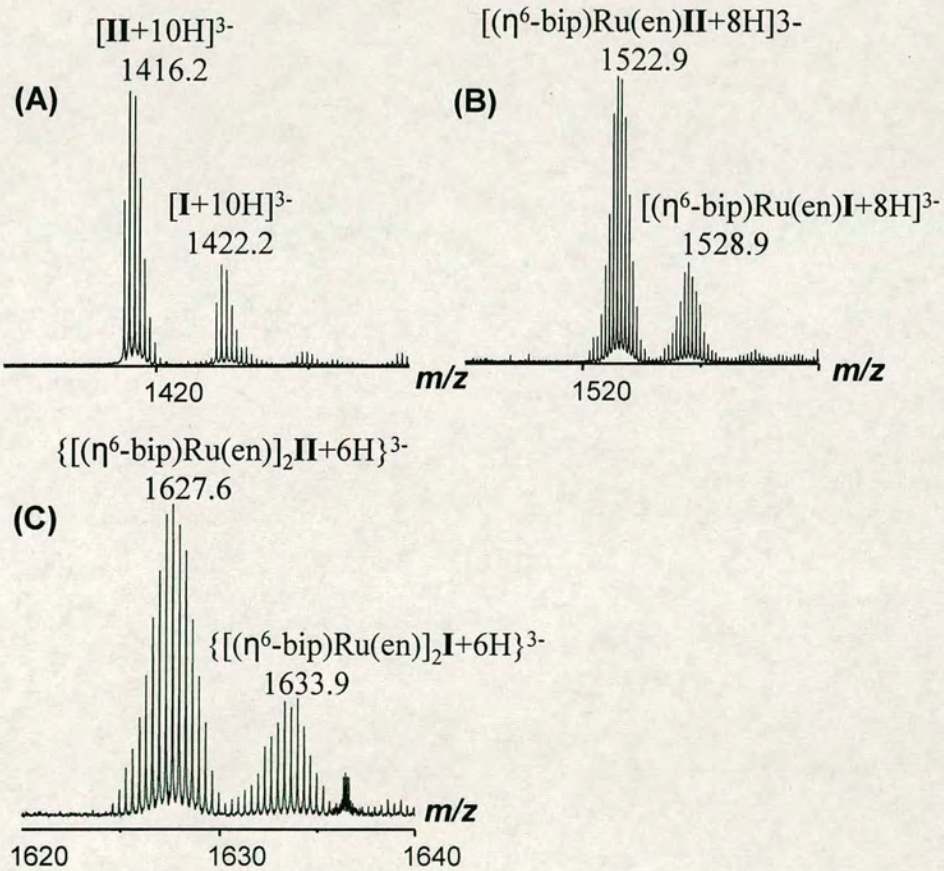

Figure 4.11 FT-ICR mass spectra for the fraction eluting from 9 to 10 min (Figure 4.13).

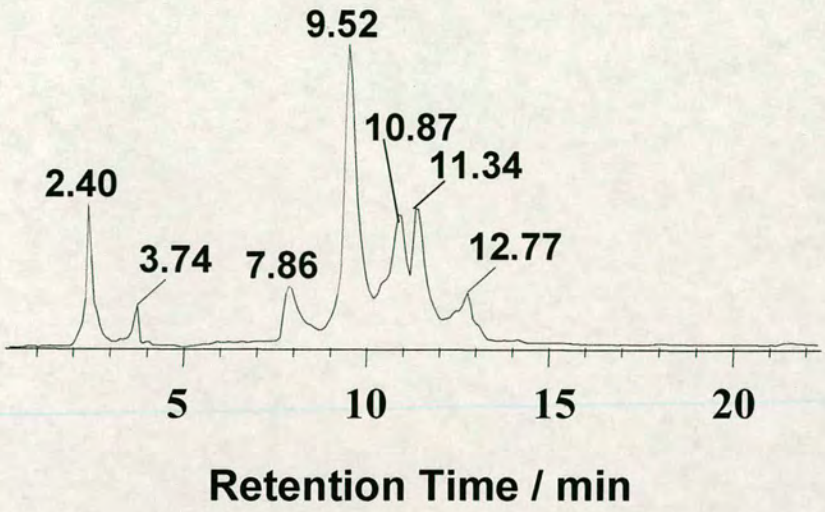

Figure 4.12 HPLC separation for the reaction of **1** (0.1 mM) with GSH (5 mM, pH 7) and duplex **III** (0.05 mM) for 16 h.

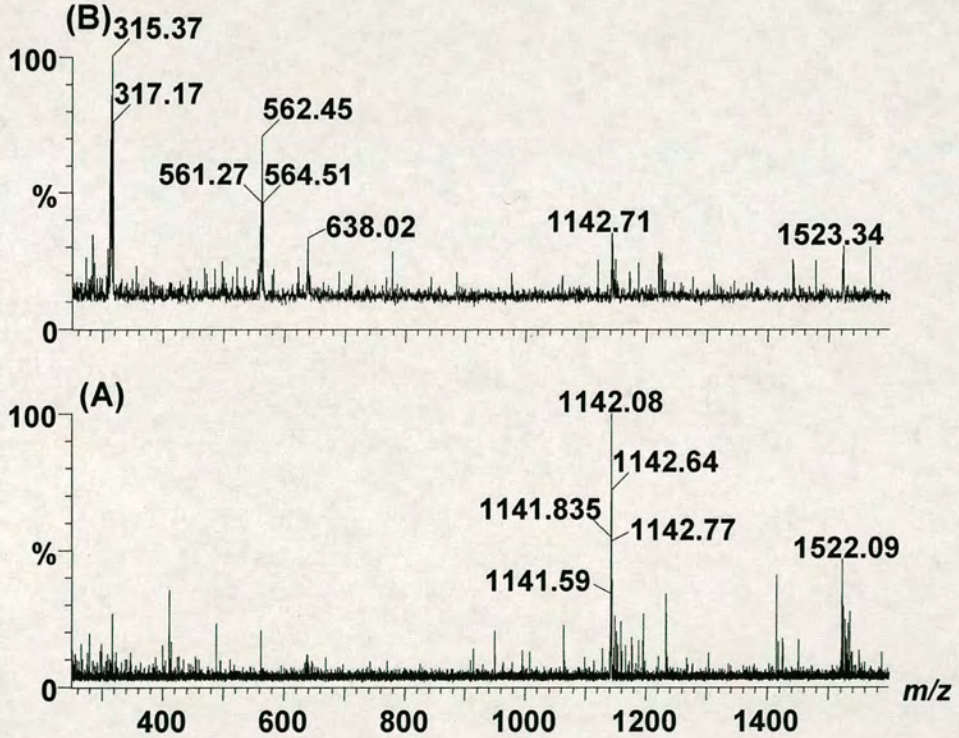

Figure 4.13 (A) ESI mass spectrum for the fractions eluting from 10.4 to 11 min (Figure 4.15); (B) ESI mass spectrum for the fractions eluting from 7.5 to 10 min (Figure 4.15).

Scheme 4.3 Pathway for reactions of **1** with GSH and DNA oligonucleotides at pH 7.

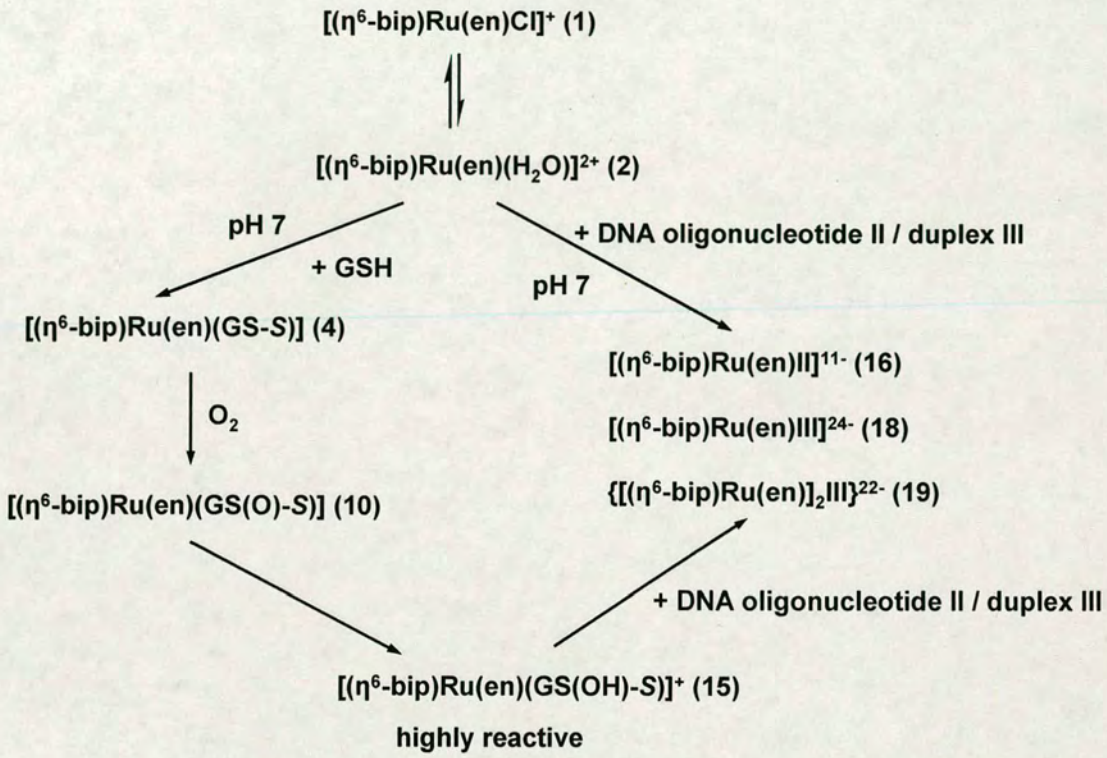

4.3.2.3 Competitive reaction of complex 12 with GSH and 14-mer duplex

Reaction mixtures of **12** (0.1 mM) and duplex **III** (0.1 mM) with or without GSH (1 mM, pH 7) for 48 h, were separated by HPLC. For each mixture, the separations (Figure 4.17) gave rise to two fractions which eluted at the same time. A series of triply-charged and penta-charged ion peaks were detected for the reaction mixtures (Figure 4.18). The ion peaks centred at *m/z* 1416.2 and 1422.2 were assigned to free single strand **II** and **I**, respectively, due to the fragmentation of duplex **III** during the ionisation, and the two ion peaks centred at *m/z* 1530.6 and 1536.6 were assignable to mono-ruthenated single strand **II** and **I** adducts **20** and **21**, respectively. The two penta-charged ion peaks centred

at *m/z* 1703.4 and 1778.5 are assignable to free duplex **III** and mono-ruthenated duplex **III** adduct **22**, respectively.

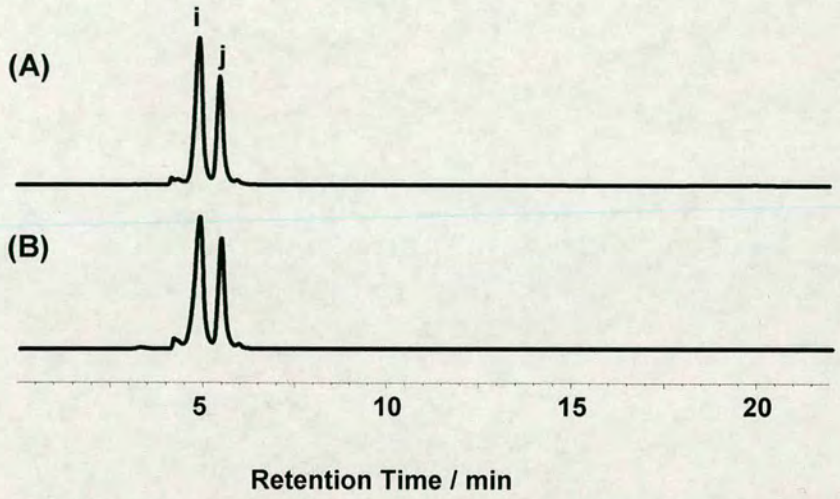

Figure 4.14 (A) HPLC separation for the reaction mixture of **12** (0.1 mM) with duplex **III** (0.1 mM) for 48 h; (B) HPLC chromatogram for the reaction mixture of **12** (0.1 mM) with GSH (1 mM, pH 7) and duplex **III** (0.1 mM) for 48 h.

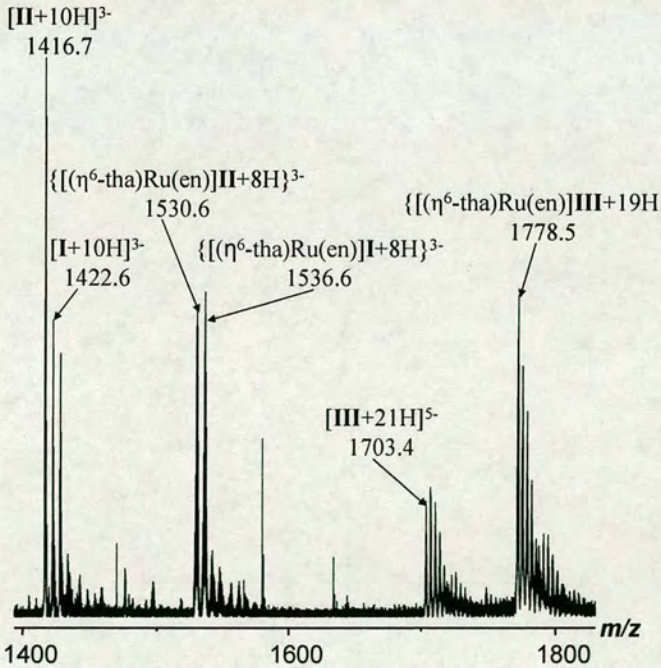

Figure 4.15 FT-ICR mass spectrum for the reaction mixture of **12** (0.1 mM) with GSH (1 mM, pH 7) and duplex **III** (0.1 mM) after 48 h.

Hydrophobic interactions between the arene ligand in these Ru(II) arene anticancer complexes, $[(\eta^6\text{-arene})Ru(en)Cl]^+$, and DNA can produce a driving force for DNA binding.[17] The most active complexes contain the most hydrophobic η^6-arene ligands.[7a] Complex **12** was used for comparison with **1** because the η^6-arene ligand in **12** (tha) is more hydrophobic that that in **1** (bip). The reaction of complex **12** with duplex **III** at the presence of GSH was shown to be similar to the reaction of **1** with **III** and GSH. GSH did not block complex **12** binding to N 7 of guanine bases in the DNA oligonucleotides.

4.4 Summary

Cells contain high (millimolar) concentrations of the tripeptide glutathione which has several binding sites for metal ions: the amino and carboxylate groups at the Glu terminus, carboxylate at the Gly terminus, and thiolate sulfur of the central Cys residue. Binding to the deprotonated amide nitrogen of Cys is possible when a N/S chelate ring can be formed, as has been observed for platinum amine complexes.[18] For heavier, "soft" transition metal ions, thiolate sulfur is a particularly strong site, and for Pt^{II}, such bonds are essentially formed irreversibly. Elevation of GSH levels therefore provides cells with detoxification and resistance mechanisms.[3,4] Therefore reactions of the organometallic Ru^{II} arene anticancer complex $[(\eta^6\text{-bip})Ru(en)Cl]^+$ with GSH and cGMP/DNA oligonucleotides were investigated, in particular, whether the presence of a large molar excess of GSH (as would be the case in cells) could prevent binding to the nucleobase guanine, the predominant binding site for $\{(\eta^6\text{-bip})Ru(en)\}^{2+}$ on DNA. The strategy used here involved separation of the products by HPLC and identification by ESI-MS, and after preparative HPLC, characterization by NMR spectroscopy. ^{15}N-labeling of the chelated ethylenediamine ligand and use of 2D [^1H, ^{15}N] HSQC NMR spectroscopy was helpful for elucidation of some of the complicated reaction pathways.

First the competitive reaction of complex **1** with 250 mol equiv GSH and 25 mol equiv cGMP[19] under the physiologically relevant conditions (phosphate buffer pH 7, 22 mM NaCl, 310 K) was investigated. This gave rise to the cGMP adduct $[(\eta^6\text{-bip})Ru(en)(cGMP\text{-}N7)]^+$ (**13**) as the major product, accounting for ca. 62% of total Ru after 72 h (Figure 4.4 and 4.6). This suggests that oxidation of coordinated glutathione in the thiolato complex **4** to the sulfenate in **10** and protonation of **10** to sulfenic acid provide a facile route for displacement of S-bound glutathione by G N7 (Scheme 4.2), a

route for RNA and DNA ruthenation even in the presence of a large excess of GSH.

1

4-mer DNA oligonucleotides were used for further studies. The reactions of **1** or **12** with GSH and DNA oligonucleotides still followed a similar pathway as that for the reaction of **1** with GSH and cGMP-giving rise to the DNA adducts **16-22** (see Figure 4.8, 4.12, 4.14 and 4.18) as final products via the sulfenate adduct **10** (Scheme 4.3).

This work has revealed unusual redox reactions of cysteinyl adducts of a monofunctional ethylenediamine Ru^{II} arene complex with glutathione, which provides a facile route for displacement of S-bound glutathione by G N7 for these Ru(II) arene anticancer complexes. In order to do the further studies on sulfenate complexes, a series of novel Ru(II) arene complexes in which SR was used as a leaving group were synthesized and investigations on the reactions for novel Ru complexes will be shown in Chapter 5.

4.5 References

[1] Morris, R. E.; Aird, R. E.; Murdoch, P. del S.; Chen, H.; Cummings, J.; Hughes, N. D.; Parsons, S.; Parkin, A.; Boyd, G.; Jodrell, D. I.; Sadler, P. J. *J. Med. Chem.* **2001**, *44*, 3616-3621.

[2] Gelasco, A.; Lippard, S. J. In *Topics in Biological Inorganic Chemistry*; Clarke, M. J., Sadler, P. J., Eds.; Springer-Verlag: Berlin, **1999**; Vol. 1, pp 1-43.

[3] Reedijk, J. *Chem. Rev.* **1999**, *99*, 2499-2510 and references therein.

[4] (a) Barnham, K. J.; Guo, Z. J.; Sadler, P. J. *J. Chem. Soc., Dalton Trans.* **1996**, 2867-2876. (b) Barnham, K. J.; Djuran, M. I.; Murdoch, P. D.; Sadler, P. J. *J. Chem. Soc., Chem. Commun.* **1994**, 721-722. (c) Barnham, K. J.; Djuran, M. I.; Murdoch, P. D.; Ranford, J. D.; Sadler, P. J. *J. Chem. Soc., Dalton Trans.* **1995**, 3721-3726. (d) Teuben, J. M.; Reedijk, J. *J. Biol. Inorg. Chem.* **2000**, *5*, 463-468. (e) Bugarcic, Z. D.; Soldatovic, T.; Jelic, R.; Alguero, B.; Grandas, A. *Dalton Trans.* **2004**, 3869-3877.

[5] Wang, F. Y.; Chen, H. M.; Parkinson, J. A.; Murdoch, P. D.; Sadler, P. J. *Inorg. Chem.* **2002**, *41*, 4509-4523.

[6] Frasca, D. R.; Clarke, M. J. *J. Am. Chem. Soc.* **1999**, *121*, 8523-8532.

[7] (a) Chen, H.; Parkinson, J. A.; Parsons, S.; Coxall, R. A.; Gould, R. O.; Sadler, P. J. *J. Am. Chem. Soc.* **2002**, *124*, 3064-3082. (b) Chen, H.; Parkinson, J. A.; Morris, R. E.; Sadler, P. J. *J. Am. Chem. Soc.* **2003**, *125*, 173-186. (c) Novakova, O.; Chen, H.; Vrana, O.; Rodger, A.; Sadler, P. J.; Brabec, V. *Biochemistry* **2003**, *42*, 11544-11554. (d) Chen, H. M.; Parkinson, J. A.; Novakova, O.; Bella, J.; Wang, F. Y.; Dawson, A.; Gould, R.; Parsons, S.; Brabec, V.; Sadler, P. J. *Proc. Natl. Acad. Sci. U.S.A.* **2003**, *100*, 14623-14628.

[8] (a) Palmer, A. G.; Cavanagh, J.; Wright, P. E.; Rance, M. *J. Magn. Reson.* **1991**, *93*, 151-170. (b) Kay, L. E.; Keifer, P.; Saarinen, T. *J. Am. Chem. Soc.* **1992**, *114*, 10663-10665. (c) Schleucher, J.; Schwendinger, M.; Sattler, M.;

Schmidt, P.; Schedletzky, O.; Glaser, S. J.; Sørensen, O. W.; Griesinger, C. *J. Biomol. NMR* **1994**, *4*, 301-306.

[9] Weigand, W.; Wunsch, R. *Chem. Ber.* **1996**, *129*, 1409-1419.

[10] The HPLC fraction b shown in Figure 5.4 was collected to lyophilize for NMR studies, and it was found to decompose within 30 min due to the protonation of **10**.

[11] (a) Murdoch, P. del S.; Kratochwil, N. A.; Parkinson, J. A.; Patriarca, M.; Sadler, P. J. *Angew. Chem., Int. Ed.* **1999**, *38*, 2949-2951. (b) Lempers, E. L. M.; Inagaki, K.; Reedijk, J. *Inorg. Chim. Acta* **1988**, *152*, 201-207.

[12] (a) Lempers, E. L. M.; Reedijk, J. *Inorg. Chem.* **1990**, *29*, 1880-1884. (b) Bose, R. N.; Moghaddas, S.; Weaver, E. L.; Cox, E. H. *Inorg. Chem.* **1995**, *34*, 5878-5883.

[13] van Boom, S.; Chen, B. W.; Teuben, J. M.; Reedijk, J. *Inorg. Chem.* **1999**, *38*, 1450-1455.

[14] Wang, F.; Bella, J.; Parkinson, J. A.; Sadler, P. J. *J. Biol. Inorg. Chem.* **2005**, *10*, 147-155.

[15] Liu, H. K.; Berners-Price, S. J.; Wang, F.; Parkinson, J. A.; Xu, J.; Bella, J.; Sadler, P. J. *Angew. Chem. Int. Ed.* **2006**, *45*, 8153-8156.

[16] Parkinson, J. A.; Chen, Y.; Guo, Z.; Murdoch, P. del S.; Berners-Price, S. J.; Brown, T.; Sadler, P. J. *Chem. Eur. J.* **2000**, *6*, 3636-3644.

[17] Ren, J.; Jenkins, T. C.; Chaires, J. B. *Biochemistry* **2000**, *39*, 8439-8447.

[18] Murdoch, P. del S.; Kratochwil, N. A.; Parkinson, J. A.; Patriarca, M.; Sadler, P. J. *Angew. Chem., Int. Ed.* **1999**, *38*, 2949-2951.

[19] Concentration chosen on the basis that 10^6 cells contain ca. 10 μg RNA and 5 μg DNA, a guanine content of 0.01 μmol, which is ca. 25 × typical intracellular Ru (380 pmol Ru/10^6 cells, for dose of **1**) 25 μM: Wang, F. Y.; Zeitlin, B.; Habtemarian, A.; Eades, L.; Aird, R.; Jodrell, D. I.; Sadler, P. J. unpublished material).

Chapter 5

Activation of Ru(II) Arene Anticancer Complexes towards Guanine Binding by Oxidation of Bound Thiolates

5.1 Introduction

"Half-sandwich" Ru(II) arene anticancer complexes were found to have good aqueous solubility which is an advantage for clinical use, and the arene ligand can be inert towards displacement under physiological conditions.[1] A typical series of half-sandwich "piano-stool" Ru(II) arene anticancer complexes is $[(\eta^6\text{-arene})Ru(en)X]^{n+}$, in which X is a leaving group providing a potential binding site for nucleotides via hydrolysis, and activities of these complexes correlated with the hydrolysis rate of the leaving group.[1,2] The leaving group X is usually a halide which is hydrolysed to form the active aqua complex,[2] and substituted by biological molecules such as guanine bases.[3,4] Recently, some novel Ru(II) arene anticancer complexes containing different leaving groups, such as SPh and SC_3H_7 (SR), were synthesized and their anticancer activities were studied in our research group. Interestingly, no hydrolysis for complex $[(\eta^6\text{-hmb})Ru(en)(SPh)]PF_6$ (**23**; hmb = hexamethylbenzene) was observed, however, it still has relatively high cytotoxicity (IC_{50} = 23 μM).[5] In Chapter 3, it was shown that GSH can be oxidized to GSOH or GSO_2H which play important roles in physiological reactions.[6,7] Furthermore, thiols are considered to have one of the most reactive functional groups found in cells, and sulfenic acids RSOH are believed to be involved in these biological reactions.[8] These acids have been proved as key intermediates in many biochemical reactions.[9,10]

In this Chapter, oxidations of complex **23** and another complex $[(\eta^6\text{-hmb})Ru(en)(S\text{-}i\text{Pr})]I$ (**24**; *i*Pr=isopropyl) were studied, and two-step reactions were discovered in which formation of final products (sulfinate adducts) occured via sulfenate complexes. The reaction of the sulfinate adduct with cGMP under physiologically-relevant conditions (phosphate buffer, pH 7, 22 mM NaCl) at 310 K, was compared to the reaction of **23** with cGMP under the same conditions, and much more monoruthenated cGMP adduct was obtained in the reaction of the sulfinate adduct with cGMP.

5.2 Experimental

5.2.1 Materials

[(η^6-hmb)Ru(en)(SPh)]PF_6 (**23**), [(η^6-hmb)Ru(en)(S-*i*Pr)]I (**24**) [(η^6-hmb)Ru(^{15}N-en)(S-*i*Pr)]I (^{15}N-**24**) and were synthesized, purified and characterised as pure unoxidised compounds using HPLC, ESI-MS and NMR spectroscopy by Dr. Holm Petzold. Glutathione (GSH, reduced), sodium chloride, disodium hydrogen phosphate, and Chelex resin (used for removal of impurity ions from phosphates) were purchased from Sigma; sodium dihydrogen phosphate and the ruthenium standard for atomic spectrometry (1003 μgRu/mL^{-1}) from Aldrich; sodium hydroxide and sodium chloride from Fisher; and trifluoroacetic acid (TFAH) from Acros. Hydrogen peroxide (30% aqueous solution) was purchased from Prolabo.

5.2.2 Methods

5.2.2.1 High Performance Liquid Chromatography (HPLC)

Columns and mobile phases were same as those described in Chapter 3. The gradient (solvent B) was as follows: 10% to 25% within 10 min, 80% from 15 to 19 min, reset to 10% from 20 to 25 min.

5.2.3 Preparation of Samples

5.2.3.1 UV-Vis

The reactions of **23** (0.1 mM)/**24** (0.1 mM) with H_2O_2 (0.6 mM) in unbuffered water at 298 K were followed by recording UV-Vis spectra every 2 min for 2 h and 3 h, respectively.

5.2.3.2 HPLC/ESI-MS/NMR

For all the reaction mixtures containing GSH, before GSH was added, the pH values of GSH were adjusted using NaOH and $HClO_4$ to ca. pH 7.

For the reaction of **23** with O_2 at 310 K for 24 h, the experiment was set up as shown in Figure 5.1. The reaction solution was connected with an oxygen cylinder. Oxygen was bubbled into the reaction solution for 24 h, and the flask was incubated in a water-bath at 310 K.

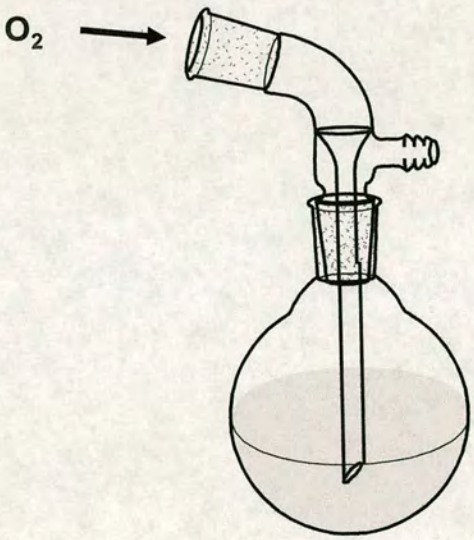

Figure 5.1 The apparatus used for the reaction of **23** with O_2 at 310 K for 24 h.

For ESI-MS samples, HPLC fractions were collected from the 24-h reaction mixture of **23** with H_2O_2 at various molar ratios in water. After lyophilization, the residue from each fraction was re-dissolved in 50% H_2O/50% CH_3CN to the final concentration of ca. 0.05 mM.

For NMR samples, the reaction mixture of **23** (1 mM) with H_2O_2 (6 mM) in MeOD at 298 K was recorded by ^1H NMR spectroscopy every 2 min for 24 h, and another reaction mixture of **24** (2 mM) with GSH (10 mM) and cGMP (4 mM) under physiologically-relevant described as above containing 10% D_2O at 310 K was recorded by 1D NMR and 2D [^1H, ^{15}N] HSQC NMR spectroscopy every 2 h for 62 h. All NMR data were processed using topspin-nmr (version 1.3, Bruker Biospin. Ltd.).

5.2.3.3 Determination of Extinction Coefficients

HPLC fractions of complex **23**, its sulfinate adducts were collected from a 10 mM equilibrium aqueous solution of **23**, the 24-h reaction mixture of complex **23** with H_2O_2 in water, 24-h reaction mixture of complex **23** with cGMP in buffer containing 22 mM NaCl. The values are listed in Table 5.1.

Table 5.1 Relative extinction coefficients at 254 nm of HPLC-isolated Ru arene complexes

Complex	Ru[a] /μg mL^{-1}	Ru /nmol	peak area[b]	ε^R_{254}[c]
[(η^6-hmb)Ru(en)(SPh]$^+$ (**23**)	1.76	87.1	3621.54	1.00
[(η^6-hmb)Ru(en)(SO_2Ph)]$^+$ (**26**)	6.04	299	19238.5	1.55

[a] Ru concentration in 5 mL aqueous sample determined by ICP-OES.
[b] Relative peak areas of HPLC fractions with UV detection at 254 nm.
[c] Relative extinction coefficient.

5.3 Results and Discussion

5.3.1 Oxidation of Pure Complex 23 or 24 to sulfenate/sulfinate adducts

Since the partial oxidation of sulphur in [(η^6-hmb)Ru(en)(SPh)]PF_6 (**23**) was observed in the x-ray crystal structure (data not shown), aqueous solutions of pure complex **23** (1 mM) containing phosphate buffer (pH 7) and 22 mM NaCl in air (i.e. not purged

with N_2) incubated at 310 K, were monitored by ^1H NMR (Figure 5.2(A), Table 5.2) to test the stability of **23** under the physiologically-relevant conditions. The empirical formula for the crystal structure $[Ru(en)(C_6Me_6)(SPh)_{0.85}(SO_2Ph)_{0.15}]PF_6$, indicated that 15% of SPh was oxidized to sulfinate SO_2Ph due to the oxidation of starting material NaSPh to $NaSO_2Ph$ during the synthesis process. The ^1H NMR spectra (Figure 5.2, Table 5.2) illustrated that the aqueous solution of **23** is stable within seven days at pH 7 (22 mM NaCl) in air at 310 K.

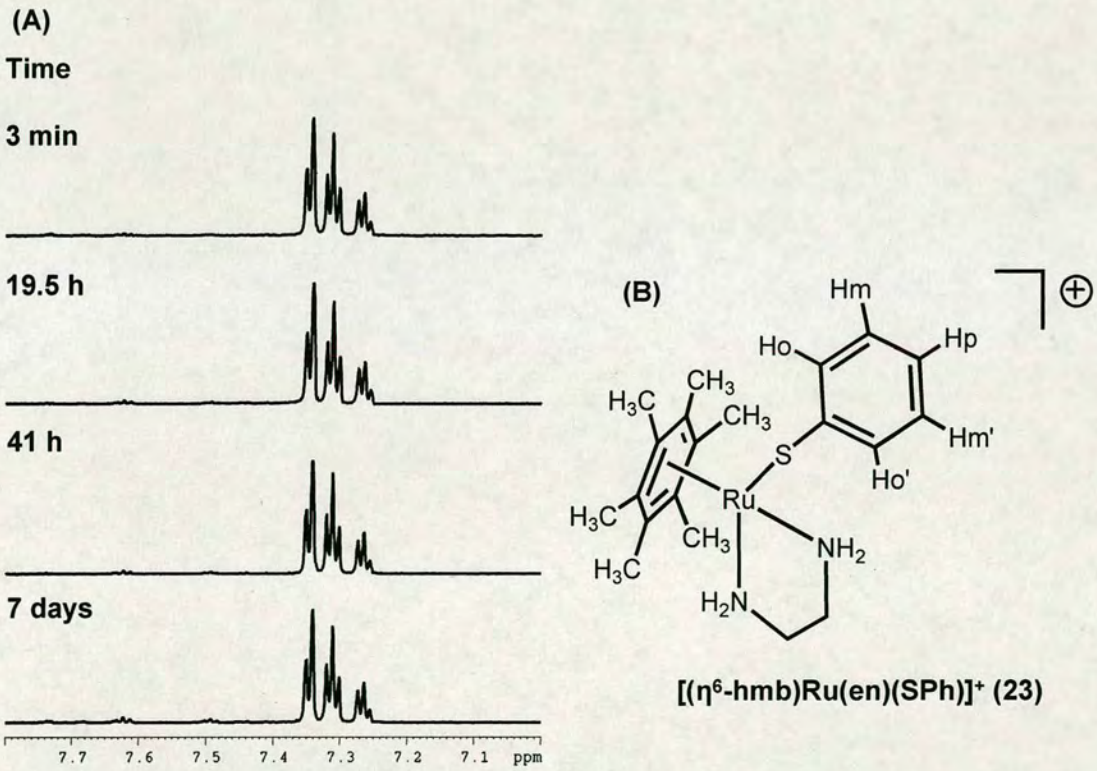

Figure 5.2 (A) Phenyl thiolate region of ^1H NMR time course for aqueous solution of pure complex **23** (1 mM) under physiologically-relevant conditions in air at 310 K The assignment for the three signals were listed in Table 5.2; (B) Chemical structure of **23**.

Table 5.2 ^{1}H NMR chemical shifts (δ) for the phenyl thiolate of pure complex [(η^6-hmb)Ru(en)(SPh)]$^+$ (**23**) (pH 7, 22 mM NaCl) in 90% H_2O/10% D_2O (310 K)

Proton	δ /ppm
Ho	7.35
Ho′	7.35
Hm	7.31
Hm′	7.31
Hp	7.26

Sulfenic acids are generally assumed to be only transient intermediates in the oxidation of thiols to both disulfides and sulfinic acids (see Scheme 5.1),[11] due to their instability. The main reason why they are very unstable and highly reactive is a facile self-condensation reaction to form the corresponding thiosulfinic-S esters RS(O)SR (thisulfinates) involving nucleophilic attack by one sulfenic acid sulphur on that of the second RSOH.[12] The X-ray crystal structure of Ru(II) arene sulfenate complex [(η^6-*p*-cymene)Ru(en)(S(O)-*i*Pr)]I (synthesized and crystallized by Dr. Holm Petzold; not shown) showed that the bond length of Ru-S(O) (2.3788(7) Å) is shorter than that of Ru-S (2.3932(7) Å) obtained from the X-ray crystal structure of Ru(II) arene thiolate complex [(η^6-*p*-cymene)Ru(en)(SPh)]I (not shown). Similar results have been obtained in the crystal structures of *cis*-dithiolate [1,5-bis(2-mercaptoethyl)-1,5-diazacy-clooctanato]nickel(II) and its sulfenato adduct.[13] Ruthenium (II) has a high affinity for sulphur-containing molecules.[14] Therefore, no hydrolysis was observed for complex **23**.[5]

Scheme 5.1 Oxidation pathways for thiols giving sulfinic acids and disulfides.

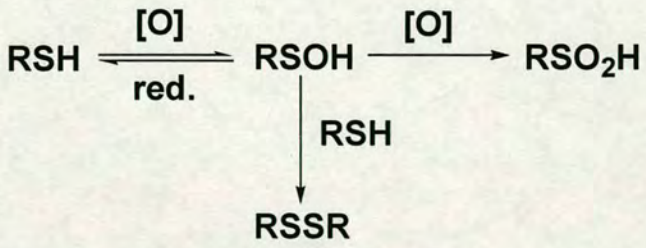

5.3.1.1 Oxidation of Pure Complex 23 by Molecular Oxygen

The reaction of pure complex **23** with pure O_2 supplied by an oxygen cylinder (the vessel is shown in Figure 5.1) for 24 h at 310 K was investigated using HPLC. Compared to the chromatogram of complex **23**, the chromatogram for the reaction mixture of **23** with O_2 at 310 K for 24 h showed that the reaction did not give rise to any new adduct (Figure 5.3), which indicated the complex cannot be readily oxidized by O_2.

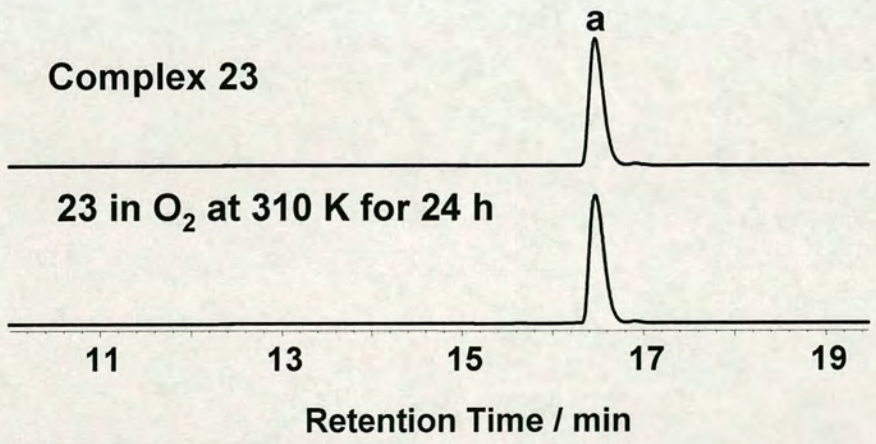

Figure 5.3 HPLC separations for pure complex **23** and the reaction mixture of complex **23** with O_2 at 310 K for 24 h. Peak assignments: (a) **23**.

5.3.1.2 Reactions with H_2O_2

The reactions of pure **23** (0.1 mM)/pure **24** (0.1 mM) with H_2O_2 (0.6 mM) in unbuffered water at 298 K were followed by UV-Vis spectroscopy (Figure 5.4 and

5.5). Figure 5.4 shows the absorption band at 252 nm decreased in intensity with time and disappeared after 6 min, and a new absorption band appeared at 327 nm and increased in intensity for the first 14 min and then decreased in intensity, and another new band at 316 nm appeared. Figure 5.5 shows a similar variation to that in Figure 5.4. The two curves in Figure 5.6 indicate that the reactions of pure **23** or **24** with H_2O_2 in aqueous solution at 298 K are two-step reactions.

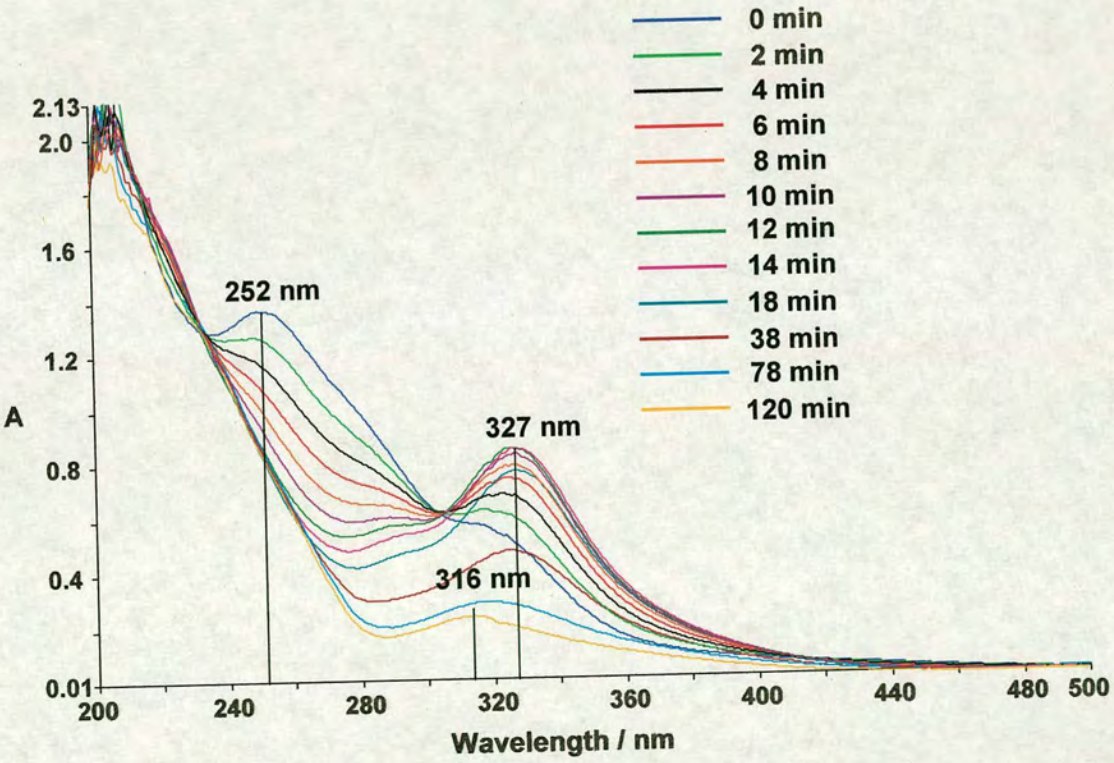

Figure 5.4 UV-Vis time course for the reaction of pure **23** (0.1 mM) with H_2O_2 (0.6 mM) in unbuffered water at 298 K.

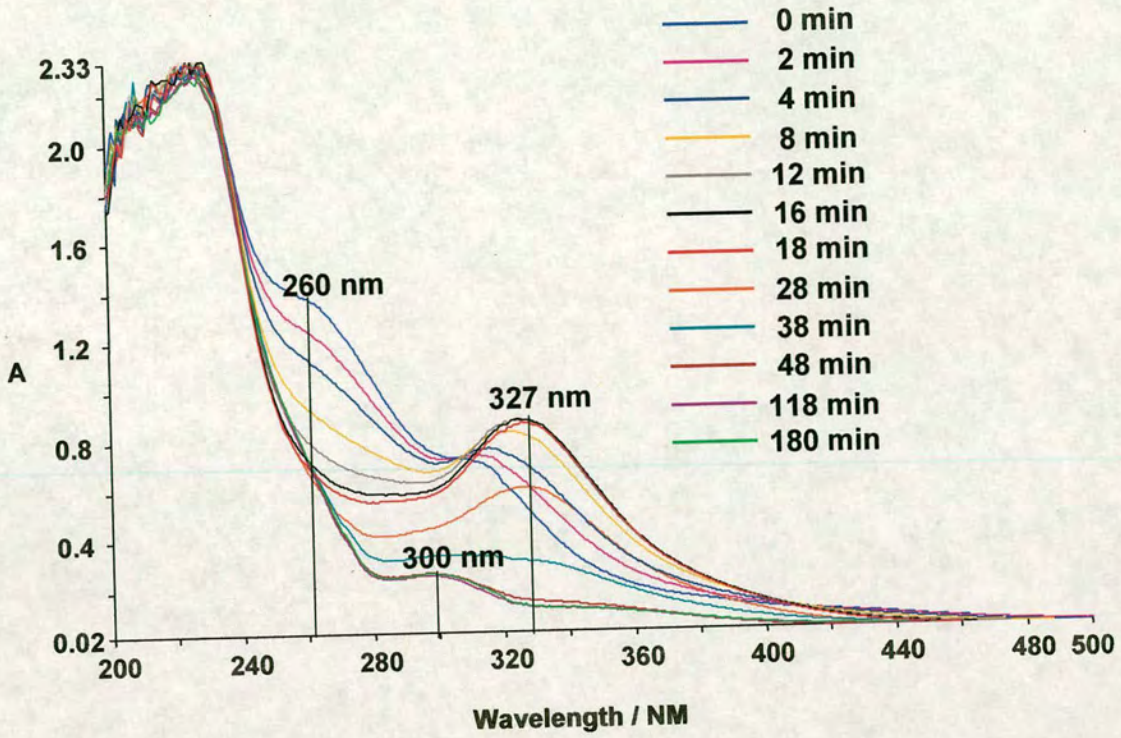

Figure 5.5 UV-Vis time course for the reaction of pure [(η^6-hmb)Ru(en)(S-*i*Pr)]I (**24**; 0.1 mM) with H_2O_2 (0.6 mM) in unbuffered water at 298 K.

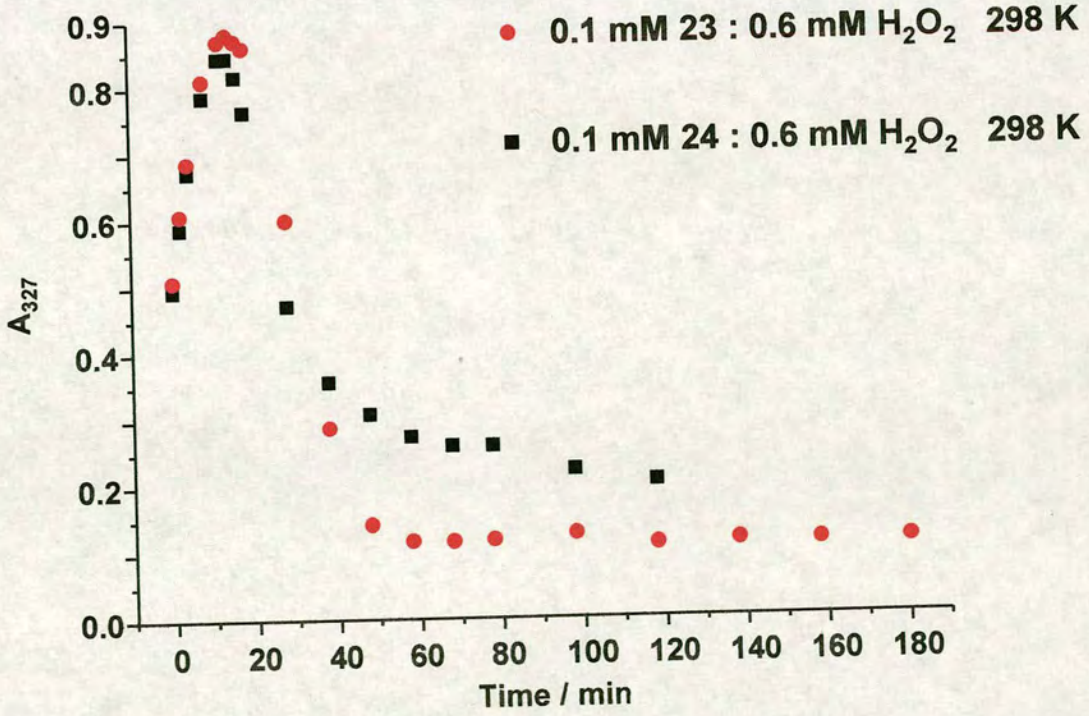

Figure 5.6 Variation of the absorption at 327 nm of the UV-Vis curves shown in Figure 5.4 and 5.5 with time.

Hydrogen peroxide produced in the human body by cells of the immune system, was used as a mild oxidant for the oxidation of thiolate complexes (**23** and **24**) giving sulfenate adducts which were further oxidized to sulfinate adducts. In the UV-Vis spectra, the peaks at 252 nm in Figure 5.4 and at 260 nm in Figure 5.5 are due to thiolato complexes **23** and **24**, respectively, while those at 327 nm in Figure 6.4 and 5.5 are due to the sulfenato complexes **25** and **27**. A similar change in the UV-Vis spectrum during the photooxidation of $[Co(III)(en)_2(S\text{-}cys)]BF_4$ has been observed.[15] Another two bands at 316 nm in Figure 5.4 and at 300 nm in Figure 5.5 are probably assignable to the sulfinato adducts.

Reaction mixtures of pure **23** and H_2O_2 at various mole ratios in water at 310 K for 24 h were prepared for HPLC and MS analysis. HPLC separations (Figure 5.7) showed that the reaction of **23** (1 mM) with H_2O_2 (ca. 0.5 mM) in water at 310 K for 24 h, gave rise to two oxidation adducts (peaks b and c), while the reaction of **23** (1 mM) with H_2O_2 (2 mM) in water at 310 K for 24 h, only gave rise to one oxidation adduct (peak d). ESI mass spectra (Figure 5.8) from HPLC fraction b (see Figure 5.7) gave an peak at *m/z* 449.2 which can be assigned to the sulfenato adduct $[(\eta^6\text{-hmb})Ru(en)(SOPh)]^+$ (**25**), and an ion peak at *m/z* 465.4 from HPLC fraction c (see Figure 5.7) assignable to the sulfinato adduct $[(\eta^6\text{-hmb})Ru(en)(SO_2Ph)]^+$ (**26**).

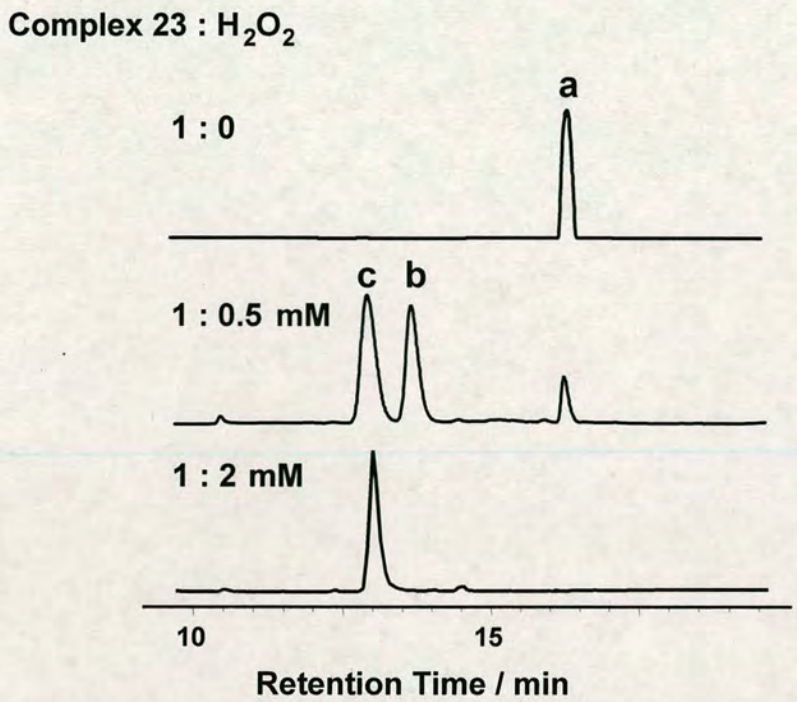

Figure 5.7 HPLC separations for reaction mixtures of **23** and H_2O_2 at various mole ratios (as indicated in the Figure) in water at 310 K for 24 h. Peak assignments: (a) complex **1**; (b) sulfenato adduct $[(\eta^6\text{-hmb})Ru(en)(SOPh)]^+$ (**25**); (c) sulfinato adduct $[(\eta^6\text{-hmb})Ru(en)(SO_2Ph)]^+$ (**26**).

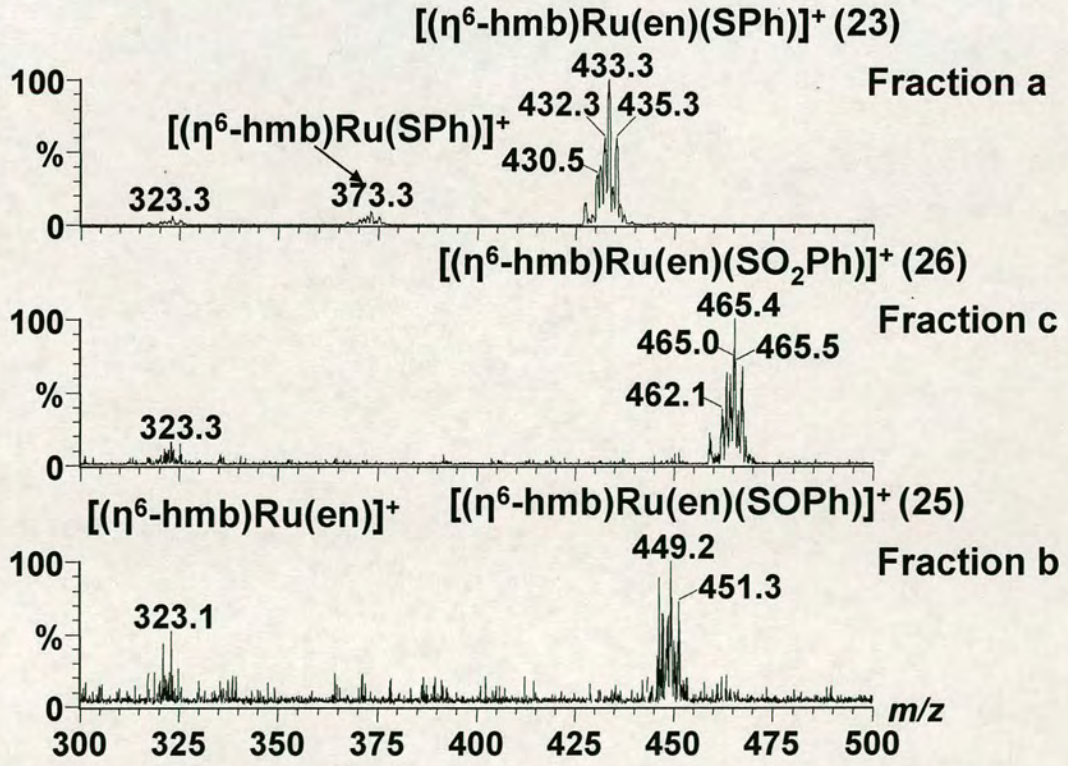

Figure 5.8 ESI mass spectra for HPLC fractions (shown in Figure 5.7) collected from the reaction of **23** (1 mM) and H_2O_2 (0.5 mM) in water at 310 K for 24 h.

The reaction of **1** (1 mM) with H_2O_2 (6 mM) in MeOD at 298 K was followed by ^1H NMR spectroscopy (see Figure 5.9(A), Table 5.3). The three blue resonances assigned to phenyl thiolate in **23** (blue in Figure 5.9(A)), decreased in intensity and disappeared at after ca. 20 min; meanwhile after ca. 8 min a new adduct $[(\eta^6\text{-hmb})Ru(en)(SOPh)]^+$ (**25**) (three new resonances coloured in red in Figure 5.9(A)) formed and increased in concentration until 20 min, and decreased in concentration, then disappeared after ca. 24 h. Another two new signals labelled in pink appeared, assignable to sulfinate adduct $[(\eta^6\text{-hmb})Ru(en)(SO_2Ph)]^+$ (**26**), and increased in intensity with time. Figure 5.9(B) illustrated that the reaction of **23** with H_2O_2 is a two-step reaction, in which **23** is oxidized to the sulfenate adduct **25**, and then **25** is further oxidized to sulfinate product **26**. It is evident that the reaction rate for the oxidation of **23** to **25** is much faster than that for the further oxidation of **25** to **26**.

Table 5.3 ^1H NMR chemical shifts for phenyl group in complex **23**, adducts $[(\eta^6\text{-hmb})Ru(en)(SOPh)]^+$ (**25**) and $[(\eta^6\text{-hmb})Ru(en)(SO_2Ph)]^+$ (**26**) in MeOD at 298 K (see Figure 5.9(A)). The labels for the protons are given in Figure 5.2(B).

Proton	Complexes		
	23	**25**	**26**
		δ/ppm	
Ho	7.24	7.29	7.67
Ho′	7.24	7.29	7.67
Hm	7.13	7.52	7.62
Hm′	7.13	7.52	7.62
Hp	7.06	7.38	7.62

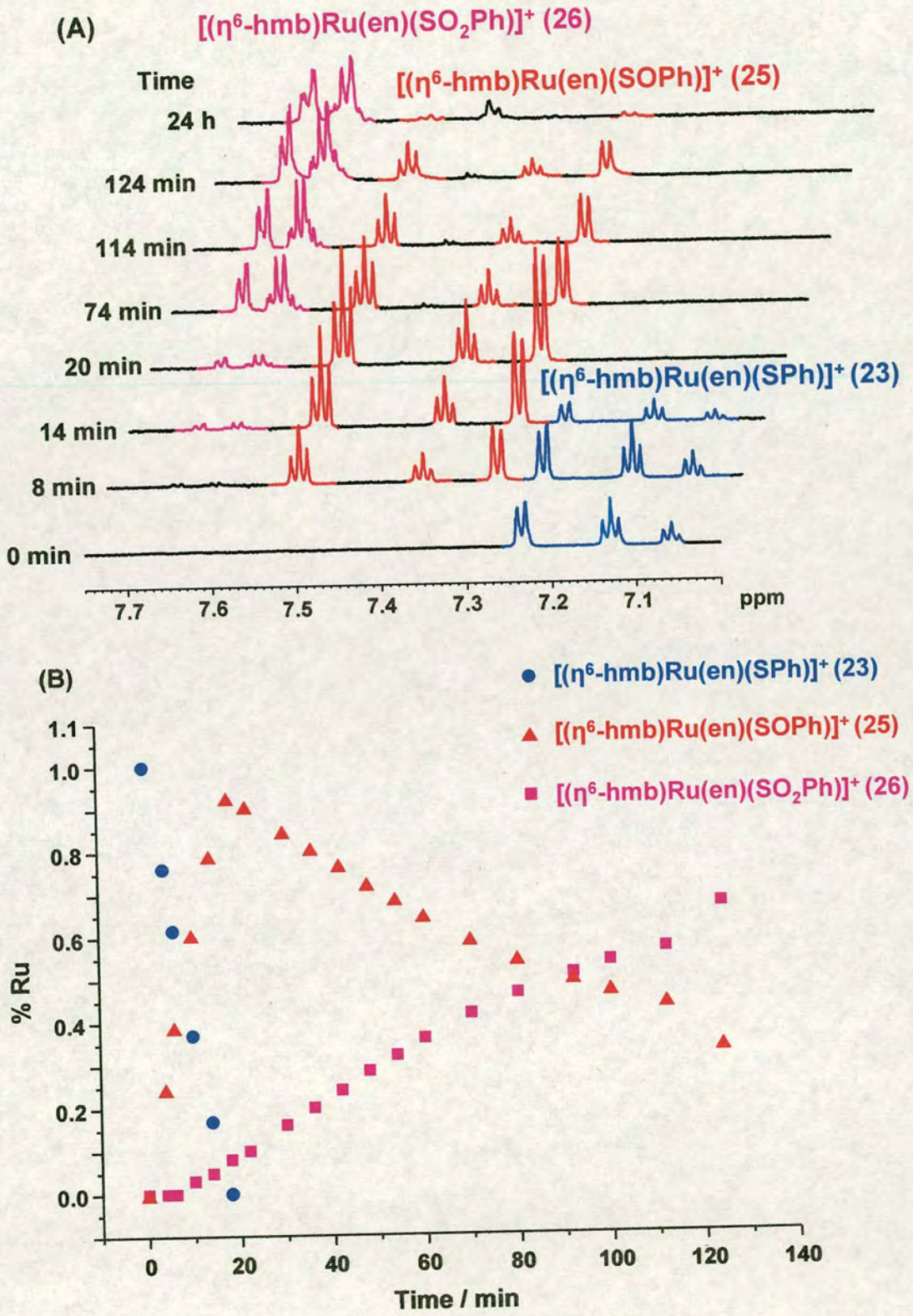

Figure 5.9 (A) Phenyl region of ^{1}H NMR time course for the reaction of **23** (1 mM) with H_2O_2 (6 mM) in MeOD at 298 K. There are three sets of signals, assignable to complex **23**, sulfenate adduct **25** and sulfinate adduct **26**, respectively; (B) Variation of the relative Ru concentrations of species detected during the reaction in (A) with time.

It has been demonstrated that in the absence of metal ions, a two-step bimolecular nucleophilic substitution mechanism is involved in thiol oxidation by hydrogen peroxide in aqueous solution, in which the rate-determining formation of a reactive sulfenic acid intermediate (RSOH) is followed by reaction with a second thiolate to form a disulfide (RSSR), the only final product observed in aqueous solutions.[16] In the presence of Ru(II), both of sulfenato adduct **25** and sulfinato product **26** were observed in the reaction of **23** with H_2O_2 at the molar ratio of 2:1 in aqueous solution at 310 K for 24 h. Even at the high ratio of H_2O_2:**23** (6:1), the sulfinato adduct **26** is the only product observed in the aqueous solution. According to Figure 5.9(B), the formation of the sulfenato adduct **25** is very fast (complete within 20 min), and further oxidation to the sulfinato adduct **26** is much slower (complete within 24 h) which is the rate-determining step. Such a reaction pathway has also been observed for the reaction of $[Co(III)(en)_2(S\text{-}cys)]BF_4$ with singlet oxygen.[15]

5.3.1.3 Oxidation of Complex 24 to Sulfenate by Air in Presence of GSH

The reaction solutions of ^{15}N-**24** (1 mM) with or without GSH (10 mM) at pH 7 containing 22 mM NaCl, were bubbled with air and incubated in water-bath at 310 K for 4 h, and then analysed by 2D [^{1}H,^{15}N] HSQC NMR. One pair of cross-peaks 24a/b in Figure 5.10(A) was assigned to $[(\eta^6\text{-hmb})Ru(^{15}N\text{-en})(S\text{-}i\text{Pr})]^+$ (^{15}N-**24**), and two pairs of cross-peaks 27a/b and 27c/d in Figure 5.10(B) are assignable to $[(\eta^6\text{-hmb})Ru(^{15}N\text{-en})(SO\text{-}i\text{Pr})]^+$ (^{15}N-**27**). The reaction of ^{15}N-**24** (1 mM) with H_2O_2 (6 mM) at pH 7 (22 mM NaCl) at 310 K for 6 h was monitored by 2D [^{1}H,^{15}N] HSQC NMR (data not shown) and used as basis for the assignment of complex **27**. The two results (Figure 5.10(A) and (B)) demonstrated that complex **24** can be readily oxidized to sulfenato adduct **27** by bubbling with air only in the presence of GSH, and GSH/O_2 acts as oxidant.

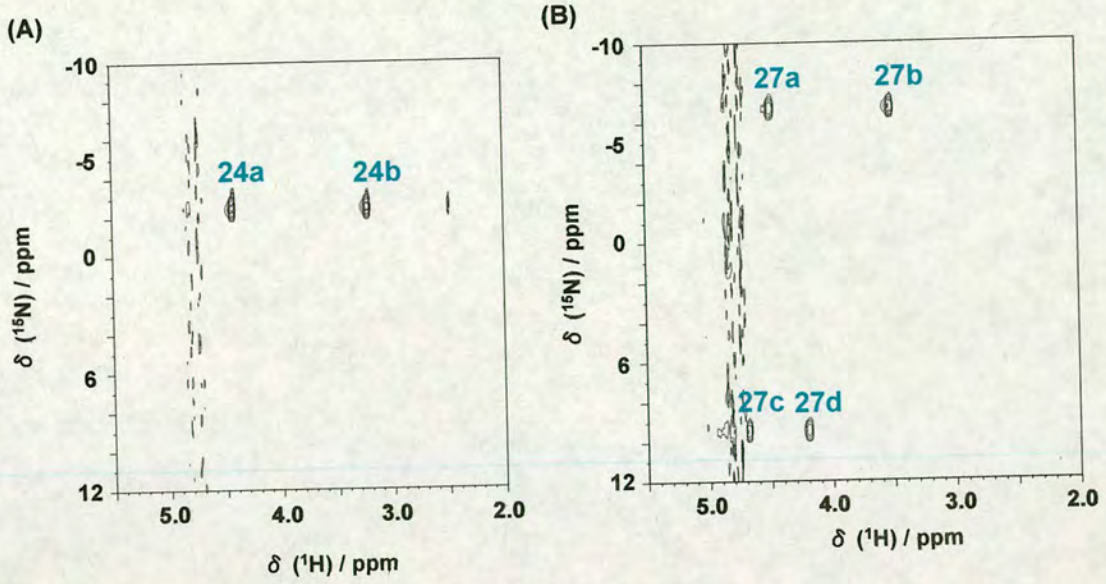

Figure 5.10 (A) 2D [^{1}H,^{15}N] HSQC NMR spectrum for the reaction of ^{15}N-**24** (1 mM) bubbled with air at 310 K for 4 h without GSH. Assignment: 24a/b [(η^6-hmb)Ru(^{15}N-en)(S-*i*Pr)]$^{+}$ (^{15}N-**24**); (B) 2D [^{1}H,^{15}N] HSQC NMR spectrum for the reaction of ^{15}N-**24** (1 mM) bubbled with air at 310 K for 4 h in presence of GSH (10 mM). Assignment: 27a/b and 27c/d [(η^6-hmb)Ru(^{15}N-en)(SO-*i*Pr)]$^{+}$ (^{15}N-**27**).

It was demonstrated that the highest rate for air oxidation of GSH to GSSG is at pH ca. 9.[17] It is believed that in the HL^{2-} form of glutathione (Figure 5.11),[18] two groups (the protonated NH_3^+ and the deprotonated S^-) interact with each other, at the average S-N distance of ca. 2.85 Å which is such that a molecule of dioxygen can be easily accommodated and activated.[17] However, the mechanism for the oxidation of GSH to GSSG are not known, still one supposed mechanism is given in Scheme 5.2. The thiolato complex **24** can only be oxidized to the sulfenato adduct **27** in presence of GSH by bubbling with Air (Figure 5.10), indicating GSH was involved in this oxidation reaction to accommodate O_2, and the supposed mechanism for this reaction is shown in Scheme 5.3. The excess of GSH was oxidized to GSSG which cannot bind to complex **24** due to the existence of sufficient O_2.

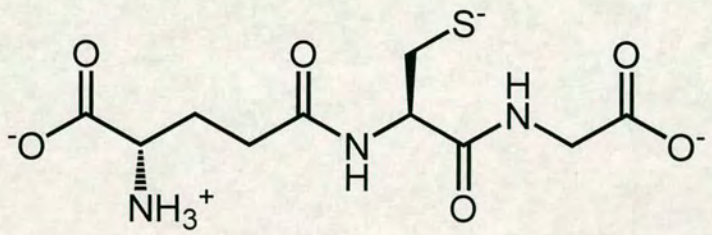

Figure 5.11 The HL^{2-} form of glutathione.[18]

Scheme 5.2 Supposed mechanism for air oxidation of GSH to GSSG.

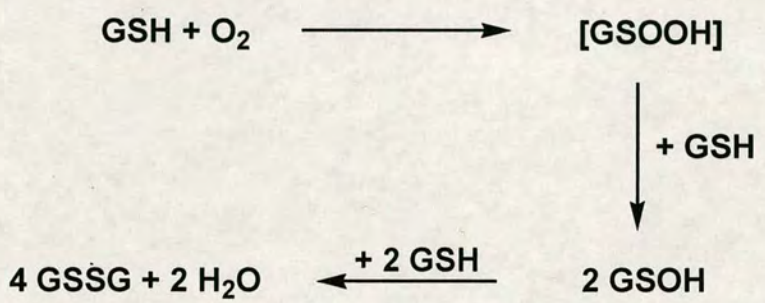

Scheme 5.3 Supposed mechanism for the reaction of **2** bubbled with air at pH 7 containing 22 mM NaCl in presence of GSH at 310 K for 4 h.

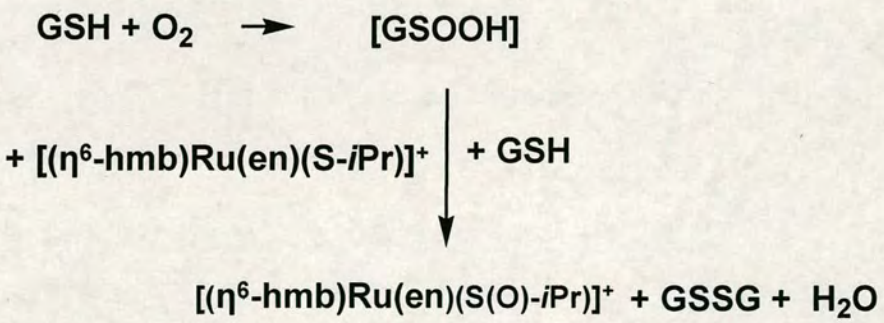

5.3.2 Hydrolysis and Acidity of Sulfenato Adduct 27

When the HPLC fraction b (see Figure 5.7) was collected for lyophilization, the sulfenato adduct **25** was found to have decomposed (^{1}H NMR obtained by Dr. Holm Petzold) due to the presence of trifluoroacetic acid (TFA) in HPLC mobile phase solvents (pH value ca. 2). Therefore, at low pH values, sulfenato complexes are

protonated to give sulfenic acid complexes which are unstable and highly reactive,[8] as shown in Scheme 5.4.

Scheme 5.4 Protonation of sulfenate complexes.

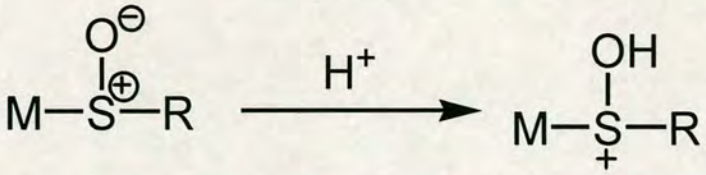

The pK_a^* value (pK_a value determined for D_2O solutions) of the sulfenato complex **27** was determined by Dr. Holm Petzold using NMR spectroscopy, which is the first time to be studied. The change in the ^1H NMR chemical shift of the CH proton in –S(O)C**H**Me_2 in **27**, [(η^6-hmb)Ru(en)(S(O)-*i*Pr)]$^+$, which predominates in equilibrium solution of **27** in D_2O at 298 K, was followed with changes in pH* (pH meter reading without correction for effects of D on glass electrode) over the range of 1.50-8.00 (Figure 5.12). The data were fitted to the Henderson-Hasselbalch equation which yielded a pK_a^* value of 3.44 for **27** (Figure 5.12).

Also the hydrolysis of sulfenato complex **27** in 90% D_2O/10% H_2O at 310 K was studied by Dr. Holm Petzold using 2D [^1H,^{15}N] HSQC NMR spectroscopy. The ^{15}N-labelled sulfenato complex (^{15}N-**27**) is relatively stable at pH* 7 (phosphate buffer) as shown in Figure 5.13(A), and at 16 h after HCl was added to change the pH* value from 7 to 2.11, two pairs of cross-peaks (27a/b and 27c/d) assignable to [(η^6-hmb)Ru(^{15}N-en)(S(O)-*i*Pr)]$^+$ (^{15}N-**27**), had disappeared, and another two new pairs of cross-peaks (28a/b and 29a/b) were obtained, which can be assigned to [(η^6-hmb)Ru(^{15}N-en)Cl]$^+$ (^{15}N-**28**) for 28a/b and [(η^6-hmb)Ru(^{15}N-en)OH_2]$^{2+}$ (^{15}N-**29**) for 29a/b, respectively (see Figure 5.13(B)) on the basis of the assignments for the hydrolysis of complex ^{15}N-**28** (Figure 5.13(C)). However, the rate of hydrolysis for **27** is quite fast, and appears to complete within hours.[19] The pathways are shown in

Scheme 5.5. The Ru-S(O) bond becomes weaker at low pH (ca. 2) due to the protonation of sulfenato complex **27**.

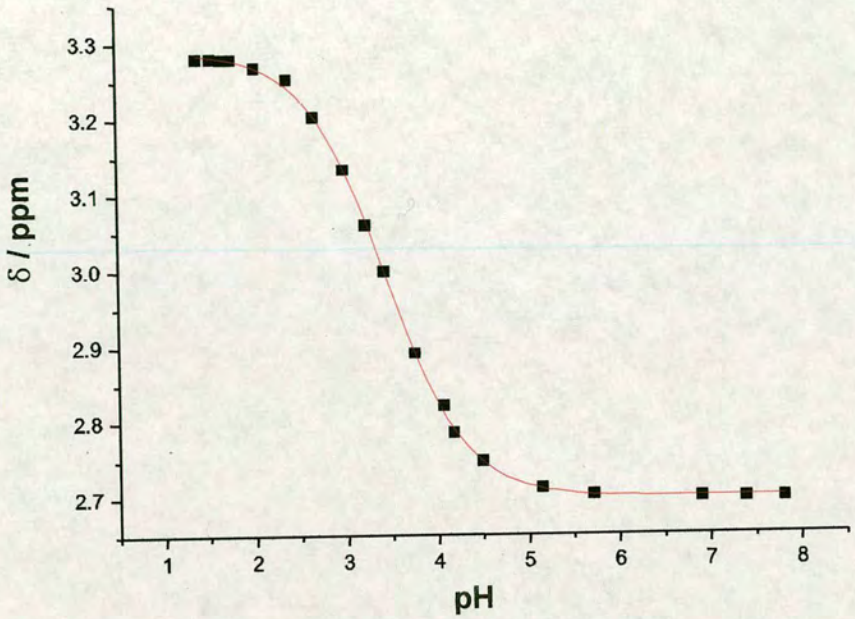

Figure 5.12 Plot of the ^{1}H NMR chemical shift versus pH at 298 K for –S(O)C**H**Me$_2$ proton of [(η^6-hmb)Ru(en)(S(O)-*i*Pr)]$^+$ (**27**) in D_2O. The curve represents the best fit to the Henderson-Hasselbalch equation and corresponds to pK_a value of 3.44 for **27** (data is from Dr. Holm Petzold).

Scheme 5.5 Pathways for the hydrolysis of the sulfenato complex **27**.

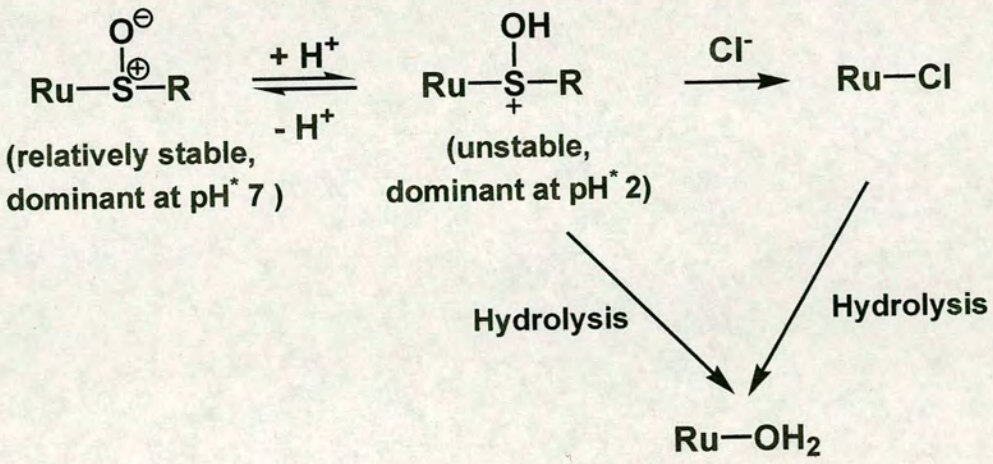

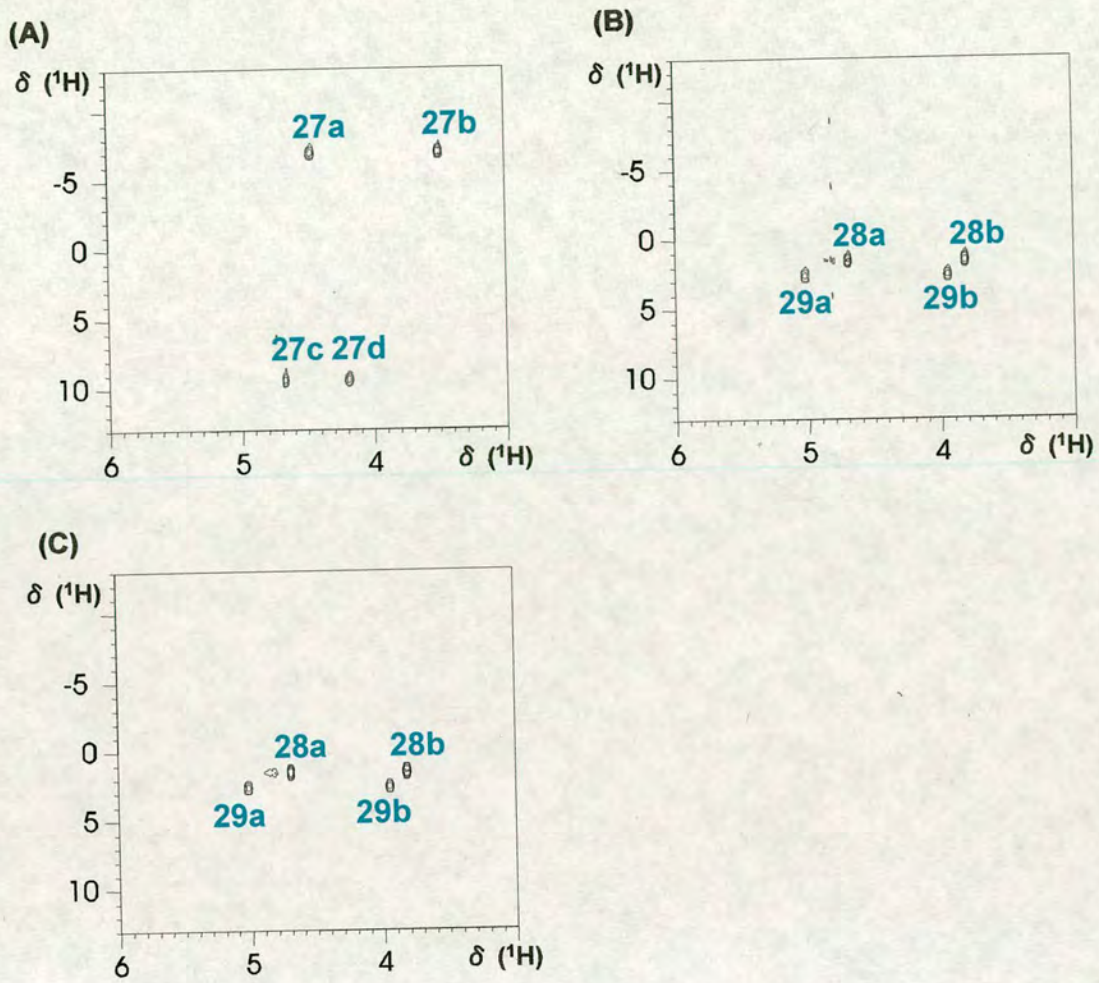

Figure 5.13 (A) 2D [^{1}H,^{15}N] HSQC NMR spectrum for sulfenato complex [(η^{6}-hmb)Ru(^{15}N-en)(S(O)-*i*Pr)]$^{+}$ (^{15}N-**27**) containing phosphate buffer (pH* 7) in 90% D_2O/10% H_2O at 310 K. (B) 2D [^{1}H,^{15}N] HSQC NMR spectrum for 16 h after HCl (in 90% D_2O/10% H_2O) was added to the solution in (A) to change the pH* to 2.11 at 310 K. (C) 2D [^{1}H,^{15}N] HSQC NMR spectrum for [(η^{6}-hmb)Ru(^{15}N-en)Cl]$^{+}$ (^{15}N-**28**; pH* 2.20) and [(η^{6}-hmb)Ru(^{15}N-en)(OH_2)]$^{2+}$ (^{15}N-**29**; pH* 2.20) in 90% D_2O/10% H_2O at 310 K, providing a basis for the assignments (Wang, F.; Xu, J.; Habtemariam, A.; Bella, J.; Sadler, P. J. *J. Am. Chem. Soc.* 2005, *127*, 17734-17743) in (B).

5.3.3 Competitive Reaction of 23 or 24 with GSH and cGMP Under Physiologically-relevant Conditions

The reaction of complex **23** (0.1 mM) with 50 mol equiv of GSH and 5 mol equiv of cGMP in air (i.e. not purged with Ar) at 310 K for 24 h, was studied by HPLC and ESI-MS. The HPLC chromatogram (Figure 5.14) showed that the reaction gave rise to three adducts (peaks b, d and e in Figure 5.14), and the three fractions were collected

and analysed by ESI-MS. In the mass spectrum of the fraction b (Figure 5.15), a singly-charged ion peak centred at *m/z* 449 was assigned to the sulfenate adduct $[(\eta^6$-hmb)Ru(en)(SOPh)$\}^+$ (**25**), and another singly-charged ion peak centred at *m/z* 323 to a fragment which had lost the SPh ligand from **25**. A singly-charged ion peak centred at *m/z* 668 obtained from fraction d is assignable to the monoruthenated cGMP adduct $[(\eta^6$-hmb)Ru(en)(cGMP-*N7*)$]^+$ (**30**), and a singly-charged ion peak centred at *m/z* 646 and a doubly-charged ion peak centred at *m/z* 323 from the fraction e are assignable to the monoruthenated glutathione sulfenate adduct $[(\eta^6$-hmb)Ru(en)(S(O)G)] (**31**).

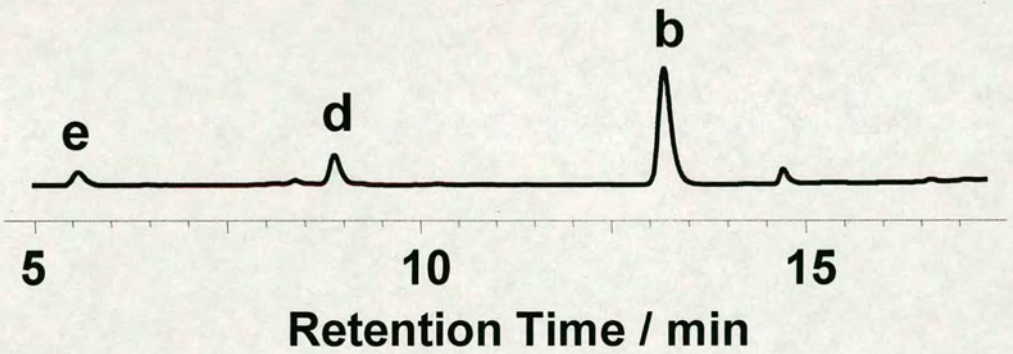

Figure 5.14 HPLC separation for the reaction of **23** (0.1 mM) with GSH (5 mM) and cGMP (0.5 mM) in air at 310 K for 24 h. Peak assignments: (c) sulfenato adduct $[(\eta^6$-hmb)Ru(en)(SOPh)$\}^+$ (**25**); (d) cGMP adduct $[(\eta^6$-hmb)Ru(en)(cGMP-*N7*)$]^+$ (**30**); (e) glutathione sulfenato adduct $[(\eta^6$-hmb)Ru(en)(S(O)G)] (**31**).

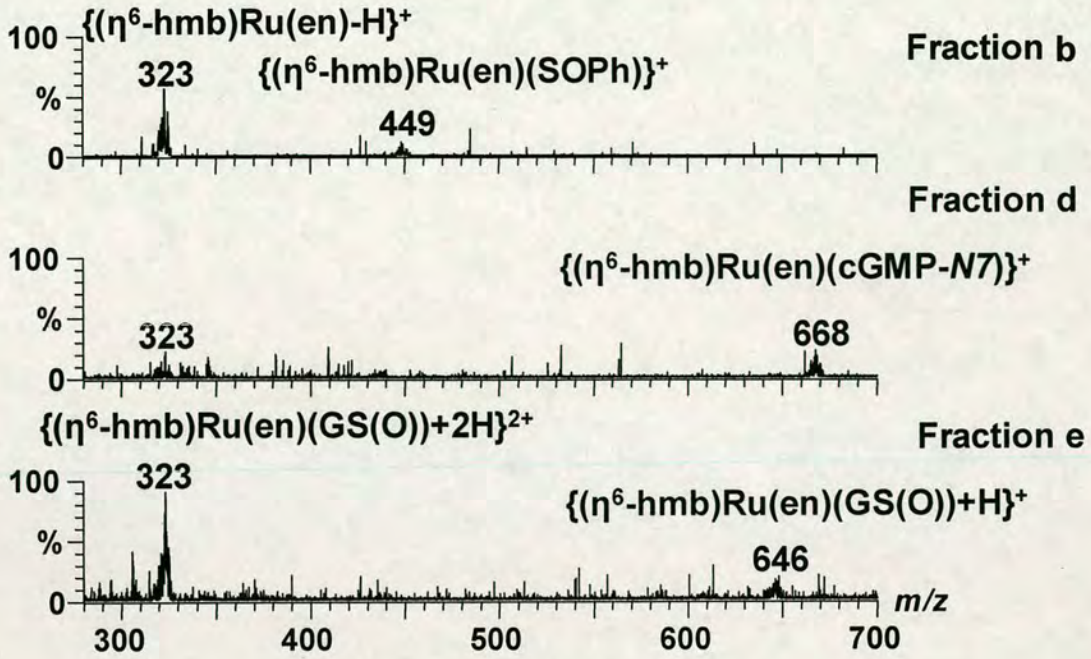

Figure 5.15 ESI mass spectra for the HPLC fractions b, d and e (see Figure 5.14) obtained from the reaction described in Figure 5.14.

Due to the broad water signal in NMR spectra for the reaction of **23** with GSH and cGMP, the competitive reaction of GSH and cGMP at millimolar concentrations (**24**:GSH:cGMP 2:10:4 mM) was followed by 2D [^{1}H,^{15}N] HSQC NMR in air (i.e. not purged with Ar) at 310 K using ^{15}N-labelled **24** (^{15}N-**24**). The spectra are shown in Figure 5.16 and ^{1}H and ^{15}N NMR chemical shifts are listed in Table 5.4. During the early stages (<2 h), a pair of new cross-peaks (32a/b) was observed for the ^{15}N-en ligand in thiolato adduct [(η^{6}-hmb)Ru(^{15}N-en)SG] (^{15}N-**32**), which increased in concentration until 36 h, and then decreased in concentration until 62 h. After 12 h, cross-peaks 27a/b and 27c/d appeared, assignable to the sulfenato adduct [(η^{6}-hmb)Ru(^{15}N-en)(S(O)-*i*Pr)]$^{+}$ (^{15}N-**27**). After 28 h, another pair of cross-peaks (31a/b and 31c) was detectable and can be assigned to the monoruthenated glutathione sulfenato adduct [(η^{6}-hmb)Ru(^{15}N-en)(S(O)G)] (^{15}N-**31**), and one cross-peak which should have same ^{15}N NMR chemical shift as that of 31c was covered by the water signal. These two sulfenato adducts **27** and **31** increased in concentrations until 62 h. All of the assignments were on the basis of the assignments from 2D [^{1}H,^{15}N] HSQC

NMR time courses for the reactions of ^{15}N-**24** (2 mM) with H_2O_2 (4 mM) containing phosphate buffer (pH 7) and 22 mM NaCl at 310 K (data not shown), and [(η^6-hmb)Ru(^{15}N-en)Cl]$^+$ (^{15}N-**28**; synthesized by Dr. Holm Petzold; 5 mM) with GSH (25 mM) at 310 K (data not show). Another reaction mixture of ^{15}N-**27** (2 mM; obtained from the reaction of ^{15}N-**24** with H_2O_2 at molar ratio of 1:1 at 310 K for 1 h) with cGMP (4 mM) at 310 K for 24 h in air, was analysed by 2D [^{1}H,^{15}N] HSQC NMR. Two pairs of cross-peaks (30a/b and 30c/d) were observed (see Figure 5.17, Table 5.4), assignable to monoruthenated cGMP adduct [(η^6-hmb)Ru(^{15}N-en)(cGMP-*N7*)]$^+$ (^{15}N-**30**) on the basis of the assignment for the ion peak at *m/z* 670 in the ESI mass spectrum for the reaction mixture (data not shown) and the assignment for the 2D [^{1}H,^{15}N] HSQC NMR spectrum of the reaction of ^{15}N-**28** (5 mM) with cGMP (50 mM) at 310 K for 24 h (data not shown; cGMP adduct **30** is the only product in the spectrum).

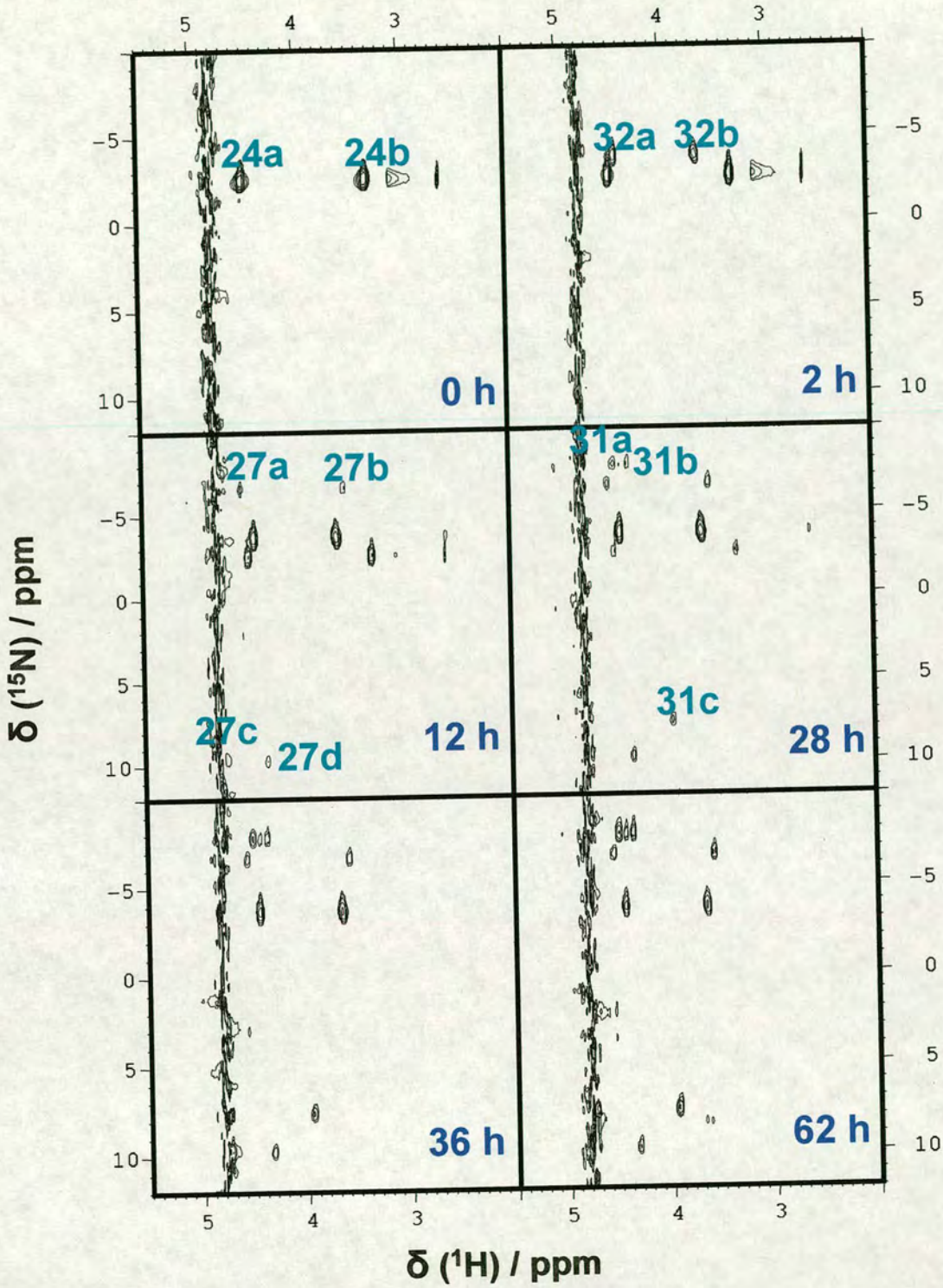

Figure 5.16 2D [^{1}H,^{15}N] HSQC NMR time course for the reaction of ^{15}N-**24** (2 mM) with GSH (10 mM) and cGMP (4 mM) in 90%H_2O / 10% D_2O containing 50 mM phosphate buffer and 22 mM NaCl in air at 310 K over a period of 62 h. Assignments: 24a/b ^{15}N-**24** [(η^6-hmb)Ru(^{15}N-en)(S-*i*Pr)]$^+$, 32a/b thiolate adduct [(η^6-hmb)Ru(^{15}N-en)SG] (^{15}N-**32**), 27a/b and 27c/d sulfenato adduct [(η^6-hmb)Ru(^{15}N-en)(S(O)-*i*Pr)]$^+$ (^{15}N-**27**), 31a/b and 31c monoruthenated glutathione sulfenato adduct [(η^6-hmb)Ru(^{15}N-en)(S(O)G)] (^{15}N-**31**).

Table 5.4 Chemical shifts of $^{1}H,^{15}N$ NMR peaks observed for reactions of ^{15}N-**24** (2 mM) with GSH (10 mM) and cGMP (4 mM) in 90%H_2O / 10% D_2O in air at 310 K (Figure 5.16), and ^{15}N-**27** (2 mM) with cGMP (4 mM) in 90%H_2O / 10% D_2O in air at 310 K for 24 h (see Figure 5.17).

complexes	(peak) δ $^{1}H/^{15}N$	
[(η^6-hmb)Ru(^{15}N-en)(S-*i*Pr)]$^+$ (^{15}N-**24**)	(2a) 4.50/-2.63	(2b) 3.32/-2.63
[(η^6-hmb)Ru(^{15}N-en)SG] (^{15}N-**32**)	(8a) 4.44/-3.73	(8b) 3.64/-3.73
[(η^6-hmb)Ru(^{15}N-en)(S(O)-*i*Pr)]$^+$ (^{15}N-**27**)	(5a) 4.55/-6.69	(5b) 3.58/-6.69
	(5c) 4.73/9.75	(5d) 4.34/9.75
[(η^6-hmb)Ru(^{15}N-en)(S(O)G)] (^{15}N-**31**)	(7a) 4.50/-7.89	(7b) 4.36/-7.89
	(7c) 3.95/7.56	
[(η^6-hmb)Ru(^{15}N-en)(cGMP-*N7*)]$^+$ (^{15}N-**30**)	(6a) 6.09/-0.11	(6b) 4.87/-0.11
	(6c) 5.01/1.10	(6d) 3.98/1.10

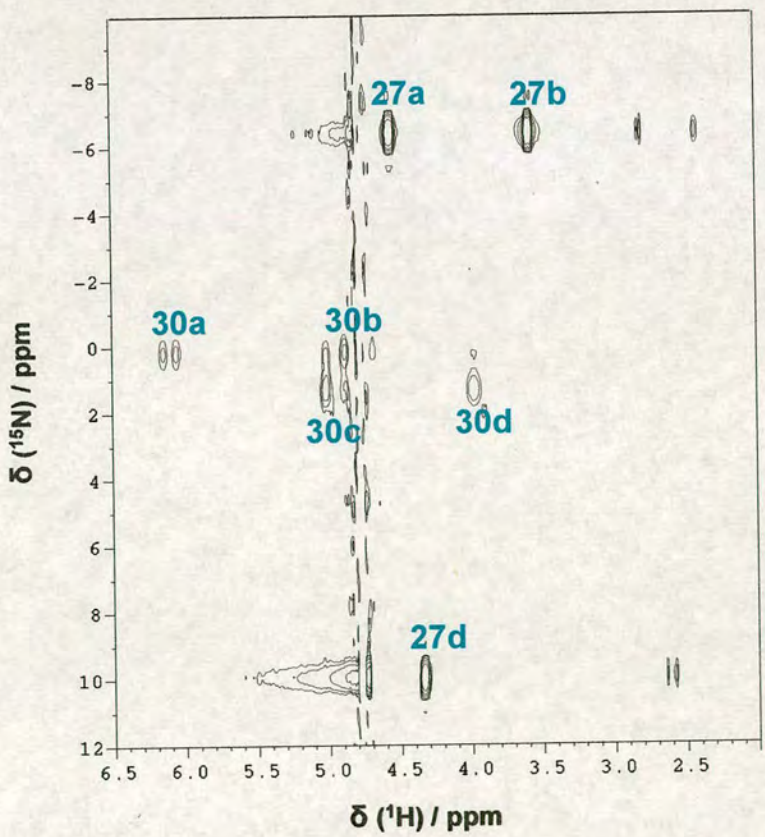

Figure 5.17 2D [$^{1}H,^{15}N$] HSQC NMR spectrum for the reaction of ^{15}N-**27** with cGMP at 310 K for 24 h. Peak assignments: 27a/b and 27c/d sulfenato adduct [(η^6-hmb)Ru(^{15}N-en)(S(O)-*i*Pr)]$^+$ (^{15}N-**27**), 30a/b and 30c/d cGMP adduct [(η^6-hmb)Ru(^{15}N-en)(cGMP-*N7*)]$^+$ (^{15}N-**30**).

The LC-ESI-MS (Figure 5.14 and 5.15) for the reaction of **23** with GSH and cGMP at 310 K for 24 h, showed peaks for three products $[(\eta^6\text{-hmb})Ru(en)(S(O)\text{-}i\text{Pr})]^+$ (**25**), $[(\eta^6\text{-hmb})Ru(en)(S(O)G)]$ (**31**) and $[(\eta^6\text{-hmb})Ru(en)(cGMP\text{-}N7)]^+$ (**30**); whereas the 2D $[^1H,^{15}N]$ HSQC NMR time course for the reaction of ^{15}N-**24** with GSH and cGMP at 310 K for 62 h demonstrated that no cGMP adduct **30** formed after 62 h, which is probably due to the presence of TFA in HPLC separation but not involved in NMR spectroscopy. Compared to the reaction of ^{15}N-**24** bubbled with air continuously in presence of GSH at 310 K for 4 h, the reaction of ^{15}N-**24** with GSH and cGMP (not purged with air continuously) at 310 K for 62 h gave rise to two glutathione adducts, a glutathione thiolato adduct $[(\eta^6\text{-hmb})Ru(^{15}N\text{-en})(SG)]$ (^{15}N-**32**) and a glutathione sulfenato adduct $[(\eta^6\text{-hmb})Ru(^{15}N\text{-en})(S(O)G)]$ (^{15}N-**31**), which is due to the deficiency of O_2, leading to the excess of GSH that reacted with **24** to give rise to **32** (not observed in section **5.3.1.3** due to the existence of sufficient O_2), indicating the adducts **32** and **31** are side products. On the basis of the studies on the hydrolysis and acidity of sulfenato complexes in section **5.3.2**, it can be concluded that only in the presence of GSH the thiolato complex **24** can be readily oxidized to the sulfenato adduct **27**, and **27** is relatively stable at pH 7 in the NMR experiment (rate of hydrolysis at pH 7 is low); whereas the protonated forms are very unstable sulfenic acid complexes $[(\eta^6\text{-hmb})Ru(en)(S(OH)\text{-}i\text{Pr})]^{2+}$ (**33**) and $[(\eta^6\text{-hmb})Ru(en)(S(OH)G)]^+$ (**34**) at pH 2 during HPLC separation. Therefore, the highly reactive sulfenic acid complexes **33** and **34** are key intermediates in the competitive reaction of **24** with GSH and cGMP. The proposed mechanism is shown in Scheme 5.6. This is the first report that Ru(II) arene complexes are oxidized to sulfenates and then protonated to sulfenic acid complexes which are active forms instead of aqua complexes as active forms shown in Chapters 3 and 4.

Scheme 5.6 Proposed pathway for the reaction of **24** with GSH and cGMP. The dashed pathway represents the side reaction.

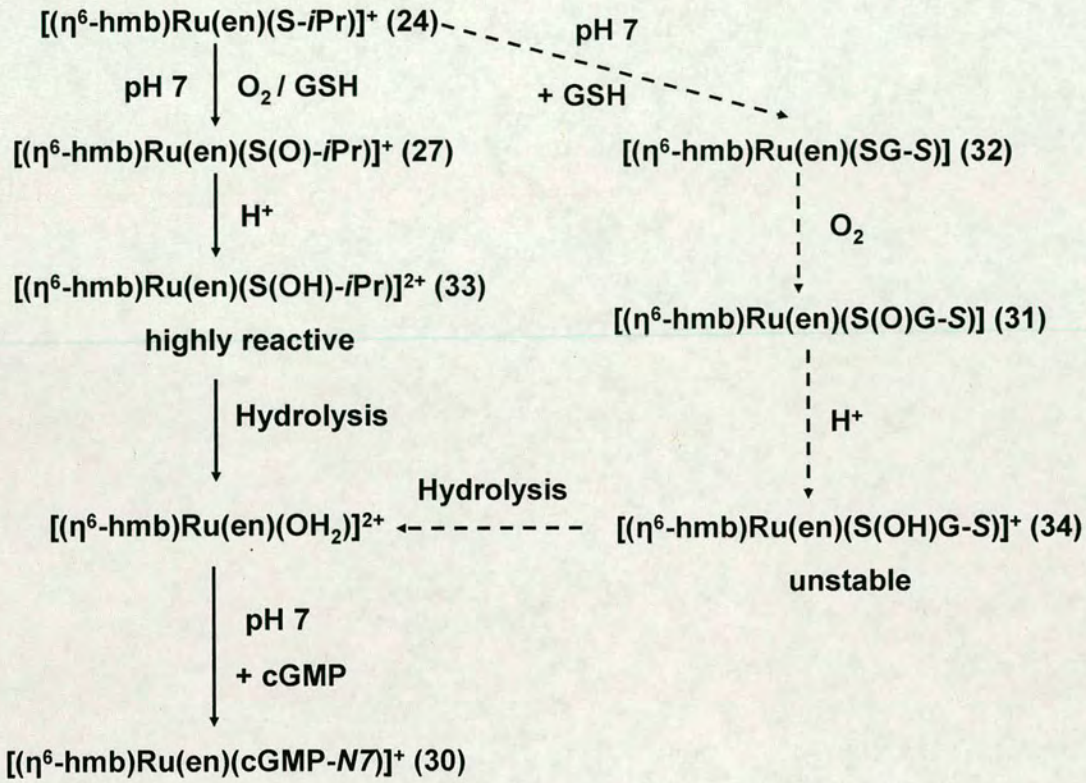

5.4 Summary

In Chapters 3 and 4, the Ru(II) arene complexes are activated by hydrolysis, however, a novel Ru(II) arene complex [(η^6-hmb)Ru(en)(SPh)]PF_6 (**23**) shown in this Chapter does not hydrolyse, but still shows activity to human ovarian cancer cell A2780 (IC_{50} = 23 μM). Thus the mechanism of activation was investigated using HPLC, ESI-MS and NMR, particularly 2D [^{1}H,^{15}N] HSQC NMR.

First the oxidation of complexes **23** and **24** was studied. The thiolato complexes **23** and **24** can be readily oxidized by air at pH 7 containing 22 mM NaCl at 310 K only in presence of GSH (Figures 5.2, 5.3 and 5.10), and the proposed mechanism is given in Scheme 5.3, in which GSH/O_2 is oxidant. The thiolato complexes **23** and **24** can be oxidized to sulfinates by H_2O_2 in aqueous solution, which are two-step reactions (Figures 5.4, 5.5 and 5.9), and sulfenato adducts are intermediates.

The competitive reactions of **23** or ^{15}N-**24** with GSH and cGMP containing phosphate buffer (pH 7) and 22 mM NaCl at 310 K were analysed by HPLC and 2D [^{1}H,^{15}N] HSQC NMR. It is proposed that in the presence of GSH, the thiolato complexes are oxidized by O_2 to sulfenato adducts which protonate slowly at pH 7, forming highly reactive sulfenic acid complexes that hydrolyse, and then bind to cGMP to form ruthenated cGMP products, as shown in Scheme 5.6.

5.5 References

[1] Yan, Y. K.; Melchart, M.; Habtemariam A.; Sadler, P. J. *Chem. Commun.* **2005**, 4764-4776.

[2] Wang, F.; Chen, H.; Parsons, S.; Oswald, I. D. H.; Davidson, J. E.; Sadler, P. J. *Chem. Eur. J.* **2003**, *9*, 5810-5820.

[3] Novakova, O.; Chen, H.; Vrana, O.; Rodger, A.; Sadler, P. J.; Brabec, V. *Biochemistry* **2003**, *42*, 11544-11554.

[4] Liu, H. K.; Wang, F.; Parkinson, J. A.; Bella, J.; Sadler, P. J. *Chem. Eur. J.* **2006**, *12*, 6151-6165.

[5] Wang, F.; Habtemariam, A.; van der Geer, E. P. L.; Fernandez, R.; Melchart, M.; Deeth, R. J.; Aird, R.; Guichard, S.; Fabbiani, F. P. A.; Lozano-Casal, P.; Oswald, I. D. H.; Jodrell, D.; Parsons, S.; Sadler, P. J. *Proc. Natl. Acad. Sci. U. S. A.* **2005**, *102*, 18269-18274.

[6] Wang, F.; Xu, J.; Habtemariam, A.; Bella, J.; Sadler, P. J. *J. Am. Chem. Soc.* **2005**, *127*, 17734-17743.

[7] Wang, F.; Weidt, S.; Xu, J.; Mackay, L. C.; Langridge-Smith, P. R. R.; Sadler, P. J. *J. Am. Soc. Mass Spectr.* submitted.

[8] Weigand, W.; Wunsch, R. *Chem. Ber.* **1996**, *129*, 1409-1419.

[9] Claiborne, A.; Miller, H.; Parsonage, D.; Ross, R. P. *FASEB* **1993**, *7*, 1483-1490.

[10] Hildebrand, U.; Taraz, K.; Budzikiewicz, H. *Tetrahedron Lett.* **1985**, *26*, 4349-4350.

[11] (a) Davis, F. A.; Jenkins, L. A.; Billmers, R. L. *J. Org. Chem.* **1986**, *51*, 1033-1040. (b) Kice, J. L. *Adv. Phys. Org. Chem.* **1980**, *17*, 65-181.

[12] Yoshimura, T.; Hamada, K.; Yamazaki, S.; Shimasaki, C.; Ono, S.; Tsukurimichi, E. *Bull. Chem. Soc. Jpn.* **1995**, *68*, 211-218.

[13] Grapperhaus, C. A.; Darensbourg, M. Y. *Acc. Chem. Res.* **1998**, *31*, 451-459.

[14] Wang, F.; Chen, H.; Parkinson, J. A.; Murdoch, P. del S.; Sadler, P. J. *Inorg. Chem.* **2002**, *41*, 4509-4523.

[15] Galvez, C.; Ho, D. G.; Azod, A.; Selke, M. *J. Am. Chem. Soc.* **2001**, *123*, 3381-3382.

[16] Luo, D.; Anderson, B. D. *Pharml. Res.* **2006**, *23*, 2239-2253.

[17] Krezel, A.; Szczepanik, W.; Sokolowska, M.; Jezowska-Bojczuk, M.; Bal, W. *Chem. Res. Toxicol.* **2003**, *16*, 855-864.

[18] Rabenstein, D. L. *J. Am. Chem. Soc.* **1973**, *95*, 2797-2803.

[19] The HPLC fraction b shown in Figure 6.7 was collected and lyophilized for NMR studies, and it was found to decompose within hours due to the protonation of **5**.

Chapter 6

Conclusions and Future Work

6.1 Conclusions

When this work began, cisplatin was known to be deactivated by S-donor amino acids, peptides and proteins, and not much was known about the competitive reactions between N-donor nucleotides and S-donor peptides Ru(II) arene anticancer complexes. The expected mono-ruthenated cGMP adduct $[(\eta^6\text{-bip})Ru(en)(cGMP\text{-}N7)]^+$ is the major product, rather than glutathione (GSH) adduct $[(\eta^6\text{-bip})Ru(en)(SG\text{-}S)]$, from the competitive reaction of $[(\eta^6\text{-bip})Ru(en)Cl]^+$ with glutathione and guanosine-3′,5′-cyclic monophosphate (cGMP) at pH 7 at 310 K for 72 h. Interestingly, the glutathione adduct was found to be susceptible to oxidation, forming the sulfenato adduct $[(\eta^6\text{-bip})Ru(en)(S(O)G\text{-}S)]$ which can protonate to form the highly reactive sulfenic acid $[(\eta^6\text{-bip})Ru(en)(S(OH)G)]^+$, providing a facile route for displacement of S-bound glutathione by G N7. Similar results were obtained for the reactions of $[(\eta^6\text{-arene})Ru(en)Cl]^+$ (arene = bip, tha) with GSH and 14-mer DNA oligonucleotides. A dinuclear Ru(0) sulfenate/sulfinate complex $\{[(\eta^6\text{-bip})Ru(0)(GSO_2)](\mu\text{-S-GSO})_2[(GSO_2)Ru(0)(\eta^6\text{-bip})]\}^{9-}$ and a tetranuclear complex $\{[(\eta^6\text{-bip})Ru(II)(GSO_2)]_2[(\eta^6\text{-bip})Ru(I)(GSO_2)]_2\}^{8-}$ were observed as products from reactions of $[(\eta^6\text{-bip})Ru(en)Cl]^+$ with GSH for the first time, and they probably play similar roles to $[(\eta^6\text{-bip})Ru(en)(S(O)G\text{-}S)]$ in some physiological reactions.

This thesis has been concerned with the mechanism of cytotoxic action of Ru(II) arene complexes with novel leaving groups, e.g. $[(\eta^6\text{-hmb})Ru(en)(SPh)]^+$ and $[(\eta^6\text{-hmb})Ru(en)(S\text{-}i\text{Pr})]^+$. $[(\eta^6\text{-hmb})Ru(en)(SPh)]^+$ was reported to exhibit anticancer activity (IC_{50} = 23 μM, A2780 cells) but cannot hydrolyse to form the active aqua species. Surprisingly, GSH/O_2 is found to be the oxidant in the oxidation of the Ru(II) thiolate $[(\eta^6\text{-hmb})Ru(en)(S\text{-}i\text{Pr})]^+$ to the sulfenato adduct $[(\eta^6\text{-hmb})Ru(en)(S(O)\text{-}i\text{Pr})]^+$ which is a key intermediate involved in formation of cGMP

adduct $[(\eta^6\text{-hmb})Ru(en)(cGMP\text{-}N7)]^+$. The sulfenate $[(\eta^6\text{-hmb})Ru(en)(S(O)\text{-}i\text{Pr})]^+$ can protonate to form the sulfenic acid complex $[(\eta^6\text{-hmb})Ru(en)(S(OH)\text{-}i\text{Pr})]^+$ which readily hydrolyses and binds to cGMP.

The following part of this Chapter explores future work which could be carried out in this project, and some of which is based on preliminary results shown in this thesis.

6.2 Future Work

6.2.1 Di- and Tetra- Nuclear Complexes

6.2.1.1 Confirmation of Structures of Complexes

In Chapter 3, a dinuclear complex and a tetranuclear complex were analysed by FT-ICR MS, and the possible structures were given, however, further confirmation is needed, such as evidence from infrared (IR) spectroscopy and extended X-ray absorption fine structure (EXAFS). It has been reported that the existence of SO, SO_2 and H-bonds (Ru–N–H····OS) can be confirmed by IR spectroscopy.[1,2] Sulfinato complexes show a two-band set, $\upsilon(SO)_{asym}$ and $\upsilon(SO)_{sym}$ in the range of 1030-1190 cm^{-1}; whereas sufenates show $\upsilon(SO)$ as single absorbance at ca. 900-920 cm^{-1}.[1] NH stretching from the ethylenediamine ligand coordinated toward the oxygen of SO group, has an absorption band range from 3150 to 3400 cm^{-1}.[2] The oxidation states of Ru in these two complexes could be confirmed by EXAFS. Therefore, the exact structures of these two complexes could be identified.

6.2.1.2 Role of Dinuclear Ruthenium Complex

The dinuclear complex was observed in the reactions both in aqueous solution and under physiological conditions (pH 7, 22 mM NaCl) bubbling with Ar, so it is supposed to play a role in the physiological reaction. The investigation on the competitive reaction of $[(\eta^6\text{-bip})Ru(en)Cl]^+$ with GSH and cGMP at pH 7 bubbling with Ar will be carried out to study the role of the dinuclear ruthenium complex in the competition between GSH and cGMP bubbling with Ar, probably it can provide a similar facile route for the displacement of S-bound GSH by guanine N7.

6.2.2 Studies on Ruthenated GST Sulfenate

6.2.2.1 Determination of Binding Sites

It was reported that besides cysteine residues, methionine and histidine residues (Figure 6.1) are also possible binding sites for ruthenium(II) arene complexes in proteins.[3,4] It suggested that the affinity of the $\{(\eta^6\text{-bip})Ru(en)\}^{2+}$ fragment for these amino acids decreases in the order L-Cys > L-Met > L-His.[5] The adducts which are from the reactions of $[(\eta^6\text{-bip})Ru(en)Cl]^+$ with L-Met or L-His are $[(\eta^6\text{-bip})Ru(en)(\text{L-Met-}S)]^{2+}$, $[(\eta^6\text{-bip})Ru(en)(\text{L-His-}N\delta)]^{2+}$ and $[(\eta^6\text{-bip})Ru(en)(\text{L-His-}N\varepsilon)]^{2+}$, respectively.[3,4,5] There are 9 methionine and 6 histidine residues in the enzyme GST used in this thesis as well as 2 reduced cysteine residues, thus determination of binding sites for $[(\eta^6\text{-bip})Ru(en)Cl]^+$ is needed. Recently, the new MS/MS method of electron capture dissociation (ECD)[6,7] for electrosprayed ions cleaves peptide backbones primarily at the C_α – N bond, was used to characterize post-translational modifications.[8,9] This new fragmentation method would be applied for determining the binding sites for bound GST.

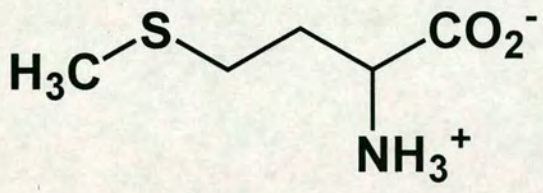

Methionine

Histidine

Figure 6.1 Structures of methionine and histidine.[5]

6.2.2.2 Competition between GST and cGMP

Hydrogen peroxide (H_2O_2), an oxidizing agent known to produce metastable sulfenic acids,[10,11] would be used to oxidize the thiolato adduct $\{[(\eta^6\text{-bip})Ru(en)]_2(GST)\}^{2+}$ to the sulfenate. FT-ICR MS can be applied to identify the formation of the sulfenate. Then cGMP could be added to the sulfenate solution to investigate the substitution of S-bound sulfenate by guanine N7.

The reaction of $[(\eta^6\text{-bip})Ru(en)Cl]^+$ with the enzyme GST and cGMP could be investigated at pH 8 at 310 K using HPLC, FT-ICR MS and NMR spectroscopy. A similar mechanism will probably be obtained, in which the sulfenate play an important role in the displacement of S-bound GST by guanine N7.

6.2.3 Investigation on the Mechanism Using ^{17}O NMR

In order to confirm the mechanism for the oxidation of $[(\eta^6\text{-hmb})Ru(en)(S\text{-}i\text{Pr})]^+$ in the presence of GSH, ^{17}O NMR spectroscopy would be applied.[12] $^{17}O_2$ would be bubbled into the an NMR tube containing a solution of $[(\eta^6\text{-hmb})Ru(en)(S\text{-}i\text{Pr})]^+$ and GSH at pH 7 at 298 K (slowing down the reaction so that good spectra could be obtained), and the reaction mixture would be monitored by ^{17}O NMR, and the ^{17}O chemical shift for $GS^{17}O^{17}OH$ is in the range of 180-300 ppm; the ^{17}O chemical shift for sulfenate is 10-50 ppm.[13] Once the mechanism is confirmed, further evidence for the possible novel mechanism of cytotoxic action of $[(\eta^6\text{-hmb})Ru(en)(SR)]^+$ (R = phenyl, isopropyl) via oxidation would be obtained.

6.2.4 Ru(II) Anticancer Complexes with Other Arenes

It was reported that anticancer activity (against A2780) appears to increase with the size of the coordinated arene: benzene (bz) < *p*-cymene (*p*-cym) < biphenyl (bip) < dihydroanthracene (dha) < tetrahydroanthracene (tha),[5] and the sequence of rates for the reactions of $[(\eta^6\text{-arene})Ru(en)Cl]^+$ with cGMP is consistent with that for analogous reactions of $[(\eta^6\text{-arene})Ru(en)(OH_2)]^{2+}$: tha > bip > dha >> *p*-cym > bz (the structures are shown in Figure 6.2).[14] $[(\eta^6\text{-tha})Ru(en)Cl]^+$ was investigated (in Chapter 4) in the competitive reaction between GSH and a 14-mer DNA oligonucleotide at pH 7 which only gave rise to the monoruthenated DNA adduct.

More investigations on competitive reactions of GSH and cGMP/14-mer DNA oligonucleotides for $[(\eta^6\text{-arene})Ru(en)Cl]^+$ (arene = dha, tha, *p*-cym and bz) can be carried out as well as the studies on the mechanisms. Similar results and mechanisms to those for $[(\eta^6\text{-bip})Ru(en)Cl]^+$ could be obtained.

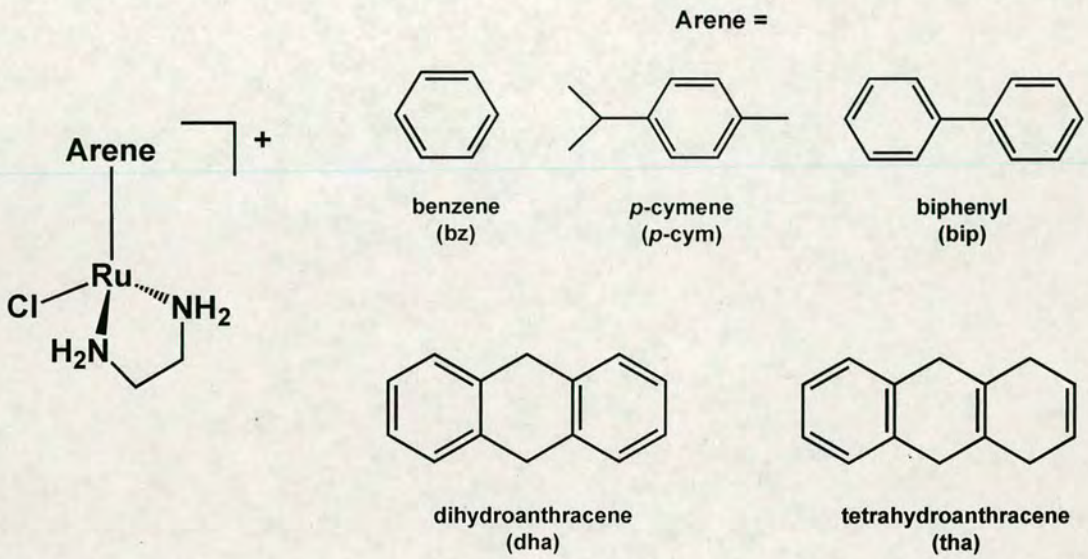

Figure 6.2 Ru(II) arene complexes with different arenes.

6.2.5 O, O-Chelated Ru(II) Arene Complexes

For the Ru(II) arene anticancer complexes containing chelating ligand enthylenediamine (en) which is a hydrogen-bond donor, there is exclusive binding to guanine nucleobases, and in the absence of guanine there is binding to cytosine or thymine, but little binding to adenine bases.[14,15] It was demonstrated that the tropolonato (trop; hydrogen-bond acceptor) complex $[(\eta^6\text{-}p\text{-cym})Ru(trop)Cl]$ reacted with guanosine (Guo) to form N7 adducts (Figure 6.3(A)) and with adenosine (Ado) to form both N7 and N1 adducts (Figure 6.3(B) and (C)), and competitive reactions with guanosine and adenosine gave rise to guanosine:adenosine adducts in a ca. 1.3:1

mol ratio.[16] It was also reported that for the anionic acetylacetonate (acac; hydrogen-bond acceptor) complex [(η^6-*p*-cym)Ru(acac)Cl] (Figure 6.4), the overall affinity for adenosine can be greater than for guanosine, and there is little binding to cytidine or thymidine.[17] However, no studies on the competition between S-donor amino acids (like cysteine, methionine) or peptides (like GSH) or proteins (like albumin) and N-donor nucleotides (like guanine and adenine) for these O, O-chelated Ru(II) arene complexes were explored. Similar investigations on these O, O-chelated Ru(II) arene complexes can be carried out.

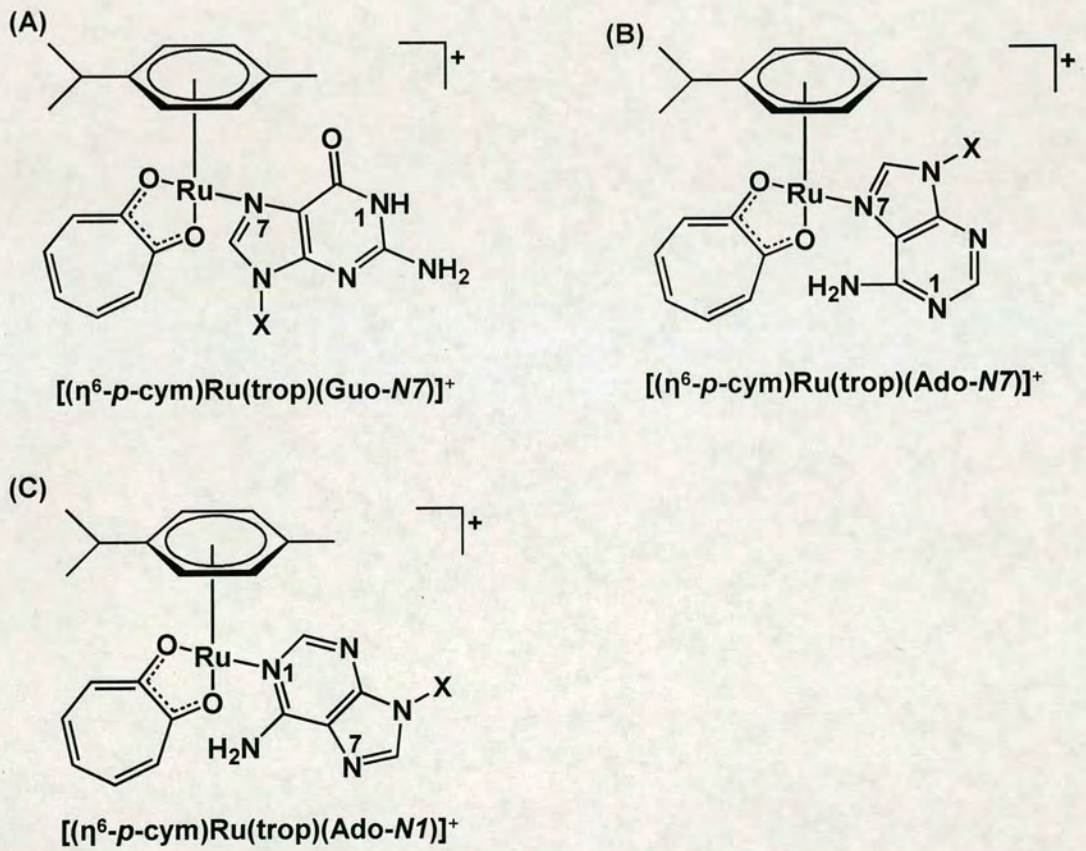

Figure 6.3 Structures of guanosine and adenosine adducts of [(η^6-*p*-cym)Ru(trop)Cl].[16]

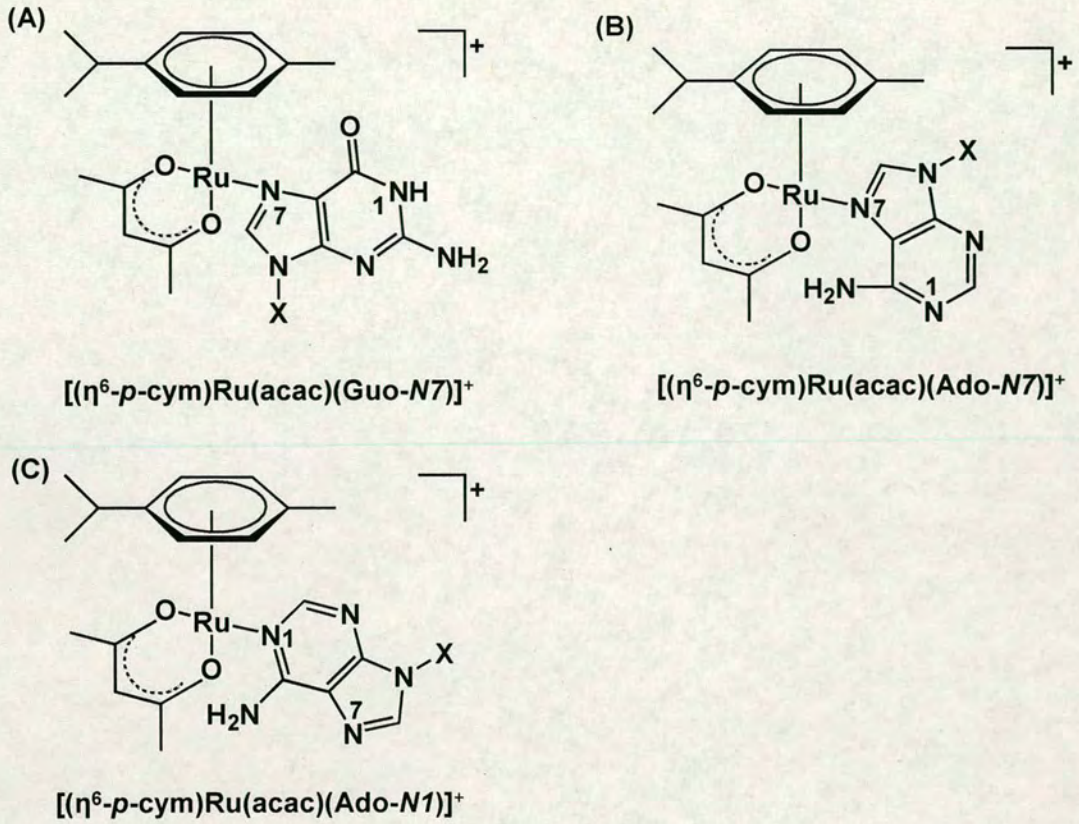

Figure 6.4 Structures of guanosine and adenosine adducts of [(η^6-*p*-cym)Ru(acac)Cl].[17]

6.3 References

[1] Buonomo, R. M.; Font, I.; Maguire, M. J.; Reibenspies, J. H.; Tuntulani, T.; Darensbourg, M. Y. *J. Am. Chem. Soc.* **1995**, *117*, 963-973.

[2] Aranyosiova, M.; Vollarova, O.; Benko, J.; Cernusak, I. *Int. J. Quantum Chem.* **2006**, *106*, 747-763.

[3] Wang, F.; Chen, H.; Parkinson, J. A.; Del S. Murdoch, P.; Sadler, P. J. *Inorg. Chem.* **2002**, *41*, 4509-

[4] Wang, F.; Bella, J.; Parkinson, J. A.; Sadler, P. J. *J. Biol. Inorg. Chem.* **2005**, *10*, 147-

[5] Yan, Y. K.; Melchart, M.; Habtemariam, A.; Sadler, P. J. *Chem. Commun.* **2005**, 4764-4776.

[6] Zubarev, R. A.; Kelleher, N. L.; McLafferty, F. W. *J. Am. Chem. Soc.* **1998**, *120*, 3265-3266.

[7] Zubarev, R. A.; Kruger, N. A.; Fridriksson, E. K.; Lewis, M. A.; Horn, D. M.; Carpenter, B. K.; McLafferty, F. M. *J. Am. Chem. Soc.* **1999**, *121*, 2857-2862.

[8] Kelleher, N. L.; Zubarev, R. A.; Bush, K.; Furie, B.; Furie, B. C.; McLafferty, F. M.; Walsh, C. T. *Anal. Chem.* **1999**, *71*, 4250-4253.

[9] Bakhtiar, R.; Guan, Z. *Biochem. Biophys. Res. Commun.* **2005**, *334*, 1-8.

[10] DeMaster, E. G.; Quast, B. J.; Redfern, B.; Nagasawa, H. T. *Biochemistry* **1995**, *34*, 11494-11499.

[11] Radi, R.; Beckman, J. S.; Bush, K. M.; Freeman, B. A. *J. Biol. Chem.* **1991**, *266*, 4244-4250.

[12] Flambard, A.; Montagne, L.; Delevoye, L. *Chem. Commun.* **2006**, 3426-3428.

[13] Boykin, D. W. *^{17}O NMR Sepctroscopy in Organic Chemistry* CRC Press, Boca Raton, USA, **1990**.

[14] Chen, H.; Parkinson, J. A.; Morris, R. E.; Sadler, P. J. *J. Am. Chem. Soc.* **2003**, *125*, 173-186.

[15] Chen, H.; Parkinson, J. A.; Parsons, S.; Coxall, R. A.; Gould, R. O.; Sadler, P. J. *J. Am. Chem. Soc.* **2002**, *124*, 3064-3082.

[16] Melchart, M.; Habtemariam, A.; Parsons, S.; Moggach, S. A.; Sadler, P. J. *Inorg. Chim. Acta* **2006**, *359*, 3020-3028.

[17] Fernandez, R.; Melchart, M.; Habtemariam, A.; Parsons, S.; Sadler, P. J. *Chem. Eur. J.* **2004**, *10*, 5173-5179.

Courses Attended

1) Transferable skills course: effective writing.

2) Undergraduate Structures of Biological Macronolecules lecture course, Dr. Dryden, 2004.

3) Undergraduate Metals in Medicine lecture course, Professor Sadler, 2005.

4) Postgraduate NMR Spectroscopy lecture course, 2004.

5) Weekly Bio-Physical and Chemical Biology Section Seminars during term time, 2004-2007.

Conferences Attended

1) 37th International Conference of Coordination Chemistry (ICCC), Cape Town, South Africa, August 2006. Poster displayed.

2) 2nd European Conference on Chemistry for Life Science (FECS), Wroclaw, Poland, September 2007. Poster displayed.

Publications

Competition between Glutathione and Guanine for a Ruthenium(II) Arene Anticancer Complex: Detection of a Sulfenato Intermediate.

Fuyi Wang, Jingjing Xu, Abraha Habtemariam, Juraj Bella, Peter J. Sadler, *Journal of the American Chemical Society* **2005**, *127*, 17734-17743.

Identification of Clusters from Reactions of Ruthenium Arene Anticancer Complex with Glutathione Using Nanoscale Liquid Chromatography Fourier Transform Ion Cyclotron Mass Spectrometry Combined with ^{18}O-Labelling.

Fuyi Wang, Stefan Weidt, Jingjing Xu, C. Logan Mackay, Pat R. R. Langridge-Smith, Peter, J. Sadler, *Submitted.*

Diversity in Guanine-Selective DNA Binding Modes for an Organometallic Ruthenium Arene Complex.

Hong-Ke, Liu, Susan J. Berners-Price, Fuyi Wang, John, A. Parkinson, Jingjing Xu, Juraj Bella, Peter J. Sadler *Angewandte Chemie International Edition* **2006**, *45*, 8153-8156.

Competitive Reactions between Glutathione and 14-mer DNA oligonucleotides for Ruthenium(II) Arene Anticancer Complexes

Jingjing Xu, Fuyi Wang, Stefan Weidt, C. Logan Mackay, Pat R. R. Langridge-Smith, Peter, J. Sadler, *on Preparation.*

Activation of Ruthenium(II) Arene Anticancer Complexes towards Guanine Binding by Oxidation of Bound Thiolates.

Jingjing Xu, Holm Petzold, Fuyi Wang, Abraha Habtemariam, Juraj Bella, Peter J. Sadler, *on Preparation.*